(12) INTERNATIONAL APPLICATION PUBLISHED UNDER THE PATENT COOPERATION TREATY (PCT)

(19) World Intellectual Property Organization
International Bureau

(43) International Publication Date
25 August 2016 (25.08.2016)

WIPO | PCT

(10) International Publication Number
WO 2016/131981 A1

(51) International Patent Classification:
A61K 38/17 (2006.01) *A61P 35/00* (2006.01)
A61K 48/00 (2006.01) *A61P 29/00* (2006.01)
A61P 27/06 (2006.01)

(21) International Application Number:
PCT/EP2016/053613

(22) International Filing Date:
19 February 2016 (19.02.2016)

(25) Filing Language: English

(26) Publication Language: English

(30) Priority Data:
15305270.9 20 February 2015 (20.02.2015) EP
15306664.2 16 October 2015 (16.10.2015) EP

(71) Applicant: **INSTITUT PASTEUR** [FR/FR]; 25-28, rue du Docteur Roux, 75015 Paris (FR).

(72) Inventors: **PETIT, Christine**; Institut Pasteur, 25-28 rue du Dr Roux, 75724 Paris Cedex 15 (FR). **AVAN, Paul**; Université d'Auvergne - Clermont 1, Facultés de Médecine et de Pharmacie, 28 place Henri Dunant BP 38, 63001 Clermont-Ferrand (FR). **DELMAGHANI, Sedigheh**; Institut Pasteur, 25-28 rue du Dr Roux, 75724 Paris Cedex 15 (FR). **DEFOURNY, Jean**; Institut Pasteur, 25-28 rue du Dr Roux, 75724 Paris Cedex 15 (FR). **AGHAIE, Asadollah**; Institut de la Vision, 17 rue Moreau, 75012 Paris (FR). **SAFIEDDINE, Saaid**; Institut Pasteur, 25-28 rue du Dr Roux, 75724 Paris Cedex 15 (FR). **EMPTOZ, Alice**; 33 rue de Reuilly, 75012 Paris (FR).

(74) Agent: **REGIMBEAU**; 20, rue de Chazelles, 75847 Paris Cedex 17 (FR).

(81) Designated States *(unless otherwise indicated, for every kind of national protection available)*: AE, AG, AL, AM, AO, AT, AU, AZ, BA, BB, BG, BH, BN, BR, BW, BY, BZ, CA, CH, CL, CN, CO, CR, CU, CZ, DE, DK, DM, DO, DZ, EC, EE, EG, ES, FI, GB, GD, GE, GH, GM, GT, HN, HR, HU, ID, IL, IN, IR, IS, JP, KE, KG, KN, KP, KR, KZ, LA, LC, LK, LR, LS, LU, LY, MA, MD, ME, MG, MK, MN, MW, MX, MY, MZ, NA, NG, NI, NO, NZ, OM, PA, PE, PG, PH, PL, PT, QA, RO, RS, RU, RW, SA, SC, SD, SE, SG, SK, SL, SM, ST, SV, SY, TH, TJ, TM, TN, TR, TT, TZ, UA, UG, US, UZ, VC, VN, ZA, ZM, ZW.

(84) Designated States *(unless otherwise indicated, for every kind of regional protection available)*: ARIPO (BW, GH, GM, KE, LR, LS, MW, MZ, NA, RW, SD, SL, ST, SZ, TZ, UG, ZM, ZW), Eurasian (AM, AZ, BY, KG, KZ, RU, TJ, TM), European (AL, AT, BE, BG, CH, CY, CZ, DE, DK, EE, ES, FI, FR, GB, GR, HR, HU, IE, IS, IT, LT, LU, LV, MC, MK, MT, NL, NO, PL, PT, RO, RS, SE, SI, SK, SM, TR), OAPI (BF, BJ, CF, CG, CI, CM, GA, GN, GQ, GW, KM, ML, MR, NE, SN, TD, TG).

Published:

— *with international search report (Art. 21(3))*

— *before the expiration of the time limit for amending the claims and to be republished in the event of receipt of amendments (Rule 48.2(h))*

— *with sequence listing part of description (Rule 5.2(a))*

WO 2016/131981 A1

(54) Title: PREVENTION AND/OR TREATMENT OF HEARING LOSS OR IMPAIRMENT

(57) Abstract: The present invention relates to the use of gasdermin, in particular of gasdermin A, gasdermin B, gasdermin C, gasdermin D, DFNA5 or DFNB59 (or pejvakin), and more particularly pejvakin for modulating cellular redox homeostasis. A particularly preferred use of gasdermin, in particular of gasdermin A, gasdermin B, gasdermin C, gasdermin D, DFNA5 or DFNB59 (or pejvakin), and more particularly pejvakin in the context of the present invention is as an antioxidant. The present invention also concerns a virally-mediated gene therapy for restoring genetically- impaired auditory and vestibular functions in subjects suffering from an Usher syndrome. More precisely, this gene therapy takes advantage of an AAV2/8 vector expressingat least one USH1 gene product, preferably SANS.

PREVENTION AND/OR TREATMENT OF HEARING LOSS OR IMPAIRMENT

PEJVAKIN AS REDOX MODULATOR AND PARTICULAR USES THEREOF AS ANTIOXIDANT

BACKGROUND OF THE INVENTION

The mammalian hearing organ, the cochlea, consists of a coiled, fluid filled membranous duct that contains the sensory epithelium responsive to sound. This sensory epithelium, termed the organ of Corti, comprises two different kinds of sensory cells, inner hair cells (IHCs) and outer hair cells (OHCs), which are surrounded by supporting cells. The apical specialization of hair cells, the hair bundle, houses the mechanotransduction machinery that transforms sound-induced mechanical stimuli into cell depolarization. This results in neurotransmitter release and the generation in spiral ganglion neurons (SGN) (auditory nerve) of action potentials that are relayed by the brainstem to the auditory cortex. Each class of sensory cells serves a different function. IHCs are the genuine sound receptors, whereas OHCs behave as active mechanical amplifiers that impart high sensitivity, sharp tuning and wide dynamic range to the cochlea. This functional difference is also evident in the afferent innervation of hair cells. Each single IHC is innervated by 15–20 type I spiral ganglion neurons that provide parallel channels for transmitting auditory information to the brain. In contrast, 30–60 OHCs are innervated by a single type II spiral ganglion neuron, thus integrating the sensory input from many different effector cells.

The basic auditory signal conveyed by spiral ganglion neurons is analysed, decoded and integrated along the afferent auditory pathway, which includes four major relays (cochlear nuclei, superior olive, inferior colliculus and medial geniculate body) before reaching the auditory cortex in the temporal lobe of the brain. Each level in the auditory pathway is tonotopically organized, paralleling the distribution of the range of sound frequencies perceived along the cochlear spiral, from base (high frequencies) to apex (low frequencies).

Most forms of **inherited sensorineural hearing impairment** are due to cochlear cell defects. However, a substantial proportion of cases, including up to 10% of all cases of permanent hearing impairment in children, are caused by a lesion located beyond the cochlea. Clinical tests for sensorineural hearing impairment include recording the auditory brainstem response

(ABR), which measures the acoustic stimulus–evoked electrophysiological response of the auditory nerve and brainstem, and otoacoustic emissions (OAEs), which are low level sounds originating from the cochlea due to the mechanical activity of OHCs. Auditory neuropathy is a type of sensorineural hearing impairment in which the ABR is absent or severely distorted while OAEs are preserved. This suggests a primary lesion located in the IHC, in the auditory nerve or in the intervening synapse, but may also include damage to neuronal populations in the auditory pathway.

Age-related hearing loss (ARHL or **presbycusis)**, which affects more than 30% people above 60 and overall, about 5 million people in France, is the result of a combination of factors, genetic and environmental (lifelong exposure to noise and to chemicals). Yet it has been shown in the 1950s that subjects who spend their lives in silent environments do not suffer from any hearing impairment even in their 80s. This, and a huge body of evidence collected in subjects occupationally exposed to noise, leads to conclude that **noise-induced hearing loss** (NIHL) is the dominant cause of hearing impairment in ageing subjects. It is one of the most frequent conditions in workers, and an increasing matter of concern as exposure to loud sound during leisure has increased dramatically, particularly in younger subjects, with the development of inexpensive portable music players. Permanent hearing loss resulting from the loss of auditory hair cells (HCs) and spinal ganglion neurons (SGNs) is irreversible because the cells are terminally developed and cannot be replaced by mitosis. Although great efforts have been made to regenerate lost HCs and SGNs in mammals, these efforts have been largely unsuccessful so far.

The *DFNB59* gene has been identified to underlie an autosomal recessive auditory neuropathy. The product of *DFNB59*, pejvakin, is known to be expressed in all the relays of the afferent auditory pathway, from the cochlea to the midbrain, and plays a critical role in the physiology of auditory neurons (Delmaghani S. et al, 2006). This first study was performed in patients affected by pure auditory neuropathies that consistently showed increased inter-wave delay of auditory brainstem responses (ABRs).

Since then, other DFNB59 patients have been reported, who display a cochlear dysfunction, as shown by the absence of OAEs. Because the latter patients were carrying truncating (nonsense or frame-shifting) *PJVK* mutations, whereas the former had missense mutations (p.T54I or p.R183W), the DFNB59 phenotypic variability has tentatively been ascribed to the difference in

the mutations (Collin et al., 2007; Ebermann et al., 2007; Hashemzadeh Chaleshtori et al., 2007; Schwander et al., 2007; Borck et al., 2012; Mujtaba et al., 2012; Zhang et al., 2015). Subsequently-reported patients, who carried the p.R183W missense mutation but lacked OAEs unlike the first reported patients (Collin et al., 2007), called into question the existence of a straightforward connection between the nature of the *PJVK* mutation and the hearing phenotype.

The precise function of pejvakin is still unknown and its role in the hearing impairment aetiology remains to be elucidated in order to identify novel treatments and/or adapt conventional ones.

Pejvakin belongs to the family of molecules called gasdermins, expressed in the epithelial cells of several tissues and whose actual functions remain unknown. In humans, the sequences of DFNB59 and DFNA5 genes share at least 50% identity and the encoded proteins belong to the gasdermin family group of proteins, which also comprises the proteins encoded respectively by the GSDMA, GSDMB, GSDMC and GSDMD genes, as demonstrated by multiple sequence alignment and phylogenetic tree of all the gasdermin family of proteins (Shi et al., 2015, Saeki and Sasaki, 2011). Of note, DFNB59 and DFNA5 are also designated as gasdermin-related proteins.

In this aim, the present inventors studied *Pjvk* knock-out mice. This study revealed an unprecedented hypervulnerability to sound exposure and allowed them to identify what the target cells and the cellular mechanisms underlying the pejvakin defect are. More precisely, they found that pejvakin is a peroxisome-associated protein involved in the division of this organelle and playing a critical role in antioxidant metabolism.

Moreover, their results show that it is possible to alleviate the hair cells and neuronal cell defects of *Pjvk*$^{-/-}$ mice by treating them with antioxidant compounds, and to fully prevent the auditory defect by gene transfer in the cochlea. These findings have major therapeutic implications, as described below.

DETAILED DESCRIPTION OF THE INVENTION

The present Inventors identified the biochemical mechanisms involved in the congenital hearing impairment and sound vulnerability observed in pejvakin deficient mice.

More precisely, they have shown that these phenomena are due to a faulty homeostasis of reactive oxygen species (ROS) in the auditory system of *Pjvk*$^{-/-}$ mice. This was demonstrated by various means: (i) the expression of some antioxidant genes, *CypA*, *Gpx2, c-Dct*, and, *Mpv17* was reduced in the *Pjvk*$^{-/-}$ mice. (ii) The reduced glutathione (GSH) content was decreased in *Pjvk*$^{-/-}$ cochlea whilst the oxidized glutathione (GSSG) content was increased. Therefore the ratio between GSH and GSSG was reduced in *Pjvk*$^{-/-}$ mice. The increase in GSSG as well as the decrease in GSH:GSSG ratio are well known as markers of oxidative stress in cells. Thus the lack of pejvakin increases oxidative stress in the *Pjvk*$^{-/-}$ cochlea. (iii) Lipids are natural targets of oxidation by ROS and the content of aldehydes that are the by-product of lipid peroxidation were shown to be increased in the cochlea of *Pjvk*$^{-/-}$, indicating *Pjvk* defect results in ROS cellular damage. (iv) Sound exposure is known to induce oxidative stress as the result of cellular hyperactivity, which is associated with an antioxidant protective response. The present Inventors herein showed that the expression levels of *Pjvk* and of some antioxidants increased in response to sound. In addition, the transcription rate of *Pjvk* increased in the physiological response to noise (sound preconditioning), indicating that it is likely involved in the immediate adaptive antioxidant response to noise.

In an aspect, the present invention relates to the use of a gasdermin, which designates a member of the gasdermin family of proteins, for modulating cellular redox homeostasis. Thus, the present invention concerns the use of a gasdermin as a redox modulator. A particularly preferred use of gasdermin in the context of the present invention is as an antioxidant. Accordingly, a gasdermin can be advantageously used as such in pharmaceutical compositions.

The terms "**modulator of cellular redox homeostasis**" or "**redox modulator**" as used herein refer to an agent or compound that modifies the redox status (or redox potential or redox state) in a cell. This agent or compound can (i) act indirectly by changing the balance of oxidants and antioxidants in a cell and/or (ii) act directly by increasing or decreasing the rate of generation or of elimination of ROS in a cell and/or by increasing or decreasing the amount of ROS in a cell.

The term "**gasdermin**" as used herein refers to any member of the gasdermin family of proteins or polypeptides, or any homolog of a member of the gasdermin family of proteins or polypeptides, in humans or non-human mammals such as primates, cats, dogs, swine, cattle, sheep, goats, horses, rabbits, rats, mice, and the like. In humans, members of the gasdermin family include, but are not limited to: gasdermin A, gasdermin B, gasdermin C, gasdermin D, DFNA5 and DFNB59 (or pejvakin) (Shi et al., 2015; Saeki and Sasaki, 2011).

In another embodiment, the term "gasdermin" also designates any fragment of a member of the gasdermin family of proteins or polypeptides, or any fragment of a homolog of a member of the gasdermin family of proteins or polypeptides, wherein said fragment retains at least one biological function that is of interest in the present context (Shi et al., 2015; Saeki and Sasaki, 2011).

In a particular embodiment, the present invention relates to the use of a gasdermin chosen among: gasdermin A, gasdermin B, gasdermin C, gasdermin D, DFNA5 and DFNB59 (or pejvakin), for modulating cellular redox homeostasis. The present invention therefore concerns the use of gasdermin A, gasdermin B, gasdermin C, gasdermin D, DFNA5 or DFNB59 (or pejvakin), as a redox modulator. A particularly preferred use of gasdermin A, gasdermin B, gasdermin C, gasdermin D, DFNA5 or DFNB59 (or pejvakin) in the context of the present invention is as an antioxidant. Accordingly, gasdermin A, gasdermin B, gasdermin C, gasdermin D, DFNA5 or DFNB59 (or pejvakin) can be advantageously used as such in pharmaceutical compositions.

In a more particular embodiment of this aspect, the present invention relates to the use of pejvakin for modulating cellular redox homeostasis. Thus, an embodiment of the present invention concerns the use of pejvakin as a redox modulator.

Regarding the role of pejvakin as a modulator of cellular redox homeostasis, the role here proposed is an indirect one, which involves an effect via an organelle, peroxisome. The glutathione is the major antioxidant within the cell and as shown by the present Inventors, the oxidized glutathione content increases in the cochlea of *Pjvk*$^{-/-}$ mice, whereas the reduced glutathione content decreases, showing an impaired anti-oxidant defence in the cochlea of these mice.

A particularly preferred use of pejvakin in the context of said particular embodiment of the present invention is as an antioxidant.

Accordingly, pejvakin can be advantageously used as such in pharmaceutical compositions.

The term "**antioxidant**" herein qualifies any molecule that is capable of modulating the redox homeostasis in a cell, preferably in an auditory cell. Such a molecule is involved in the subtly orchestrated balance of redox status in cells, or in the delicate balance between the ROS generation and elimination. Consequently, it is very important for the proper functioning of these cells. In a particular embodiment, "antioxidant molecules" herein designate any molecule that is capable of restoring the normal function of one or more organelles selected from peroxisomes, lysosomes, mitochondria, and endoplasmic reticulum in a cell, e.g., in an auditory cell.

An "antioxidant" compound may not be able to eliminate the Reactive Species (ROS or RNS) directly (e.g., by physical interaction). It is thus not a "RS inhibiting compound" as meant in the present invention (see below).

For example, said antioxidant compounds may be a gasdermin, and preferably a gasdermin-related protein chosen among: pejvakin (DFNB59), gasdermin A, gasdermin B, gasdermin C, gasdermin D, DFNA5, cyclophilin A, c-dopachrome tautomerase or Mpv17.

Pejvakin or autosomal recessive deafness type 59 protein or PJVK is a protein belonging to the gasdermin family. In human, it has the sequence SEQ ID NO:1 (NCBI Reference Sequence: NP_001036167.1). In mouse, it has the sequence SEQ ID NO:2 (NCBI Reference Sequence: NP_001074180). It is known to be expressed in all the relays of the afferent auditory pathway from the cochlea to the midbrain and is thought to play a critical role in the physiology of auditory neurons (Delmaghani S. et al, 2006). Several impairing mutations have been described (Collin et al., 2007; Ebermann et al., 2007; Hashemzadeh Chaleshtori et al., 2007; Schwander et al., 2007; Borck et al., 2012; Mujtaba et al., 2012; Zhang et al., 2015).

Human pejvakin is encoded by the *DFNB59* gene of SEQ ID NO:3 in human (NCBI Reference Sequence: NM_001042702.3, the coding sequence being comprised between the nucleotides 357 and 1415). The mouse *DFNB59* gene is of SEQ ID NO:4 (NCBI Reference Sequence: NM_001080711.2, the coding sequence being comprised between the nucleotides 150 and 1208).

In the context of the invention, the term "pejvakin" herein designates a polypeptide having the amino acid sequence SEQ ID NO:1 (human PJVK) or SEQ ID NO:2 (mouse PJVK) or an homologous sequence thereof. Said latter **homologous sequence** is for example the PJVK protein of another animal species, the polypeptide having said latter homologous sequence retains at least one biological function of human PJVK or mouse PJVK that is of interest in the present context. This latter homologous sequence shares preferably at least 50%, preferably at least 60%, more preferably at least 70%, more preferably at least 80%, and even more preferably at least 90% identity with SEQ ID NO:1 or SEQ ID NO:2. Preferably, the identity percentage between said homologous sequence and SEQ ID NO:1 or SEQ ID NO:2 is identified by a global alignment of the sequences in their entirety, this alignment being performed by means of an algorithm that is well known by the skilled person, such as the one disclosed in Needleman and Wunsch (1970). Accordingly, sequence comparisons between two amino acid sequences can be performed for example by using any software known by the skilled person, such as the "needle" software using the "Gap open" parameter of 10, the "Gap extend" parameter of 0.5 and the "Blosum 62" matrix.

In another embodiment, the term "pejvakin" also designates any polypeptide encoded by a *DFNB59* gene. In a preferred embodiment, said *DFNB59* gene is chosen in the group consisting of: SEQ ID NO:3, SEQ ID NO:4, or any homologous gene of another animal species, said homologous gene whose encoding protein shares at least 50%, similarity with SEQ ID NO:3 or SEQ ID NO:4 and more particularly preferably at least 50%, preferably at least 60%, more preferably at least 70%, more preferably at least 80%, and even more preferably at least 90% identity with SEQ ID NO:3 or SEQ ID NO:4.

In another embodiment, the term "pejvakin" also designates any fragment of human PJVK or mouse PJVK or any fragment of a polypeptide having a homologous sequence as defined above, wherein said fragment retains at least one biological function of human PJVK or mouse PJVK that is of interest in the present context. This fragment shares preferably at least 30%, preferably at least 40%, more preferably at least 50%, more preferably at least 60%, and even more preferably at least 70% identity with SEQ ID NO:1 or SEQ ID NO:2.

Gasdermin A is a protein which belongs to the gasdermin family. In human, it has the sequence SEQ ID NO:21 (NCBI Reference Sequence: NP_835465.2). In mouse, gasdermin A has the sequence SEQ ID NO:22 (NCBI Reference Sequence: NP_067322.1), gasdermin A2 has the

sequence SEQ ID NO:23 (NCBI Reference Sequence: NP_084003.2) and gasdermin A3 has the sequence SEQ ID NO:24 (NCBI Reference Sequence: NP_001007462.1). It is known to be expressed predominantly in the gastrointestinal tract and in the skin. It was discovered as a potential tumour suppressor with a different expression pattern in normal stomach and human gastric cancer cells. Gasdermin A was reported as a target of LIM domain only 1 (LMO1) in human gastric epithelium and induced apoptosis in a transforming growth factor-β–dependent manner and mouse gasdermin A3 has been reported to cause autophagy followed by cell death (Shi P *et al.*, 2015).Human gasdermin A is encoded by the mRNA of SEQ ID NO:25 (NCBI Reference Sequence: NM_178171.4). The mouse gasdermin A gene is of SEQ ID NO:26 (NCBI Reference Sequence: NM_021347.4), the gasdermin A2 gene is of SEQ ID NO:27 (NCBI Reference Sequence: NM_029727.2) and the gasdermin A3 gene is of SEQ ID NO:28 (NCBI Reference Sequence: NM_001007461.1).

In the context of the invention, the term “gasdermin A” herein designates a polypeptide having the amino acid sequence SEQ ID NO:21 (human gasdermin A) or SEQ ID NO:22, SEQ ID NO:23 or SEQ ID NO:24 (mouse gasdermin A, GSDM A2 and GSDM A3 respectively) or an homologous sequence thereof. Said latter **homologous sequence** is for example the gasdermin A protein of another animal species, the polypeptide having said latter homologous sequence retains at least one biological function of human gasdermin A or mouse gasdermin A, GSDM A2 or GSDM A3 that is of interest in the present context. This latter homologous sequence shares preferably at least 50%, preferably at least 60%, more preferably at least 70%, more preferably at least 80%, and even more preferably at least 90% identity with SEQ ID NO:21, SEQ ID NO:22, SEQ ID NO:23 or SEQ ID NO:24.

Preferably, the identity percentage between said homologous sequence and SEQ ID NO:21, SEQ ID NO:22, SEQ ID NO:23 or SEQ ID NO:24 is identified by a global alignment of the sequences in their entirety, this alignment being performed by means of an algorithm that is well known by the skilled person, such as the one disclosed in Needleman and Wunsch (1970). Accordingly, sequence comparisons between two amino acid sequences can be performed for example by using any software known by the skilled person, such as the “needle” software using the “Gap open” parameter of 10, the “Gap extend” parameter of 0.5 and the “Blosum 62” matrix.

In another embodiment, the term "gasdermin A" also designates any polypeptide encoded by a gasdermin A gene. In a preferred embodiment, said gasdermin A gene is chosen in the group consisting of: SEQ ID NO:25, SEQ ID NO:26, SEQ ID NO:27, SEQ ID NO:28 or any homologous gene of another animal species, said homologous gene sharing preferably at least 50%, more preferably at least 60%, more preferably at least 70%, more preferably at least 80%, and even more preferably at least 90% identity with SEQ ID NO:25, SEQ ID NO:26, SEQ ID NO:27 or SEQ ID NO:28.

In another embodiment, the term "gasdermin A" also designates any fragment of human gasdermin A or mouse gasdermin A, GSDM A2 or GSDM A3 or any fragment of a polypeptide having an homologous sequence as defined above, wherein said fragment retains at least one biological function of human gasdermin A or mouse gasdermin A, GSDM A2 or GSDM A3 that is of interest in the present context. This fragment shares preferably at least 30%, preferably at least 40%, more preferably at least 50%, more preferably at least 60%, and even more preferably at least 70% identity with SEQ ID NO:21, SEQ ID NO:22, SEQ ID NO:23 or SEQ ID NO:24.

Gasdermin B is a protein which belongs to the gasdermin family. In human, gasdermin B isoform 3 has the sequence SEQ ID NO:29 (NCBI Reference Sequence: NP_001159430.1). It is known to be expressed in oesophagus, stomach, liver, and colon. The function of gasdermin B is not known. The gene Gsdmb was not identified in mouse genome.

Human gasdermin B is encoded by the transcript variant 3 (mRNA) of SEQ ID NO:30 in human (NCBI Reference Sequence: NM_001165958.1).

In the context of the invention, the term "gasdermin B" herein designates a polypeptide having the amino acid sequence SEQ ID NO:29 (human gasdermin B) or an homologous sequence thereof. Said latter **homologous sequence** is for example the gasdermin B protein of another animal species, the polypeptide having said latter homologous sequence retains at least one biological function of human gasdermin B that is of interest in the present context. This homologous sequence shares preferably at least 50%, preferably at least 60%, more preferably at least 70%, more preferably at least 80%, and even more preferably at least 90% identity with SEQ ID NO:29.

Preferably, the identity percentage between said homologous sequence and SEQ ID NO:29 is identified by a global alignment of the sequences in their entirety, this alignment being performed by means of an algorithm that is well known by the skilled person.

In another embodiment, the term "gasdermin B" also designates any polypeptide encoded by a gasdermin B gene. In a preferred embodiment, said gasdermin B gene is chosen in the group consisting of: SEQ ID NO:30 or any homologous gene of another animal species, said homologous gene sharing preferably at least 50%, more preferably at least 60%, more preferably at least 70%, more preferably at least 80%, and even more preferably at least 90% identity with SEQ ID NO:30.

In another embodiment, the term "gasdermin B" also designates any fragment of human gasdermin B or any fragment of a polypeptide having a homologous sequence as defined above, wherein said fragment retains at least one biological function of human gasdermin B that is of interest in the present context. This fragment shares preferably at least 30%, preferably at least 40%, more preferably at least 50%, more preferably at least 60%, and even more preferably at least 70% identity with SEQ ID NO:29.

Gasdermin C is a protein which belongs to the gasdermin family. In human, it has the sequence SEQ ID NO:31 (NCBI Reference Sequence: NP_113603.1). In mouse, gasdermin C has the sequence SEQ ID NO:32 (NCBI Reference Sequence: NP_113555.1), gasdermin C2 has the sequence SEQ ID NO:33 (NCBI Reference Sequence: NP_001161746.1), gasdermin C3 has the sequence SEQ ID NO:34 (NCBI Reference Sequence: NP_899017.2). It is known to be expressed in oesophagus, stomach, trachea, spleen, and skin and its function is not known.

Human gasdermin C is encoded by the mRNA of SEQ ID NO:35 (NCBI Reference Sequence: NM_031415.2). The mouse gasdermin C gene is of SEQ ID NO:36 (NCBI Reference Sequence: NM_031378.3), the gasdermin C2 gene is of SEQ ID NO:37 (NCBI Reference Sequence: NM_001168274.1) and the gasdermin C3 gene is of SEQ ID NO:38 (NCBI Reference Sequence: NM_183194.3)

In the context of the invention, the term "gasdermin C" herein designates a polypeptide having the amino acid sequence SEQ ID NO:31 (human gasdermin C) or SEQ ID NO:32, SEQ ID NO:33, SEQ ID NO:34 (mouse gasdermin C, gasdermin C2 and gasdermin C3 respectively) or an homologous sequence thereof. Said latter **homologous sequence** is for example the gasdermin

C protein of another animal species, the polypeptide having said latter homologous sequence retains at least one biological function of human gasdermin C or mouse gasdermin C, C2 or C3 that is of interest in the present context. This homologous sequence shares preferably at least 50%, preferably at least 60%, more preferably at least 70%, more preferably at least 80%, and even more preferably at least 90% identity with SEQ ID NO:31, SEQ ID NO:32, SEQ ID NO:33 or SEQ ID NO:34.

Preferably, the identity percentage between said homologous sequence and SEQ ID NO:31, SEQ ID NO:32, SEQ ID NO:33 or SEQ ID NO:34 is identified by a global alignment of the sequences in their entirety, this alignment being performed by means of an algorithm that is well known by the skilled person.

In another embodiment, the term “gasdermin C” also designates any polypeptide encoded by a gasdermin C gene. In a preferred embodiment, said gasdermin C gene is chosen in the group consisting of: SEQ ID NO:35, SEQ ID NO:36, SEQ ID NO:37, SEQ ID NO:38, or any homologous gene of another animal species, said homologous gene sharing preferably at least 50%, more preferably at least 60%, more preferably at least 70%, more preferably at least 80%, and even more preferably at least 90% identity with SEQ ID NO:35, SEQ ID NO:36, SEQ ID NO:37 or SEQ ID NO:38.

In another embodiment, the term “gasdermin C” also designates any fragment of human gasdermin C or mouse gasdermin C, C2 or C3 or any fragment of a polypeptide having a homologous sequence as defined above, wherein said fragment retains at least one biological function of human gasdermin C or mouse gasdermin C, C2 or C3 that is of interest in the present context. This fragment shares preferably at least 30%, preferably at least 40%, more preferably at least 50%, more preferably at least 60%, and even more preferably at least 70% identity with SEQ ID NO:31, SEQ ID NO:32, SEQ ID NO:33 or SEQ ID NO:34.

Gasdermin D is a protein belonging to the gasdermin family. In human, it has the sequence SEQ ID NO:39 (NCBI Reference Sequence: NP_001159709.1). In mouse, it has the sequence SEQ ID NO:40 (NCBI Reference Sequence: NP_081236.1). It is known to be expressed in oesophagus and stomach and is involved in pyroptotic cell death (Shi J et al., 2015; Kayagaki et al., 2015). This activity appears upon a cleavage of the protein by caspase-11.

Human gasdermin D is encoded by the mRNA of SEQ ID NO:41 in human (NCBI Reference Sequence: NM_001166237.1). The mouse gasdermin D gene is of SEQ ID NO:42 (NCBI Reference Sequence: NM_026960.4).

In the context of the invention, the term "gasdermin D" herein designates a polypeptide having the amino acid sequence SEQ ID NO:39 (human gasdermin D) or SEQ ID NO:40 (mouse gasdermin D) or an homologous sequence thereof. Said latter **homologous sequence** is for example the gasdermin D protein of another animal species, the polypeptide having said gasdermin D homologous sequence retains at least one biological function of human gasdermin D or mouse gasdermin D that is of interest in the present context. This homologous sequence shares preferably at least 50%, preferably at least 60%, more preferably at least 70%, more preferably at least 80%, and even more preferably at least 90% identity with SEQ ID NO:39 or SEQ ID NO:40.

Preferably, the identity percentage between said homologous sequence and SEQ ID NO:39 or SEQ ID NO:40 is identified by a global alignment of the sequences in their entirety, this alignment being performed by means of an algorithm that is well known by the skilled person.

In another embodiment, the term "gasdermin D" also designates any polypeptide encoded by a gasdermin D gene. In a preferred embodiment, said gasdermin D gene is chosen in the group consisting of: SEQ ID NO:41, SEQ ID NO:42, or any homologous gene of another animal species, said homologous gene sharing preferably at least 50%, more preferably at least 60%, more preferably at least 70%, more preferably at least 80%, and even more preferably at least 90% identity with SEQ ID NO:41 or SEQ ID NO:42.

In another embodiment, the term "gasdermin D" also designates any fragment of human gasdermin D or mouse gasdermin D or any fragment of a polypeptide having a homologous sequence as defined above, wherein said fragment retains at least one biological function of human gasdermin D or mouse gasdermin D that is of interest in the present context. This fragment shares preferably at least 30%, preferably at least 40%, more preferably at least 50%, more preferably at least 60%, and even more preferably at least 70% identity with SEQ ID NO:39 or SEQ ID NO:40.

DFNA5 is a protein which belongs to the gasdermin family. In human, it has the sequence SEQ ID NO:43 (NCBI Reference Sequence: NP_004394.1). In mouse, non-syndromic hearing

impairment protein homolog has the sequence SEQ ID NO:44 (NCBI Reference Sequence: NP_061239.1). It is known to be expressed in placenta, brain, heart, kidney, lung, liver, skin, eye, and cochlea. The role of the protein is not yet known. However, the N-terminal of DFNA5 has been showed to induce apoptosis in transfected human cell lines (Op de Beeck et al., 2011). In addition, it has been shown that endogenous DFNA5 is epigenetically silenced by hypermethylation in several forms of cancer and it is considered as a tumour suppressor gene (Akino et al., 2007; Kim et al, 2008a,b; Wang et al., 2013). Several impairing mutations have been described. These mutations are located in either intron 7 or intron 8 of DFNA5 and resulted in skipping of exon 8 and premature termination of the encoded protein (Van Laer et al., 1998; Yu et al., 2003; Bischoff et al., 2004; Cheng et al., 2007; Park et al., 2010; Chai et al., 2014; Nishio et al., 2014; Li-Yang et al., 2015).

Human DFNA5 is encoded by the *DFNA5 transcript variant 1 (mRNA)* of SEQ ID NO:45 in human (NCBI Reference Sequence: NM_004403.2). The mouse *DFNA5* gene is of SEQ ID NO:46 (NCBI Reference Sequence: NM_018769.3).

In the context of the invention, the term "DFNA5" herein designates a polypeptide having the amino acid sequence SEQ ID NO:43 (human DFNA5) or SEQ ID NO:44 (mouse DFNA5) or an homologous sequence thereof. Said latter **homologous sequence** is for example the DFNA5 protein of another animal species, the polypeptide having said DFNA5 homologous sequence retains at least one biological function of human DFNA5 or mouse DFNA5 that is of interest in the present context. This homologous sequence shares preferably at least 50%, preferably at least 60%, more preferably at least 70%, more preferably at least 80%, and even more preferably at least 90% identity with SEQ ID NO:43 or SEQ ID NO:44.

Preferably, the identity percentage between said homologous sequence and SEQ ID NO:43 or SEQ ID NO:44 is identified by a global alignment of the sequences in their entirety, this alignment being performed by means of an algorithm that is well known by the skilled person.

In another embodiment, the term "DFNA5" also designates any polypeptide encoded by a *DFNA5* gene. In a preferred embodiment, said *DFNA5* gene is chosen in the group consisting of: SEQ ID NO:45, SEQ ID NO:46, or any homologous gene of another animal species, said homologous gene sharing preferably at least 50%, more preferably at least 60%, more preferably at least 70%, more preferably at least 80%, and even more preferably at least 90% identity with SEQ ID NO:45 or SEQ ID NO:46.

In another embodiment, the term "DFNA5" also designates any fragment of human DFNA5 or mouse DFNA5 or any fragment of a polypeptide having a homologous sequence as defined above, wherein said fragment retains at least one biological function of human DFNA5 or mouse DFNA5 that is of interest in the present context. This fragment shares preferably at least 30%, preferably at least 40%, more preferably at least 50%, more preferably at least 60%, and even more preferably at least 70% identity with SEQ ID NO:43 or SEQ ID NO:44.

Besides (alternatively or additionally, depending on the embodiment under consideration) gasdermins, one can use other antioxidants compounds such as those described below.

Cyclophilin A is involved in the reduction of hydrogen peroxide (H_2O_2) into H_2O, indirectly *via* the activation of several peroxiredoxins (Lee et al., 2001; Evans and Halliwell, 1999).

c-dopachrome tautomerase decreases cell sensitivity to oxidative stress by increasing reduced glutathione (GSH) level, the major small antioxidant molecule of the cell (Michard et al., 2008a; 2008b).

Although Mpv17 has a yet unknown activity, Mpv17-defect in both human and mouse results in a hepatocerebral mitochondrial DNA depletion syndrome with profound deafness (Binder et al., 1999) reported in the mutant mice and reactive oxygen species (ROS) accumulation (Meyer zum Gottesberge et al., 2001).

With the present results, it is the first time that a gasdermin, pejvakin, is pinpointed as a key element in NIHL affecting outer hair cells, inner hair cells and neurons of the auditory pathways. Its role is of high importance to prevent ROS induced cellular damages in auditory cells.

In the aspect of the present invention yet described above, it is related to the use of a gasdermin for modulating cellular redox homeostasis. Thus, the present invention concerns the use of a gasdermin as a redox modulator.

In a particular embodiment of this aspect, the present invention relates to the use of a gasdermin chosen among: gasdermin A, gasdermin B, gasdermin C, gasdermin D, DFNA5 and DFNB59 (or pejvakin) for modulating cellular redox homeostasis. Thus, the present invention concerns the use of a gasdermin chosen among: gasdermin A, gasdermin B, gasdermin C, gasdermin D, DFNA5 and DFNB59 (or pejvakin), as a redox modulator.

In a preferred embodiment, a gasdermin, in a particular embodiment: gasdermin A, gasdermin B, gasdermin C, gasdermin D, DFNA5 or DFNB59 (or pejvakin) and in a more particular embodiment: pejvakin, is therefore used to prevent and/or reduce ROS-induced cellular damages, especially in cochlear hair cells, afferent auditory neurons and neurons of the auditory brainstem and auditory central pathway, in a subject in need thereof. In a preferred embodiment, a gasdermin, in a particular embodiment: gasdermin A, gasdermin B, gasdermin C, gasdermin D, DFNA5 or DFNB59 (or pejvakin), and in a more particular embodiment: pejvakin, is used to prevent and/or reduce ROS-induced cellular damages in Inner Hair Cells (IHC), Outer Hair Cells (OHC), or neurons of the auditory pathway.

More generally, a gasdermin, in a particular embodiment: gasdermin A, gasdermin B, gasdermin C, gasdermin D, DFNA5 or DFNB59 (or pejvakin), and in a more particular embodiment: PJVK, is likely to be a key element in preventing and/or treating the noise-induced damages affecting auditory cells such as cochlear hair cells, afferent auditory neurons and neurons of the auditory brainstem and auditory central pathway, in a subject in need thereof.

Although noise exposure is known to induce oxidative stress as the result of cellular hyperactivity, which is normally associated with an antioxidant protective response, it is herein reported for the first time that even exposure to low energy sound induces an antioxidant protective response.

In a preferred embodiment, a gasdermin, in a particular embodiment: gasdermin A, gasdermin B, gasdermin C, gasdermin D, DFNA5 or DFNB59 (or pejvakin), and in a more particular embodiment: pejvakin, is thus used to prevent and/or reduce ROS-induced cellular damages due to noise exposure. These ROS-induced cellular damages are for example diagnosed in subjects suffering from noise-induced hearing loss (NIHL). NIHL encompasses all types of permanent hearing losses resulting from excessive exposure to intense sounds, which induces mechanical deleterious effects (e.g., to stereocilia bundles and to the plasma membrane of auditory hair cells) and metabolic disturbances (e.g., leading to a swelling of the synaptic regions of IHCs and auditory neurons, in relation to the excitotoxicity of the neurotransmitter, glutamate).

Presbycusis, which affects more than 30% people above 60 and overall, about 5 million people in France, is the result of a combination of factors, genetic and environmental (lifelong

exposure to noise and to chemicals). Yet it has been shown in the 1950s that subjects who spend their lives in silent environments do not suffer from any hearing loss even in their 80s. This, and a huge body of evidence collected in subjects occupationally exposed to noise, leads to conclude that noise-induced hearing loss (NIHL) is the dominant cause of hearing impairment in ageing subjects.

In a more preferred embodiment, a gasdermin, in a particular embodiment: gasdermin A, gasdermin B, gasdermin C, gasdermin D, DFNA5 or DFNB59 (or pejvakin) and in a more particular embodiment: pejvakin, is used to prevent and/or treat **presbycusis** or age-related hearing impairment.

ROS-induced damages may also be due to an acoustic trauma, which may occur after a single, short exposure to extremely loud noise (>120 dB SPL). As a matter of fact, it is thought that, after such an acoustic trauma, subjects experience protracted worsening of their hearing lesions in relation to disrupted ROS metabolism and its consequences on cellular homeostasis, even when these subjects have a normal antioxidant equipment. Likely, their antioxidant defences can be easily overwhelmed by the after-effects of the acoustic trauma. A gasdermin, and in particular pejvakin could improve the way that these patients heal and recover hearing after a damaging exposure. Thus, in a more preferred embodiment, a gasdermin: gasdermin A, gasdermin B, gasdermin C, gasdermin D, DFNA5 or DFNB59 (or pejvakin) and, and in particular pejvakin, is used to prevent and/or treat sensorineural hearing losses due to an **acoustic trauma**.

In normal subjects exposed to loud sound, even below the legal limit, and who might suffer damage to their auditory structures (e.g., the so-called hidden hearing impairment reported by Kujawa and Liberman (2009), with loss of a specific population of auditory neurons which leads to poor understanding in noise and to hyperacusis and tinnitus despite the lack of elevation in hearing thresholds, shows that this situation is conceivable and possibly widespread), controlled intake of pejvakin should increase the level of protection of the auditory system and protect against 'hidden' forms of neuropathic presbycusis.

In a more preferred embodiment, a gasdermin, in a particular embodiment gasdermin A, gasdermin B, gasdermin C, gasdermin D, DFNA5 or DFNB59 (or pejvakin) and in a more particular embodiment: pejvakin, is therefore used to prevent and/or treat hearing impairment including, e.g., hearing loss and auditory threshold shift.

In addition to direct effects of noise exposure, other factors also involve ROS metabolism and increased oxidative stress, notably chemical substances known for their **ototoxicity**. A targeted application of a gasdermin, and in particular pejvakin, should be able to alleviate these side-effects, even when the initial insult that triggers ROS production is not mechanical, but chemical.

In a preferred embodiment, the present invention therefore targets a gasdermin, in a particular embodiment gasdermin A, gasdermin B, gasdermin C, gasdermin D, DFNA5 or DFNB59 (or pejvakin), and in a more particular embodiment PJVK, for use for preventing and/or treating auditory damages induced by exposure to **ototoxic substances**. Said ototoxic substances can be medication or chemical substances on which a subject has been unfortunately or voluntarily exposed.

There are more than 200 known ototoxic medications (prescription and over-the-counter) on the market today. These include medicines used to treat serious infections, cancer, and heart disease. Ototoxic medications known to cause permanent damage include certain aminoglycoside antibiotics, such as gentamicin, and cancer chemotherapy drugs, such as cisplatin and carboplatin.

Other medications may reversibly affect hearing. This includes some diuretics, aspirin and NSAIDs, and macrolide antibiotics. On October 18, 2007, the U.S. Food and Drug Administration (FDA) announced that a warning about possible sudden hearing impairment would be added to drug labels of PDE5 inhibitors, which are used for erectile dysfunction.

In addition to medications, hearing impairment including hearing loss and auditory threshold shift may result from specific drugs, metals (such as lead, mercury, trimethyltin), solvents (such as toluene, for example found in crude oil, gasoline and automobile exhaust, styrene, xylene, n-hexane, ethyl benzene, white spirit, carbon disulfide, perchloroethylene, trichloroethylene, or p-xylene), pesticides / herbicides (organophosphates) and asphyxiating agents (carbon monoxide, hydrogen cyanide).

To conclude, a gasdermin, in a particular embodiment: gasdermin A, gasdermin B, gasdermin C, gasdermin D, DFNA5 or DFNB59 (or pejvakin) and in a more particular embodiment: PJVK may be used to prevent and/or treat acquired sensorineural hearing impairments that involve ROS metabolism and increased oxidative stress. These disorders may be due to direct effect of

noise exposure (e.g. intense acoustic trauma, presbycusis) or to chemical substances that are known for their ototoxicity.

In a preferred embodiment, a gasdermin, in a particular embodiment: gasdermin A, gasdermin B, gasdermin C, gasdermin D, DFNA5 or DFNB59 (or pejvakin) and in a more particular embodiment: PJVK is thus used to prevent and/or treat presbycusis, noise-induced hearing loss or sudden sensorineural hearing impairment or auditory damages induced by acoustic trauma or ototoxic substances, in a subject in need thereof.

As used herein, the term “hearing impairment” refers to a hearing defect that can either be congenital or not.

As used herein, the term “hearing loss” refers to a hearing defect that develops in previously normal hearing individual. It can appear at any age.

As used herein the term "**auditory threshold shift**" is intended to mean any reduction in a subject's ability to detect sound. Auditory threshold shift is defined as a 10 decibel (dB) standard threshold shift or greater in hearing sensitivity for two of 6 frequencies ranging from 0.5-6.0 (0.5, 1 , 2, 3, 4, and 6) kHz (cited in Dobie, R.A. (2005)). Auditory threshold shift can also be only high frequency, and in this case would be defined as 5 dB auditory threshold shift at two adjacent high frequencies (2-6 kHz), or 10dB at any frequency above 2kHz.

As used herein, the term "**treating**" is intended to mean the administration of a therapeutically effective amount of one of the antioxidant compound of the invention to a subject who is suffering from a disease, e.g., a loss or impairment of hearing, in order to minimize, reduce, or completely impair the symptoms of same, e.g., the loss of hearing. “Treatment” is also intended to designate the complete restoration of hearing function regardless of the cellular mechanisms involved.

In the context of the present invention, the term "**preventing**" a disease, e.g., presbycusis, herein designates impairing or delaying the development of the symptoms of said disease, e.g., delaying the impairment of hearing sensitivity within the aforesaid frequency range, particularly at the high frequency range above 3-4 kHz.

Some **congenital hearing impairments** are known to affect ROS homeostasis in the auditory system. These disorders are for example the Usher syndrome (USH), Alport syndrome (AS), Alstrom syndrome (ALMS), Bardet-Biedl syndrome (BBS), Cockayne syndrome (CS),

spondyloepiphyseal dysplasia congenital (SED), Flynn-Aird syndrome, Hurler syndrome (MPS-1), Kearns-Sayre syndrome (CPEO), Norrie syndrome, and Albers-Schonberg disease (ADO II). Thus, in another embodiment a gasdermin: gasdermin A, gasdermin B, gasdermin C, gasdermin D, DFNA5 or DFNB59 (or pejvakin) and in a more particular embodiment: pejvakin may be used for restoring the auditory capacities in subjects suffering from these congenital hearing impairments.

As explained in the experimental part below, localization of pejvakin to peroxisomes, organelles that are major effectors in the response to oxidative stress, ultrastructural anomalies of this organelle in *Pjvk*$^{-/-}$ mice and transfection experiments suggested a role of pejvakin in stress-induced peroxisome proliferation. More generally, administration of a gasdermin: gasdermin A, gasdermin B, gasdermin C, gasdermin D, DFNA5 or DFNB59 (or pejvakin) and in a more particular embodiment: pejvakin, would help treating peroxisomal disorders.

In another embodiment, the present invention therefore relates to a gasdermin, in a particular embodiment: gasdermin A, gasdermin B, gasdermin C, gasdermin D, DFNA5 or DFNB59 (or pejvakin) and in a more particular embodiment: pejvakin, for use as antioxidant for treating subjects suffering from peroxisomal disorders or mitochondrial disorders leading to ROS production.

Said peroxisomal disorders are preferably chosen in the group consisting of: the Zellweger syndrome (ZS), the infantile Refsum disease (IRD), neonatal adrenoleukodystrophy (NALD) and the rhizomelic chondrodysplasia punctata type 1 (RCDP1). More precisely, pejvakin would improve the hearing capacity of subjects suffering from said peroxisomal disorders.

In a preferred embodiment, a gasdermin, in a particular embodiment: gasdermin A, gasdermin B, gasdermin C, gasdermin D, DFNA5 or DFNB59 (or pejvakin) and in a more particular embodiment: pejvakin, is used for restoring peroxisome and/or mitochondria-mediated homeostasis in auditory cells from said subjects.

Sensorineural hearing disorders were already reported as part of the picture of extremely severe diseases, which belong to the spectrum of Zellweger disease and occur when the biogenesis of peroxisomes is defective. In these cases, metabolism is impaired in many organs. The patients die in early childhood, except when they are affected by milder forms of this spectrum of diseases, notably those with late onset (e.g., in relation to *PEX6* mutations, Tran et

al., 2014). Presence of hearing impairment has been reported in most of these patients, and usually ascribed to abnormal neural conduction in relation to adrenoleukodystrophy-like dysfunctions.

In a particular embodiment, a gasdermin, in a particular embodiment: gasdermin A, gasdermin B, gasdermin C, gasdermin D, DFNA5 or DFNB59 (or pejvakin) and in a more particular embodiment pejvakin, is used as antioxidant for improving the hearing in subjects suffering from the **Zellweger disease** or from other peroxisomal disorders that come with hearing impairment.

Other severe conditions are thought to involve failure of ROS metabolism, which might be improved by the use of a gasdermin, in a particular embodiment: gasdermin A, gasdermin B, gasdermin C, gasdermin D, DFNA5 or DFNB59 (or pejvakin) and in a more particular embodiment: pejvakin, as it is able to activate important protective pathways much more specifically and powerfully than existing drugs. For example, it may be possible to use a gasdermin, and in particular pejvakin, to treat other neurodegenerative disorders involving peroxisomal defects, such as Parkinson's disease (PD), Alzheimer's disease (AD), Familial Amyotrophic Lateral Sclerosis (FALS), as well as other age-related disorders including age-related macular degeneration (ARMD), type 2 diabetes, atherosclerosis, arthritis, cataracts, osteoporosis, hypertension, skin aging, skin pigmentation, and cardiovascular diseases.

As previously mentioned, pejvakin belongs to gasdermins, whose actual functions remain unknown. Nonetheless, some gasdermins have been incriminated in oesophageal and gastric cancers, hepatocarcinomas and breast carcinomas. It is acknowledged that the redox status of cancer cells usually differs from that of normal cells, and that the regulation of oxidative stress and of the metabolism of ROS is a key element of tumour growth and of responses to anticancer therapies. The potent role of pejvakin in the protection of auditory structures against effects of oxidative stress suggests that this molecule could influence or modulate cancer development.

In a preferred embodiment, a gasdermin, in a particular embodiment: gasdermin A, gasdermin B, gasdermin C, gasdermin D, DFNA5 or DFNB59 (or pejvakin) and in a more particular embodiment: pejvakin, is thus used for treating subjects suffering from cancer, inflammatory diseases and ischemia-reperfusion injury.

Typically, said cancer is chosen in the group consisting of: breast cancer, head and neck cancer, lung cancer, ovarian cancer, pancreatic cancer, colorectal carcinoma, breast carcinoma, hepatocarcinoma, cervical cancer, sarcomas, brain tumours, renal cancer, prostate cancer, melanoma and skin cancers, oesophageal or gastric cancer, multiple myeloma, leukaemia or lymphoma.

In a preferred embodiment, said cancer is an oesophageal or a gastric cancer, a hepatocarcinoma or a breast carcinoma.

In another embodiment, gasdermin is used as a modulator of cellular redox homeostasis for preventing and/or reversing skin aging and/or skin pigmentation. Preferably, said gasdermin is pejvakin. Said gasdermin may be used in a subject normally expressing gasdermin.

Here, said gasdermin can be either therapeutically applied to treat and/or prevent pathological disorders, states, diseases, conditions, or cosmetically applied to attenuate, alleviate, slow down, remedy, reduce, overcome, reverse, delay, limit, and/or prevent aesthetic skin troubles due to normal aging.

In one embodiment, gasdermin is cosmetically used for preventing, delaying, attenuating, overcoming, reducing, slowing down, limiting, alleviating, and/or reversing skin aging and skin pigmentation. Said gasdermin may be used in a subject normally expressing gasdermin.

More generally, it would be possible to use a gasdermin, in a particular embodiment: gasdermin A, gasdermin B, gasdermin C, gasdermin D, DFNA5 or DFNB59 (or pejvakin) and in a more particular embodiment pejvakin, to treat all the diseases due to the failure of ROS metabolism, especially those that are age-related such as Parkinson's disease (PD), Alzheimer's disease (AD), Familial Amyotrophic Lateral Sclerosis (FALS), age-related macular degeneration (ARMD), type 2 diabetes, atherosclerosis, arthritis, cataracts, osteoporosis, hypertension, skin aging, skin pigmentation, and cardiovascular diseases.

As used herein, the term "**subjects**" is intended to mean humans or non-human mammals such as primates, cats, dogs, swine, cattle, sheep, goats, horses, rabbits, rats, mice and the like. In a preferred embodiment, said subjects are human subjects.

In another preferred embodiment, said subjects do not suffer from a hereditary hearing impairment.

In a more preferred embodiment, said subjects have a normal expression of endogenous gasdermin, in a particular embodiment: gasdermin A, gasdermin B, gasdermin C, gasdermin D, DFNA5 or DFNB59 (or pejvakin) and in a more particular embodiment: pejvakin.

By "**normal expression of gasdermin**" it is herein meant that gasdermin, and in particular the *GSDMA*, *GSDMB*, *GSDMC*, *GSDMD*, *DFNA5* and *DFNB59* genes are normally expressed in the treated subject (i.e., neither the GSDMA, GSDMB, GSDMC, GSDMD, DFNA5 and/or *DFNB59* genes nor their transcription are altered as compared with healthy subjects), and that the endogenously encoded gasdermin polypeptides are normally expressed (i.e., they are functional and expressed at a normal level as compared with healthy subjects). As a matter of fact, the use of a gasdermin for restoring the auditory capacity of subjects having an altered expression level of a gasdermin is not encompassed within the scope of the present invention.

Expression of gasdermin, and in particular of pejvakin, in a subject may be assessed by any conventional means, such as RT-PCR or ELISA on a blood sample, *in situ* hybridization (ISH) and/or immunohistochemistry (IHC) on a tissue biopsy when available, or by clinical imaging.

In all of these applications, it is possible to combine the gasdermin, in a particular embodiment: gasdermin A, gasdermin B, gasdermin C, gasdermin D, DFNA5 or DFNB59 (or pejvakin) and in a more particular embodiment: PJVK treatment with another antioxidant treatment or with a RS inhibiting compound as defined below.

In vivo administration of gasdermin, and in particular pejvakin: vectors

The gasdermin, in a particular embodiment: gasdermin A, gasdermin B, gasdermin C, gasdermin D, DFNA5 or DFNB59 (or pejvakin) and in a more particular embodiment: pejvakin, polypeptide can be administered directly to the subject. In this case, the gasdermin, in a particular embodiment: gasdermin A, gasdermin B, gasdermin C, gasdermin D, DFNA5 or DFNB59 (or pejvakin) and in a more particular embodiment: pejvakin polypeptide is advantageously included in a pharmaceutical composition as disclosed below.

In a preferred embodiment, the gasdermin, in a particular embodiment: gasdermin A, gasdermin B, gasdermin C, gasdermin D, DFNA5 or DFNB59 (or pejvakin) and in a more particular embodiment: pejvakin polypeptide is produced *in situ* in the appropriate auditory cells by *in vivo* gene therapy.

Two alternative strategies for gene therapy can be contemplated for treating animal subjects. One strategy is to administer a vector encoding the gene of interest directly to the subject. The second is to use cells that have been i) removed from the target subject and ii) treated *ex vivo* with a vector expressing the gene of interest; these cells are then re-administered to the same subject.

Different methods for gene therapy are known in the art. These methods include, yet are not limited to, the use of DNA plasmid vectors as well as DNA and RNA viral vectors. In the present invention, such vectors may be used to express the pejvakin coding gene, *DFNB59,* in cells of the auditory pathway such as cochlear hair cells, afferent auditory neurons and neurons of the auditory brainstem pathway.

In another aspect, the present invention therefore relates to a vector encoding a gasdermin, in a particular embodiment: gasdermin A, gasdermin B, gasdermin C, gasdermin D, DFNA5 or DFNB59 (or pejvakin) and in a more particular embodiment the Pejvakin polypeptide, for use to prevent and/or treat noise-induced damages to auditory cells or peroxisomal disorders or cancer or inflammatory diseases or ischemia-reperfusion injury.

Preferably, said noise-induced damages lead to an acoustic trauma, presbycusis, noise-induced hearing loss (NIHL).

This vector may also be used to prevent and/or treat auditory damages due to ototoxic substance exposure.

Preferably, said peroxisomal disorders are chosen in the group consisting of: Zellweger syndrome (ZS), the infantile refsum disease (IRD), neonatal adrenoleukodystrophy (NALD) and the rhizomelic chondrodysplasia punctata type 1 (RCDP1).

Preferably, said cancer is chosen in the group consisting of: an esophageal, a gastric cancer, a hepatocarcinoma and a breast carcinoma.

In a preferred embodiment, said vector is a viral vector that is able to transfect the cells of the auditory pathway such as cochlear hair cells, afferent auditory neurons and neurons of the auditory brainstem pathway. These vectors are well-known in the art. They are for example lentiviruses, adenoviruses and Adeno-associated viruses (AAV).

The AAV vectors display several advantages such as i) a long lasting expression of synthesized genes (Cooper et al, 2006), ii) a low risk for pathogenic reactions (because they are artificially manufactured and not ototoxic), iii) they trigger low immunogenic response, and iv) they do not integrate the human genome (Kaplitt et al., 1994). AAV is therefore preferred to transfer the pejvakin coding gene in order to efficiently protect the auditory pathway.

In a more preferred embodiment, said vector is therefore an AAV vector.

The AAV vectors targeted by the present invention are any adeno-associated virus known in the art including, but not limited to AAV1, AAV2, AAV3, AAV4, AAV5, AAV6, AAV7, AAV8, AAV9, and AAV10.

In a more preferred embodiment, the serotype of said vector is AAV8, AAV5, or AAV1.

In order to increase the efficacy of gene expression, and prevent the unintended spread of the virus, genetic modifications of AAV can be performed. These genetic modifications include the deletion of the E1 region, deletion of the E1 region along with deletion of either the E2 or E4 region, or deletion of the entire adenovirus genome except the cis-acting inverted terminal repeats and a packaging signal. Such vectors are advantageously encompassed by the present invention.

Moreover, genetically modified AAV having a mutated capsid protein may be used so as to direct the gene expression towards a particular tissue type, e.g., to auditory cells. In this aim, modified serotype-2 and -8 AAV vectors in which tyrosine residues in the viral envelope are substituted for alanine residues can be used. In the case of tyrosine mutant serotype-2, tyrosine 444 can be substituted with alanine (AAV2-Y444A). In the case of serotype 8, tyrosine 733 can be substituted with an alanine reside (AAV8-Y733A).

Specific AAV vectors that would be able to carry a gasdermin, in particular the pejvakin, coding gene to auditory cells and methods to administer same are for example disclosed in WO 2011/075838. In the context of the invention, it would be for example possible to use the mutated tyrosine AAVs disclosed in WO 2011/075838 to deliver the pejvakin coding gene in auditory cells. These mutated vectors avoid degradation by the proteasome, and their transduction efficiency is significantly increased. Mutated tyrosine residues on the outer surface of the capsid proteins include, for example, but are not limited to, mutations of Tyr252 to Phe272 (Y252F), Tyr272 to Phe272 (Y272F), Tyr444 to Phe444 (Y444F), Tyr500 to Phe500

(Y500F), Tyr700 to Phe700 (Y700F), Tyr704 to Phe704 (Y704F), Tyr730 to Phe730 (Y730F) and Tyr733 to Phe733 (Y733F). These modified vectors facilitate penetration of the vector across the round window membranes, which allow for non-invasive delivery of the vectors to the hair cells/spiral ganglion neurons of the cochlea. For example, by using AAV2-Y444A or AAV8-Y733A, it is possible to increase gene transfer by up to 10,000 fold, decreasing the amount of AAV necessary to infect the sensory hair cells of the cochlea.

The skilled person would easily determine if it is required, prior to the administration of the vector of the invention, to enhance the permeability of the round window membrane as proposed in WO 2011/075838, depending on the target cell.

For instance, an appropriate vector in the context of the invention is an AAV8 vector. More particularly, it can be a vector having the nucleotide sequence of an AAV2 genome that is modified so as to encode AAV8 capsid proteins.

Another aspect of the present invention relates to a vector encoding pejvakin short hairpin RNA (shRNA), for use for treating cancer, inflammatory diseases or ischemia-reperfusion injury.

Use for treating congenital hearing impairment due to altered DFNB59 gene expression or deficiency

The present inventors studied for the first time the effect of antioxidants on the auditory function of *Pjvk*$^{-/-}$ mice.

A further aspect of the present invention concerns a *Pjvk*$^{-/-}$ mouse model, as described in detail in the Examples below.

N-acetyl L cysteine (NaC), and taurine, two antioxidant compounds, were administered to these mice. Their results show that these molecules have a protective effect on IHCs. Although the dose at which the molecules were administered was difficult to control, as mouse pups received the treatment via the milk delivered by their orally treated mother, in N-acetyl cysteine treated mice, the number of auditory neurons that responded to sound stimulation in synchrony was restored. Conversely, sound amplification by the cochlea and some aspects of neuronal conduction remained defective, unaffected by the treatment.

In another aspect, the present invention therefore relates to:

- either a RS inhibiting compound and an antioxidant compound, such as N-acetyl cysteine or taurine or glutathione or a gasdermin, in a particular embodiment: gasdermin A or gasdermin B or gasdermin C or gasdermin D or DFNA5 or pejvakin or cyclophilin A or c-dopachrome tautomerase or Mpv17, or
- a RS inhibiting compound (such as N-acetyl cysteine or taurine or glutathione) or an antioxidant compound (with the exception of a gasdermin, and in particular with the exception of gasdermin A, gasdermin B, gasdermin C, gasdermin D, DFNA5, pejvakin) such as cyclophilin A or c-dopachrome tautomerase or Mpv17,

for use (alone or in combination with one or more other active compounds) to treat subjects suffering from congenital hearing impairment due to altered *DFNB59* gene expression or deficiency.

"Congenital hearing impairment due to altered *DFNB59* gene expression or deficiency" herein designates the so-called "DFNB59 patients" described in the art. These patients exhibit an endogenous PJVK that is either truncated or mutated, and consequently not functional. These mutations are for example p.T54I, p.R183W, p.C343S, p.K41S*fs*X18, p.R167X and p.V330L*fs*X7 (Collin et al., 2007; Ebermann et al., 2007; Hashemzadeh Chaleshtori et al., 2007; Schwander et al., 2007; Borck et al., 2012; Mujtaba et al., 2012; Zhang et al., 2015).

A "RS inhibiting compound" herein designates any compound that is able to degrade/scavenge a Reactive Species such as ROS (Reactive Oxygen Species) or RNS (Reactive Nitrogen Species), namely superoxide, H_2O_2, hydroperoxide, lipid peroxide, lipoxygenase products, superoxide anion, hydroxyl- or alkoxyl-radicals. It is for example an enzyme (such as superoxide dismutase (SOD), catalase (CAT), Glutathione peroxidase (GPx), Glutathione reductase (GR)), or a metabolic compound (such as uric acid, creatine, cysteine, N-acetyl-cysteine, glutathione, 2-oxo-thiazolidine-4-carbixylate, and other thiol-delivering compounds, N-butyl-phenylnitrone, carnitine, lipoic acid, ubiquinone, or CoQ10) or a nutritional compound (such as Vitamin E, Vitamin C, selenium-containing compound ebselen, selenomethionine, and selenocysteine, polyphenols, flavonoids or a carotenoïd). This definition applies to all aspects and embodiments of the invention.

Preferably, said RS inhibiting compound is neither gasdermin A, gasdermin B, gasdermin C, gasdermin D, DFNA5 or PJVK nor a vector encoding same.

More preferably, said RS inhibiting compound is chosen in the group consisting of: salicylate, N-acetyl cysteine, taurine, glutathione, and D-methionine.

In a preferred embodiment, said RS inhibiting compound is combined with an antioxidant compound of the invention. Said antioxidant compound is preferably, a gasdermin, and in particular gasdermin A, gasdermin B, gasdermin C, gasdermin D, DFNA5 or PJVK or a vector encoding same.

Other antioxidant compounds useful in the present invention are for example: cyclophilin A, glutathione peroxidase 2, c-dopachrome tautomerase, Mpv17, or any combination thereof.

In a particularly preferred embodiment, said antioxidant compound is a gasdermin, and in particular gasdermin A, gasdermin B, gasdermin C, gasdermin D, DFNA5 or PJVK, or a vector encoding same, which is combined with at least one other compound chosen in the group consisting of: cyclophilin A, glutathione peroxidase 2, c-dopachrome tautomerase, Mpv17, N-acetyl cysteine, or any combination thereof.

In another aspect, the present invention therefore targets a pharmaceutical composition comprising:

- either an antioxidant compound (according to the present invention, including a gasdermin, and in particular gasdermin A, gasdermin B, gasdermin C, gasdermin D, DFNA5 or pejvakin) and at least one RS inhibiting compound (as defined above), or
- an antioxidant compound according to the present invention (with the exception of a gasdermin, and in particular with the exception of gasdermin A, gasdermin B, gasdermin C, gasdermin D, DFNA5 and pejvakin), or at least one RS inhibiting compound (as defined above),

for use to treat subjects suffering from congenital hearing impairment due to altered *DFNB59* gene expression or deficiency.

Use for treating hearing impairments other than those due to altered DFNB59 gene expression or deficiency

Exposure to sound of high energy is known to induce oxidative stress as the result of cellular hyperactivity, which is associated with an antioxidant protective response. It is now shown that this also applies upon exposure to normally harmless sound energy.

A strong emphasis is now placed on the part played by ROS and oxidative stress as a possible common background to noise-induced damage to auditory sensory cells. For example it has been proposed that sound exposure results in an increased cytoplasmic concentration of Ca^{2+}, which may powerfully interact with mitochondrial metabolism and activate ROS production by mitochondria. When the amount of the produced ROS exceeds some limit, or when ROS homeostasis in the stimulated cells is inappropriate, pathophysiological responses may be triggered, which lead to increased cell damage and ultimately, cell death. Normally, the cells of the auditory system are thought to be abundantly equipped with molecules (e.g., melanin, glutathione) and pathways (e.g. superoxide dismutase) that keep their ROS metabolism under control. It is also widely thought that the abundance of these molecules in the cochlea bears some relationship with the metabolically demanding processes of hearing transduction.

In another aspect, the present invention therefore relates to an antioxidant compound for use to treat subjects suffering from hearing impairment, said hearing impairment being preferably due to noise (e.g., because of an acoustic trauma, presbycusis, or in case of hidden hearing impairment) or to ototoxic substances, with the exception of congenital hearing impairment due to altered DFNB59 gene expression or deficiency.

Said "**antioxidant compound**", as defined earlier, is capable of modulating the redox homeostasis of cells, preferably of auditory cells (for example by restoring the normal function of peroxisomes in auditory cells). In a preferred embodiment, it is not able to down-regulate Reactive Species (ROS or RNS) directly (e.g., by physical interaction leading to RS-degradation or scavenging).

In a preferred embodiment, said compound is any antioxidant compound capable of modulating the redox homeostasis of cells, including a gasdermin, and in particular gasdermin A, gasdermin B, gasdermin C, gasdermin D, DFNA5 or PJVK.

More preferably, said antioxidant compound is chosen in the group consisting of: gasdermins (and in particular among gasdermin A, gasdermin B, gasdermin C, gasdermin D, DFNA5, PJVK) cyclophilin A, glutathione peroxidase 2, c-dopachrome tautomerase, Mpv17 or combination thereof.

In another preferred embodiment, said subject has a normal expression of endogenous gasdermin A, gasdermin B, gasdermin C, gasdermin D, DFNA5 or pejvakin.

In a preferred embodiment, said antioxidant compound is combined with any of the RS inhibiting compound defined above. Said RS inhibiting compound is preferably chosen in the group consisting of: taurine, salicylate, N-acetyl cysteine, D-methionine and glutathione.

In another aspect, the present invention therefore targets a pharmaceutical composition comprising an antioxidant compound (according to the present invention) and optionally at least one RS inhibiting compound (as defined above), for use to treat subjects suffering from hearing impairment, such as a hearing loss preferably due to noise (e.g., because of an acoustic trauma, presbycusis, or in case of hidden hearing impairment) or to ototoxic substances, with the exception of congenital hearing impairment due to altered *DFNB59* gene expression or deficiency.

In a preferred embodiment, said pharmaceutical composition contains a gasdermin, in a particular embodiment said pharmaceutical composition comprises gasdermin A, gasdermin B, gasdermin C, gasdermin D, DFNA5 or PJVK, or a vector encoding same, as an antioxidant compound.

Pharmaceutical compositions

The antioxidant compounds (e.g., a gasdermin, in particular PJVK, or a vector encoding same, etc.) and/or RS inhibiting compounds of the invention are advantageously incorporated into pharmaceutical compositions suitable for an administration to a subject.

In another aspect, the present invention also relates to the use of the antioxidant compounds (e.g., gasdermin A, gasdermin B, gasdermin C, gasdermin D, DFNA5, PJVK or a vector encoding same, etc.) and/or RS inhibiting compounds of the invention for manufacturing

pharmaceutical compositions intended to prevent and / or treat subjects suffering from the above-cited disorders.

More particularly, the present invention relates to the use of gasdermin A, gasdermin B, gasdermin C, gasdermin D, DFNA5, pejvakin, or a vector encoding same for manufacturing pharmaceutical compositions intended to treat subjects suffering from hearing impairment, from a peroxisomal disorder or from cancer. In a preferred embodiment, said hearing loss is due to noise or to ototoxic substances, as disclosed above, but not of genetic reasons (congenital hearing impairment due to DFNB59 deficiency being notably excluded). In another preferred embodiment, said peroxisomal disorders are chosen in the group consisting of: Zellweger syndrome (ZS), the infantile refsum disease (IRD), neonatal adrenoleukodystrophy (NALD) and the rhizomelic chondrodysplasia punctata type 1 (RCDP1). In another preferred embodiment, said cancer is an oesophageal or a gastric cancer, a hepatocarcinoma or a breast carcinoma.

Moreover, the present invention relates to the use of RS inhibiting compounds - other than gasdermin A, gasdermin B, gasdermin C, gasdermin D, DFNA5 or PJVK - for manufacturing pharmaceutical compositions intended to treat subjects suffering from congenital hearing impairment due to altered *DFNB59* gene expression or deficiency.

The present invention also relates to pharmaceutical compositions comprising the antioxidant compounds and/or RS inhibiting compounds (chemical substances, polypeptides and/or vectors encoding same) described above, and a pharmaceutically acceptable carrier.

As used herein, "**pharmaceutically acceptable carrier**" includes any and all solvents, dispersion media, coatings, antibacterial and antifungal agents, isotonic and absorption delaying agents, and the like that are physiologically compatible. Examples of pharmaceutically acceptable carriers include one or more of water, saline, phosphate buffered saline, dextrose, glycerol, ethanol and the like, as well as combinations thereof. In many cases, it can be preferable to include isotonic agents, for example, sugars, polyalcohols such as mannitol, sorbitol, or sodium chloride in the composition. Pharmaceutically acceptable carriers can further comprise minor amounts of auxiliary substances such as wetting or emulsifying agents, preservatives or buffers, which enhance the shelf life or effectiveness of the antioxidant compounds or of the pharmaceutical compositions containing same.

The pharmaceutical compositions of the invention may be in a variety of forms. These include, for example, liquid, semi-solid and solid dosage forms, such as liquid solutions (e.g., injectable and infusible solutions), dispersions or suspensions, tablets, pills, powders, liposomes and suppositories. The form used depends on the intended mode of administration and therapeutic application. Typical compositions are in the form of injectable or infusible solutions, such as compositions similar to those used for passive immunization of humans.

In the context of the invention, the typical mode of administration of the composition of the invention is intratympanic (in the middle ear), intracochlear, or parenteral (e.g., intravenous, subcutaneous, intraperitoneal, intramuscular, intrathecal). In one example, the pharmaceutical composition of the invention is administered by intravenous infusion or injection. In another example, the pharmaceutical composition of the invention is administered by intramuscular or subcutaneous injection. In another example, the composition of the invention is administered perorally. In yet another example, the pharmaceutical composition of the invention is delivered to a specific location using stereostatic delivery, particularly through the tympanic membrane or mastoid into the middle ear.

Pharmaceutical compositions typically must be sterile and stable under the conditions of manufacture and storage. The pharmaceutical composition of the invention is preferably formulated as a solution, microemulsion, dispersion, liposome, or other ordered structure suitable to high drug concentration. Sterile injectable solutions can be prepared by incorporating the antioxidant compounds and/or RS inhibiting compounds of the invention in the required amount in an appropriate solvent optionally with one or a combination of ingredients enumerated above, as required, followed by filtered sterilization. Generally, dispersions are prepared by incorporating the antioxidant compounds and/or RS inhibiting compounds of the invention into a sterile vehicle that contains a basic dispersion medium and optionally other ingredients from those enumerated above, as required. In the case of sterile lyophilized powders for the preparation of sterile injectable solutions, the preferred methods of preparation are vacuum drying and spray-drying that yields a powder of the active ingredient plus any additional desired ingredient from a previously sterile-filtered solution thereof. The proper fluidity of a solution can be maintained, for example, by the use of a coating such as lecithin, by the maintenance of the required particle size in the case of dispersion and by the use of surfactants. Prolonged absorption of injectable compositions can

be achieved by including an agent in the composition that delays absorption, for example, monostearate salts and gelatine.

The pharmaceutical composition of the invention can be administered by a variety of methods known in the art. As will be appreciated by the skilled artisan, the route and/or mode of administration will vary depending upon the desired results. In certain embodiments, the antioxidant compounds and/or RS inhibiting compounds of the invention may be prepared with a carrier that will protect same against rapid release, such as a controlled release formulation, including implants, transdermal patches, and microencapsulated delivery systems. Biodegradable, biocompatible polymers can be used, such as ethylene vinyl acetate, polyanhydrides, polyglycolic acid, collagen, polyorthoesters, and polylactic acid. Many methods for the preparation of such formulations are generally known to those skilled in the art.

The pharmaceutical compositions of the invention include a "**therapeutically effective amount**" or a "**prophylactically effective amount**" of the antioxidant compounds and/or RS inhibiting compounds of the invention. A "therapeutically effective amount" refers to the amount of the antioxidant compounds and/or RS inhibiting compounds of the invention that is effective, at dosages and for periods of time necessary, to achieve the desired therapeutic result, in this case for both prophylaxis and treatment of hearing impairment or peroxisomal disorders or cancer without unacceptable toxicity or undesirable side effects.

A therapeutically effective amount of the antioxidant compounds and/or RS inhibiting compounds of the invention can vary according to factors such as the disease state, age, sex, and weight of the subject, and the ability of said compound to elicit a desired response in same. A therapeutically effective amount can also be one in which any toxic or detrimental effects of the claimed compounds are outweighed by the therapeutically beneficial effects. A "prophylactically effective amount" refers to an amount of the antioxidant compounds and/or RS inhibiting compounds of the invention that is effective, at dosages and for periods of time necessary, to achieve the desired prophylactic result. Typically, since a prophylactic dose can be used in subjects prior to or at an earlier stage of disease, the prophylactically effective amount is usually less than the therapeutically effective amount.

Dosage regimens can be adjusted to provide the optimum desired response (e.g., a therapeutic or prophylactic response). For example, a single bolus can be administered, several

divided doses can be administered over time or the dose can be proportionally reduced or increased as indicated by the exigencies of the therapeutic situation. It can be especially advantageous to formulate parenteral compositions in dosage unit form for ease of administration and uniformity of dosage. Dosage unit form as used herein refers to physically discrete units suited as unitary dosages for the mammalian subjects to be treated; each unit containing a predetermined quantity of the antioxidant compound and/or RS inhibiting compounds of the invention calculated to produce the desired therapeutic effect in association with the required pharmaceutical carrier. The specification for the dosage unit forms can be dictated by and directly dependent on (a) the unique characteristics of the antioxidant compound and/or RS inhibiting compounds and the particular therapeutic or prophylactic effect to be achieved, and (b) the limitations inherent in the art of formulating such antioxidant compound and/or RS inhibiting compounds for treating or preventing hearing impairment or peroxisomal disorders in a subject.

Method to diagnose and treat a hypervulnerability to sound

Acoustic energy is the main factor that determines the damaging effects of exposure to loud sounds. To evaluate chronic exposure to sound, one uses the LEX index, the level of a stable sound which, presented over an eight-hour working shift, would deliver the same acoustic energy. This LEX calculates the energies delivered by sounds with different levels and time courses, and allows their detrimental potential to be compared. For occupational noise exposure, the LEX must not exceed a legally-fixed limit above which it is estimated that permanent hearing loss may occur if the exposure is a long-lasting one (e.g., an 8-h working shift, 5 days / week, 48 weeks / year, for 40 years). The legal limit for LEX in western countries varies from 80 to 90 dB (e.g., 80 dB in the European Community; 90 dB in the USA – OSHA-; A-weighted, i.e., measured through a filter which reproduces the frequency-dependence of human hearing sensitivity).

The present Inventors have discovered that mouse mutants in which pejvakin is defective or absent, and which, as a result, suffer from congenital sensorineural hearing impairment, are inordinately vulnerable to short exposure to loud sound, to the point that a single exposure to a LEX of 63 dB leads to about 30 dB hearing threshold elevation which persists more than a week. In comparison, a legally acceptable LEX of 80 dB for a whole life of work normally leads

to no hearing threshold elevation at all (and in the USA law, it is assumed that 90 dB is equally tolerable). As the dB scale is a logarithmic one, a two-fold increase in power translates into a 3-dB increase, and a ten-fold increase in power, in a 10-dB increase. Thus the LEX, which damages hearing in *Pjvk*$^{-/-}$ mice, is several orders of magnitude lower than the normally harmless dose of loud sound. This has never been reported before. Up until this observation, the lowest LEX reported in mutant animals and able to produce hearing loss, was 73 dB (10 times more energetic than our exposures). Furthermore, this loss was temporary, with recovery within the next few tens of hours; it had to reach 99 dB for the hearing loss to fail to recover rapidly (these mice were defective for an ATP receptor (Housley et al., 2013), as against 63 dB in *Pjvk*$^{-/-}$ mice. Another report showing that noise exposure may result in permanent neuronal damage in the absence of hearing threshold elevation used LEXs of 94 dB (1,000 times more energetic than our exposures).

The Inventors furthermore observed that DFNB59 patients, who carry deleterious mutations in the *Pjvk* gene, display the same astonishing sensitivity to loud sound exposure as *Pjvk*$^{-/-}$ mice. This was proved by recording their auditory-evoked potentials in response to impulse sounds. At a LEX = 57 dB, these sounds, routinely used for audiological diagnosis at much higher levels, induced in all tested patients large changes in their evoked responses, with an increase in latency of all identifiable waves, which often exceeded 0.5 ms for wave V, and a strong two- to three-fold decrease in intensity. Such changes were never observed in control subjects who could be exposed to at least four times as much acoustic energy without suffering any change in latency or amplitude of their auditory evoked potentials. These phenomena were therefore unique to DFNB59 patients, and, akin to auditory fatigue, were fortunately reversible after 10 min in silence.

In another aspect, the present invention relates to a method for diagnosing an acoustic hypervulnerability in a subject, comprising the steps of:

a) measuring the expression level of the pejvakin polypeptide in said subject, and/or

b) detecting the presence of inactivating mutations in the pejvakin polypeptide in said subject, and/or

c) clinically audiological testing for sensorineural hearing impairment, e.g., by recording the auditory brainstem response (ABR) and otoacoustic emissions (OAEs) in said subject.

As a matter of fact, if the expression level of the pejvakin polypeptide is decreased in said subject (as compared to healthy individuals) or if the pejvakin polypeptide is expressed in normal amounts but is biologically unfunctional in said subject, or if the auditory cells of said subject exhibit altered peroxisomes (as compared with those of healthy individuals), then said subject is likely to be highly susceptible to noise exposure.

As observed in DFNB59 patients, this may lead to irreversible deafness.

Preferably, steps a) and b) are performed on auditory cells of said subject, more precisely on cochlear hair cells, afferent auditory neurons and neurons of the auditory brainstem pathway. Alternatively, they may be performed on blood samples.

In the context of the invention, the "**expression level of the pejvakin polypeptide is decreased**" in a subject if the transcription and/or the translation of the endogenous *DFNB59* gene is impaired. Accordingly, the amount of the pejvakin transcript or of the pejvakin polypeptide is diminished as compared with the level of pejvakin transcript or of the pejvakin polypeptide expressed in healthy individuals. The skilled person well knows how to measure the amount of the pejvakin transcript or of the pejvakin polypeptide in a subject, e.g., in blood samples.

"**Biologically unfunctional**" pejvakin may be produced when the endogenous *DFNB59* gene contains nonsense mutations (leading to the generation of truncated pejvakin) or missense mutations. Some of them have already been disclosed (Collin et al., 2007; Ebermann et al., 2007; Hashemzadeh Chaleshtori et al., 2007; Schwander et al., 2007; Borck et al., 2012; Delmaghani et al., 2006; Mujtaba et al., 2012; Zhang et al., 2015). As shown in these articles, the skilled person well knows how to detect these mutations, e.g., in blood samples.

"Peroxisomal alteration" may be detected by any conventional technique. Examples thereof are disclosed in the experimental part below. Altered peroxisomes are observed for example when their size is significantly enlarged and/or when their density is significantly decreased as compared with control cells (that is, cells of the same category, but from healthy individuals).

Conventional intervention in case of sensorineural hearing impairment includes sound amplification by hearing aids and cochlear implant fitting, depending on the degree of impairment. However, conventional hearing aids, routinely used in severely hearing-impaired patients, might have harmful results in DFNB59 patients, as exposure to amplified sound is

expected to lead to long-lasting damage to cochlear sensory cells and auditory neurons. Cochlear implant, an acoustico-electronic device that bypasses the cochlea and delivers a direct electrical stimulation to the primary auditory neurons, which is particularly beneficial for patients affected by profound deafness of cochlear origin, should similarly increase ROS in these neurons, thereby threatening their long-term survival. In both cases, specific protection against the production or the effects of the ROS is anticipated to be mandatory.

The case of pejvakin deficits, which induce a non-life-threatening impairment, is the first in which several potentially damaging effects of sound amplification on sensory cells and neurons emerge, at levels of sound energy-induced activity of auditory cells that are several orders of magnitude lower than normal in the absence of pejvakin.

Hence, when a subject has been diagnosed to suffer from noise hypervulnerability according to the above mentioned method, it is important not to use sound amplification by hearing aids or by cochlear implant fitting, unless irreversible ROS-induced damages may be induced.

For these patients, alternative treatments should therefore be contemplated. These treatments include administration of RS inhibiting compounds and/or antioxidant compounds, wherein, depending on the considered treatment, said antioxidant compounds are or are not gasdermin (in particular gasdermin A, gasdermin B, gasdermin C, gasdermin D, DFNA5, DFNB59 (or pejvakin)).Such antioxidant compound can advantageously be selected from : cyclophilin A, c-dopachrome tautomerase and Mpv17.

In a related aspect, the present invention therefore relates to a method for treating subjects in need thereof, comprising the steps of performing the above-mentioned diagnostic method and, if said subject is diagnosed to suffer from noise hypervulnerability, administering to said subject an RS inhibiting compound.

In a preferred embodiment, the present invention relates to a method for treating subjects in need thereof, comprising the step of:

a) administering to said subjects a therapeutic amount of a RS inhibiting compound (such as taurine or N- acetyl-cysteine) and/or of an antioxidant compound (such as a gasdermin, and in particular: gasdermin A, gasdermin B, gasdermin C, gasdermin D, DFNA5, pejvakin, or cyclophilin A, c-dopachrome tautomerase or Mpv17).

In particular, when said subjects suffer from congenital hearing impairment due to altered *DFNB59* gene expression or deficiency, then step a) is for administering to said subjects a therapeutic amount of:

- either a RS inhibiting compound (such as taurine or N- acetyl-cysteine) and an antioxidant compound (such as a gasdermin, and in particular: gasdermin A, gasdermin B, gasdermin C, gasdermin D, DFNA5, pejvakin, cyclophilin A, c-dopachrome tautomerase or Mpv17); or
- a RS inhibiting compound (such as taurine or N- acetyl-cysteine) or an antioxidant compound (such as cyclophilin A, c-dopachrome tautomerase or Mpv17) with the exception of a gasdermin, and in particular with the exception of gasdermin A, gasdermin B, gasdermin C, gasdermin D, DFNA5 and pejvakin.

Yet in particular, when said subjects suffer from hearing impairments other than those due to altered *DFNB59* gene expression or deficiency, then step a) is for administering to said subjects a therapeutic amount of a RS inhibiting compound (such as taurine or N- acetyl-cysteine) and/or of an antioxidant compound (such as a gasdermin, and in particular: gasdermin A, gasdermin B, gasdermin C, gasdermin D, DFNA5, pejvakin, cyclophilin A, c-dopachrome tautomerase or Mpv17).

In another preferred embodiment, the present invention relates to a method for treating subjects in need thereof, comprising the steps of:

a) measuring the expression level of the pejvakin polypeptide in said subjects, and/or

b) detecting the presence of inactivating mutations in the pejvakin polypeptide in said subjects, and/or

c) clinically audiological testing for sensorineural hearing impairment, e.g., by recording the auditory brainstem response (ABR) and otoacoustic emissions (OAEs) in said subjects; and

d) administering to said subjects a therapeutic amount of a gasdermin, and in particular: gasdermin A, gasdermin B, gasdermin C, gasdermin D, DFNA5, pejvakin, optionally along with other antioxidant compound and/or RS inhibiting compounds, as defined above.

In particular, when said subjects suffer from congenital hearing impairment due to altered *DFNB59* gene expression or deficiency, then step d) is for administering to said subjects a therapeutic amount of:

- either a RS inhibiting compound (such as taurine or N- acetyl-cysteine) and an antioxidant compound (such as a gasdermin, and in particular: gasdermin A, gasdermin B, gasdermin C, gasdermin D, DFNA5, pejvakin, cyclophilin A, c-dopachrome tautomerase or Mpv17); or
- a RS inhibiting compound (such as taurine or N- acetyl-cysteine) or an antioxidant compound (such as cyclophilin A, c-dopachrome tautomerase or Mpv17) with the exception of a gasdermin, and in particular with the exception of gasdermin A, gasdermin B, gasdermin C, gasdermin D, DFNA5 and pejvakin.

Yet in particular, when said subjects suffer from hearing impairments other than those due to altered *DFNB59* gene expression or deficiency, then step d) is for administering to said subjects a therapeutic amount of a RS inhibiting compound (such as taurine or N- acetyl-cysteine) and/or of an antioxidant compound (such as a gasdermin, and in particular: gasdermin A, gasdermin B, gasdermin C, gasdermin D, DFNA5, pejvakin, cyclophilin A, c-dopachrome tautomerase or Mpv17).

As used herein, the term "**subjects**" is intended to designate humans and non-human mammals such as primates, cats, dogs, swine, cattle, sheep, goats, horses, rabbits, rats, mice and the like. In a preferred embodiment, said subjects are human subjects.

BRIEF DESCRIPTION OF THE DRAWINGS

Figure 1 describes the strategy for targeted replacement of the *Pjvk* wild-type allele with a floxed allele. (**A**) Schematic representation of the murine *Pjvk* gene and the targeting construct used to produce a floxed *Pjvk* allele ($Pjvk^{fl}$) with loxP sequences (triangles) flanking exon 2, followed by a *PGK-neo* cassette. *DTA*: diphtheria toxin A fragment. An additional *Sac*I site was engineered before the first loxP site for Southern blot analysis. Small arrows indicate the positions of PCR primers used to screen recombinant ES cell clones. Right panel: Southern blot analysis of *Sac*I-digested genomic DNA of wild-type (+/+) and $Pjvk^{fl/+}$ (fl/+) mice. Exon 2 of *Prkra* (a gene flanking *Pjvk* on the centromeric side) was used as the probe for Southern blot

analysis. The probe hybridizes to a 4.6 kb fragment from the floxed allele and to a 7.2 kb fragment from the wild-type allele. (**B**) RT-PCR analysis of the *Pjvk* transcript in inner ears of $Pjvk^{+/+}$ and $Pjvk^{-/-}$ P7 mice. $Pjvk^{-/-}$ mice were obtained by crossing $Pjvk^{fl/fl}$ mice with transgenic mice carrying the cre recombinase under the control of the ubiquitous *PGK* promoter. The expected 1059 bp amplicon is seen in the $Pjvk^{+/+}$ mouse (lane 1), while a 963 bp fragment is detected in the $Pjvk^{-/-}$ mouse (lane 2), because of the deletion of exon 2. M, DNA size marker: φX174 DNA *Hae*III digest.

Figure 2 describes the hearing loss variability and increased sensitivity to "controlled sound exposure" in $Pjvk^{-/-}$ mice. (**A**) ABR thresholds for 10 kHz pure tones in 1-month old $Pjvk^{-/-}$ and wild-type littermates. (**B**) DPOAE thresholds at $2f_1$- f_2 (in dB SPL) in $Pjvk^{-/-}$ and $Pjvk^{+/+}$ mice for identical levels of sound stimuli at f_1 (8 kHz) and f_2 (10 kHz). Stimulus level was kept below 80 SPL to avoid any contribution of instrumental distortion. In ears with no DPOAE even for 75 dB SPL stimulus levels, DPOAE thresholds were arbitrarily set at 80 dB SPL. (**C**) Natural acoustic environment effect on ABR thresholds for 10 kHz pure tones in P21 $Pjvk^{-/-}$ mice. ABR thresholds show a highly significant correlation with the number of pups (2 to 10) present in the cage (R^2 = 0.51; $p < 0.001$). (**D**) Effect of a 1-min exposure to 10-kHz, 105 dB SPL tone-bursts (2-ms plateau) separated by 60-ms silent intervals on the ABR threshold of $Pjvk^{-/-}$ mice. Re-measured just after sound exposure, ABR threshold increased to 21.7 ± 10.3 dB ($p < 0.001$) in $Pjvk^{-/-}$ mice whilst producing no effect in $Pjvk^{+/+}$ mice (2.2 ± 2.4 dB; $p = 0.3$, NS).

Figure 3 represents effects of a brief exposure to moderately intense stimuli on the auditory function in $Pjvk^{-/-}$ and $Pjvk^{fl/fl}$*Myo15*-$cre^{+/-}$ mice. (**A-C**) ABR wave I amplitude (**A**), DPOAE amplitude (**B**) and ABR interwave I-IV latency (**C**) in $Pjvk^{-/-}$ and $Pjvk^{fl/fl}$*Myo15*-$cre^{+/-}$ mice, before (left) and after (right) "controlled sound exposure", which reveals hypervulnerability to sound of IHCs, OHCs, and auditory pathway (the latter, only in $Pjvk^{-/-}$ mice, not in $Pjvk^{fl/fl}$*Myo15*-$cre^{+/-}$ mice with a pejvakin defect only in hair cells), respectively. (**D**) EEBR wave EIV amplitude before and after "controlled electrical exposure" in $Pjvk^{-/-}$ and $Pjvk^{fl/fl}$*Myo15*-$cre^{+/-}$ mice, showing that this amplitude is abnormal and hypervulnerable only when pejvakin is absent from auditory neurons. (**E** and **F**) Examples of ABRs before and after "controlled sound exposure" of $Pjvk^{-/-}$ and $Pjvk^{fl/fl}$*Myo15*-$cre^{+/-}$ mice; wave I is affected by exposure in both mice, and wave IV undergoes an additional latency increase only in $Pjvk^{-/-}$ mice. (**G-I**) Examples of EEBRs before and after "controlled electrical stimulation" in $Pjvk^{+/+}$, $Pjvk^{-/-}$ and $Pjvk^{fl/fl}$*Myo15*-$cre^{+/-}$ mice; EEBRs are affected by controlled electric exposure only in $Pjvk^{-/-}$ mice. (**J-L**) Effects

of neuronal function rescuing in *Pjvk*$^{-/-}$ mice by injection of AAV8-Pjvk, on ABR interwave I-IV latency (**J**), EEBR wave EIV amplitude before and after "controlled electrical stimulation" (**K**) and EEBR interwave EII-EIV latency (one example in L), showing that transfected ears tend to normalize and lose their hypersensitivity to "controlled electric exposure". n.s., not statistically significant; *** $p < 0.001$. Error bars indicate ± SEM.

Figure 4 shows progressive degeneration of the organ of Corti in *Pjvk*$^{-/-}$ mice (Figure 4A) and increased lipid peroxidation in the cochlea of *Pjvk*$^{-/-}$ mice (Figure 4B). (A) Upper panels: Scanning electron micrographs showing surface views of the organ of Corti in the *basal turn* of the *cochlea* from P60 *Pjvk*$^{+/+}$ and *Pjvk*$^{-/-}$ mice. In the *Pjvk*$^{-/-}$ mouse, many outer hair cells (OHCs), inner hair cells (IHCs), and pillar cells (PCs) are missing. Scale bars are 5 µm. Lower panels: Light micrographs of cross sections taken from the middle turn of the cochlea in *Pjvk*$^{+/+}$ and *Pjvk*$^{-/-}$ mice on P90. In the *Pjvk*$^{-/-}$ mouse, OHCs, IHCs, and supporting cells can't be identified anymore, and the organ of Corti has degenerated (arrow). In addition, the numbers of nerve fibres and cochlear ganglion neurons (arrowheads) are markedly decreased. Scale bars are 80 µm. **(B)** Cryosections of the organ of Corti (middle turn, upper panels) and of the cochlear ganglion (apical and basal turns, lower panels) from P60 *Pjvk*$^{+/+}$ and *Pjvk*$^{-/-}$ mice, immunolabelled for 4-HNE, a by-product of lipid peroxidation (green), and stained with DAPI (blue) to show cell nuclei. Asterisks indicate the nuclei of OHCs and IHCs. In the *Pjvk*$^{-/-}$ mouse, some OHCs and cochlear ganglion neurons are missing, but the OHCs present are highly immunoreactive for 4-HNE (arrows), as are the cochlear ganglion neurons, especially in the basal turn. Scale bars are 20 µm.

Figure 5 represents increased oxidative stress and ROS-induced cell damage in the *Pjvk*$^{-/-}$ cochlea. (**A**) Reduced-glutathione (GSH) (left bar chart), oxidized-glutathione (GSSG) (middle bar chart) contents, and GSH:GSSG ratio (right bar chart), in P21 *Pjvk*$^{-/-}$ versus *Pjvk*$^{+/+}$ cochlea. Error bars represent the SEM of 3 independent experiments. (**B**) Marked decrease in the BK α-subunit immunolabelling in *Pjvk*$^{-/-}$ IHCs. Left: P20 *Pjvk*$^{+/+}$ and *Pjvk*$^{-/-}$ IHCs. Scale bar is 5 µm. Right: quantitative analysis of BK channel clusters. Error bars represent the SD. * $p < 0.05$, *** $p < 0.001$.

Figure 6 shows that Pejvakin is a peroxisome-associated protein involved in the oxidative stress-induced peroxisomal proliferation. (**A, B**) Immunolabelling of PMP70 and endogenous pejvakin in a HepG2 cell (**A**) and in two P20 *Pjvk*$^{+/+}$ *IHCs* (**B**). (**C**) Number of peroxisomes in *Pjvk*$^{+/+}$ and *Pjvk*$^{-/-}$ mouse embryonic fibroblasts (MEFs) subjected to 0.5 mM H_2O_2, versus

untreated MEFs (n = 30 cells for each condition). (**D**) Untransfected HeLa cells (NT), and transfected cells producing either EGFP alone or EGFP together with the wild-type pejvakin (Pjvk) or a mutated Pjvk (p.T54I, p.R183W, p.C343S, or p.V330L*fs**7). Left panel: Bar chart showing the numbers of peroxisome per cell 48 hours after transfection. There were on average 33% more peroxisomes in cells producing both EGFP and Pjvk (n = 200) than in cells producing EGFP alone (n = 150). Right panel: for every range of enlarged peroxisome size, x (0.6-0.8 µm, 0.8-1.0 µm, and > 1.0 µm), in two perpendicular directions, the proportion of cells containing at least one peroxisome. (**E**) Abnormalities in shape and distribution of peroxisomes in mature *Pjvk*$^{-/-}$ OHCs detected by TEM (transmission electron microscopy; *P30 Pjvk*$^{-/-}$ (middle and right panels) and *Pjvk*$^{+/+}$ (left panel) OHCs). Insets (middle panel) show enlarged views of individual peroxisomes. In *Pjvk*$^{+/+}$ OHCs, peroxisomes are grouped just under the cuticular plate (CP) (arrowheads), with none detected in the perinuclear region (*n = 33 sections,* upper bar chart). In *Pjvk*$^{-/-}$ OHCs, some peroxisomes remain under the CP (arrowheads), but catalase-containing structures, misshapen peroxisomes (arrows), are detected in the perinuclear region (n = 24 sections, upper bar chart). Peroxisomes located under the CP are larger in *Pjvk*$^{-/-}$ *OHCs* (n = 92 peroxisomes) than in *Pjvk*$^{+/+}$ *OHCs (*n = 89 peroxisomes) (lower bar chart). N: cell nucleus. ** $p < 0.01$, *** $p < 0.001$. Error bars represent the SEM. Scale bars are 5 µm in (**A**) and (**B**), and 0.5 µm in (**E**).

Figure 7 shows that Pejvakin is associated with peroxisomes in transfected HeLa cells (A), the specificity of the antibody (B) and the immunostaining of dividing peroxisomes (C). (**A**) Transfected HeLa cells producing pejvakin (Pjvk-EGFP, upper panel) and untransfected cells (lower panel) were immunostained with both an anti-pejvakin antibody (Pjvk-G21) and an antibody against peroxisome membrane protein 70 (PMP70). Cell nuclei were stained with DAPI (dark grey). Colocalization of the immunostainings of pejvakin (light grey) and PMP70 (white) was observed in transfected cells (see inset for higher magnification of the boxed area). Pejvakin was not detected in untransfected cells. (**B**) **Absence of immunolabelling in inner hair cells (IHCs) from P21 *Pjvk*$^{-/-}$ and *Pjvk*$^{fl/fl}$Myo15-*cre*$^{+/-}$ mice with the Pjvk-G21 antibody** demonstrates the specificity of this antibody (see Figure 6B for immunolabelling in *Pjvk*$^{+/+}$ IHCs). (**C**) **Pejvakin immunostaining of dividing peroxisomes.** Double immunolabelling of HepG2 cells for pejvakin (light grey) and PMP70 (white). Upper panel: arrowheads indicate pejvakin-immunoreactive protrusions from pre-existing peroxisomes. Lower panel: boxed areas show pejvakin-immunoreactive string-of-beads structures corresponding to elongated

and constricted peroxisomes (preceding final fission). Scale bar is 10 μm in (A), 5 μm in (B), and 2 μm in (C).

Figure 8 shows the role of pejvakin in the proliferation and maintenance of peroxisomes. This figure shows larger numbers and enlargement of peroxisomes in transfected HeLa cells producing wild-type and mutant forms of pejvakin, respectively. In cells producing EGFP alone, EGFP and wild-type pejvakin (Pjvk), or EGFP and the p.T54I, p.R183W, p.C343S, or p.V330L*fs**7 mutated forms of pejvakin, peroxisomes were identified on the basis of their PMP70-immunoreactivity. The upper panel shows F-actin (medium grey), DAPI (dark grey), EGFP (light grey), and PMP70 (white) staining, whereas the lower panel shows only the PMP70 immunostaining of individual cells delimited by a white border. The number of peroxisomes is larger in cells producing wild-type pejvakin, and smaller in the cells producing any of the mutated forms of pejvakin, than in cells producing EGFP alone (see quantification in Figure 6D). In addition, cells producing the mutated forms of pejvakin contain enlarged peroxisomes (arrowheads, and see insets for magnification; see also quantification in Figure 6D). Scale bar is 10 μm.

Figure 9 shows the effect of loud sound exposure on the expression of *Pjvk* and other antioxidant genes in the organ of Corti. (**A**) The levels of *Pjvk* transcripts and of *CypA*, *Gpx2, c-Dct*, and *Mpv17* transcripts (genes that are down-regulated in $Pjvk^{-/-}$ mice) were measured by qRT-PCR in the organ of Corti of sound-exposed (5-40 kHz, 105 dB during 1 hour) P21 wild-type mice at various times (1, 3, 6, and 18 hours in a silent environment) after the sound exposure. In the sound-exposed animals, the *Pjvk* transcript showed an almost 2-fold increase at 1 hour and a 4-fold increase at 6 hours, and had returned to pre-exposure level at 18 hours. The levels of *CypA*, *c-Dct*, and *Mpv17* transcripts, and of *Hsp70* and *c-Fos* transcripts (used as a positive control of the response to sound stimulation), but not that of the *Gpx2* transcript, also increased in variable proportions after sound exposure. (**B**) Sound exposure at 5-40 kHz, 90 dB, during 1 hour, also leads to a marked increase of the levels of *Pjvk* and *CypA* transcripts, but only a moderate (less than 2-fold) increase in the levels of *c-Dct* and both *Hsp70* and *c-Fos* transcripts 6 hours after the sound exposure. This indicates that *Pjvk* and *CypA* are involved in the early physiological response to noise. Error bars indicate ± SEM.

Figure 10 highlights the hypervulnerability of DFNB59 patients to sound. (**A**) ABR waves in a patient carrying the *PJVK* p.T54I mutation, in response to 250, 500, and 1000 impulse stimuli (clicks) at 99 dB above normal detection threshold (dB nHL), delivered to one ear. After 250 clicks, waves were spotted at normal latencies. A dramatic decrease in amplitude of waves III

and V (the equivalents of waves II and IV of mice) was observed after 500 clicks, with a shift in their latencies after 1000 clicks. (**B**) A second test was carried out on the same ear after 10 minutes spent in a silent environment. Initially, full recovery of amplitude and latency of ABR waves was observed, but prolonged exposure to clicks produced even more dramatic changes. (**C, D**) In the tested sample of p.T54I patients (n = 8 ears), a significant decrease in the amplitude of wave V (**C**) and an increase in its latency were observed, whereas in a control group of patients with sensorineural hearing impairments of cochlear origin and matched ABR thresholds (n = 13), the same sound exposure (even when prolonged beyond 4000 clicks) had no effect, either on the amplitude of ABR waves or on wave V latency.

Figure 11 shows the effect of exposure to loud sounds on the number of peroxisomes in cochlear hair cells and ganglion neurons. Peroxisome proliferation in P21 *Pjvk*$^{+/+}$ hair cells and cochlear ganglion neurons after sound-exposure (same conditions as in A). Peroxisomes were counted 48 hours after sound-exposure. OHCs, IHCs, and neuronal processes stained for F-actin, myosin VI, and neurofilament protein NF200, respectively. In OHCs and IHCs, the peroxisomes are located below the CP and throughout the cytoplasm, respectively. For OHCs, both a lateral view and a transverse optical section at the level of CP (scheme on the right) are shown. The number of peroxisomes was increased in OHCs, IHCs, and dendrites after sound-exposure. N: cell nucleus. *** $p < 0.001$. Error bars represent the SEM. Scale bars are 5 μm.

Figure 12 discloses the therapeutic effect of N-acetyl cysteine on the auditory function of *Pjvk*$^{-/-}$ mice. The pregnant *Pjvk*$^{-/-}$ mice were treated with either N-acetyl cysteine (NAC) or taurine (TAU), two antioxidant drugs, in the drinking water. The treatment was continued until pups reached P21, the age that auditory tests were performed. (**A**) ABR thresholds at 10, 20, 32, and 40 kHz. A slight recovery of ABR thresholds is observed in *Pjvk*$^{-/-}$ mice treated with NAC compared to both TAU-treated and untreated mice. (**B**) ABR wave I amplitude fell within the normative range in NAC-treated *Pjvk*$^{-/-}$ compared to the untreated *Pjvk*$^{-/-}$ and TAU-treated *Pjvk*$^{-/-}$ mice, but no significant recovery of ABR wave I latency and ABR interwave I-IV was observed in treated *Pjvk*$^{-/-}$ mice (**C, D**). (**E, F**) EEBRs of NAC-treated *Pjvk*$^{-/-}$ mice, unlike those of untreated *Pjvk*$^{-/-}$ mice, resisted to high-rate (a rate of 200/s for 1 minute) electrical stimulation of the auditory nerve, as the amplitude of wave E IV remained unaffected. (**E**). Full recovery of neuronal function (unchanged amplitudes and latencies) was obtained 5 minutes after high-rate electrical stimulation in this NAC-treated *Pjvk*$^{-/-}$ ear (**F**).

Figure 13 shows the preventing hair cell dysfunction by adenovirus-mediated gene transfer in *Pjvk*$^{-/-}$ mice. *Pjvk*$^{-/-}$ P3 mice were injected with AAV2/8-Pjvk-IRES-EGFP, which specifically transduces in IHCs and OHCs, in one cochlea through round window. (**A, B**) Effect of the transfection on DPOAE thresholds at 10 kHz in treated ears compared to contralateral (untreated) ears. The improved DPOAE thresholds in treated ears correlate with the number of GFP-tagged OHCs (**B**), in relation to the partial recovery of OHC function. (**C, D**) The amplitudes of ABR wave I in response to 10 kHz, 105 dB SPL sound stimulations become normal in the treated ears compared to contralateral ears, and this reversion is highly correlated with the number of GFP-tagged IHCs (D). Error bars represent the SD. *** $p < 0.001$

Figure 14 represents the effect of AAV2/8-Pjvk-IRES-EGFP on the peroxisomes in *Pjvk*$^{-/-}$ IHCs. Upper and lower panels show and quantify (bar charts) the peroxisomes in untreated mice 48 hours after sound-exposure (5-40 kHz, 105 dB SPL for 1 hour) (peroxisome abnormalities are indicated by arrowheads). Error bars represent the SEM.** $p < 0.01$, *** $p < 0.001$.

EXAMPLES

I. Material and Methods

Animal handling

Animals were housed in the Institut Pasteur animal facilities accredited by the French Ministry of Agriculture to perform experiments on live mice (accreditation 75-15-01, issued on September 6th, 2013 in appliance of the French and European regulations on care and protection of the Laboratory Animals (EC Directive 2010/63, French Law 2013-118, February 6th, 2013). The corresponding author confirms that protocols were approved by the veterinary staff of the Institut Pasteur animal facility, and were performed in compliance with the NIH Animal Welfare Insurance #A5476-01 issued on 31/07/2012. C57Bl/6 wild-type mice were obtained from Janvier laboratories.

Gene targeting, genotyping, and RT-PCR

A targeting vector was designed, in which exon 2 of *Pjvk* and the neomycin selection cassette were flanked with loxP sites. A negative selection cassette coding for diphtheria toxin A fragment (*DTA*) was inserted at the 3'-end of the targeting *Pjvk* sequence (Figure 1A). CK35 embryonic stem (ES) cells (Kress et al., 1998), derived from a 129/Sv mouse embryo, were

electroporated with the purified, linearized targeting vector, and plated on G418 selective medium as reported (Matise et al., 1999). Approximately 300 recombinant ES cell clones were obtained, of which 12 were correctly targeted. The homologous recombinant event was confirmed on the left and right sides by PCR, using the primers specific to the 5' and 3' genomic sequence, outside of the region used in the targeting vector, and specific to the *neo* sequence. The sequences of the PCR primers used to genotype the floxed *Pjvk* allele are available on request. Integration of the recombinant DNA construct was confirmed by Southern blot analysis and PCR amplification of genomic DNA extracted from the mouse tails. Two independent clones were used to create germ line-transmitting chimeric mice by injection into C57BL/6J blastocysts. Mating of male chimeras with C57BL/6J females produced heterozygous animals. Mice heterozygous for the floxed *Pjvk* allele were mated with PGK-Cre^{m} deleter mice carrying the cre recombinase gene driven by the early acting ubiquitous phosphoglycerate kinase-1 gene promoter (Lallemand et al., 1998), to obtain *Pjvk* knock-out ($Pjvk^{-/-}$) mice. Targeted deletion of exon 2 was confirmed by PCR analysis.

To obtain *Pjvk* conditional knockout mice ($Pjvk^{fl/fl}$*Myo15*-$cre^{+/-}$), in which expression of the deleted *Pjvk* was restricted to the inner ear sensory cells, mice carrying the floxed *Pjvk* allele were mated with transgenic mice expressing the cre-recombinase under the control of the myosin 15 gene promoter (Caberlotto et al., 2011). Analyses of the auditory function were performed in ubiquitous knock-out and conditional knockout mice. All studies were performed on mixed C57BL/6J-129/Sv genetic background.

For RT-PCR analysis of the *Pjvk* transcript, total RNA was extracted from inner ears of $Pjvk^{+/+}$ and $Pjvk^{-/-}$ P7 mice with NucleoSpin® RNA II (Macherey-Nagel). In the $Pjvk^{+/+}$ mice, a transcript of 1059 bp in length was detected, while in the $Pjvk^{-/-}$ mice a transcript of 963 bp lacking the exon 2 sequence was detected.

Audiological studies in mice

Auditory tests were performed in an anechoic room. They consisted of distortion-product otoacoustic emissions (DPOAEs), auditory brainstem responses (ABRs), electrically-evoked brainstem responses (EEBRs), and cochlear potentials. Mice were anesthetized with an intraperitoneal injection of a ketamine and levomepromazin mixture (100 mg/kg: 5 mg/kg) and their core temperature was kept at 37°C with the help of a servo-controlled heating pad. The DPOAE at frequency $2f_1$-f_2 was recorded in response to two equal level primary tones, f_1 and f_2,

with f_2/f_1=1.20 (Cub^{e}Dis system, Mimosa Acoustics; ER10B microphone, Etymotic Res.). Frequency f_2 was swept at 1/10th octave steps from 4 to 20 kHz, and DPOAE level was plotted against frequency f_2 (primary tone levels increased from 20 to 70 dB SPL in 10 dB steps, then to 75 dB SPL). DPOAE threshold was defined as the smallest primary level giving rise to a detectable DPOAE. ABRs in response to calibrated short tone bursts in the 5-40 kHz range (repetition rate 17/s) were derived from the synchronous averaging of electroencephalograms recorded between subcutaneous stainless steel electrodes at the vertex and ipsilateral mastoid, with the help of a standard digital averaging system (CED1401+). A hundred responses to the tone bursts were averaged except within 10 dB of the ABR threshold (defined as the smallest tone-burst level giving rise to at least one repeatable wave above noise background level, 150 nV in an anesthetized animal), for which 300 tone bursts were used. Once ABR thresholds had been assessed, ABRs in response to 95 and 105 dB SPL tone bursts (100 averages) were collected for analysis of suprathreshold ABR waveforms, amplitudes and latencies. Controlled sound exposure was applied with the same acoustic probe used for ABRs without moving the sound system, so that pre- and post-exposure ABRs shared the same calibration. Intense stimuli were the same tone-bursts used for ABR measurements at 105 dB SPL, presented 1,000 times at the same repetition rate of 17/s.

Electrical stimulations of the eighth cranial nerve were delivered by a silver electrode placed in the round-window niche and excited by biphasic electrical impulses (neutral electrode in neck muscles; peak amplitude of electrical stimulus about 0.5 V; duration of the positive and negative phases 150 microseconds; adjustable repetition rate). EEBRs were extracted using the same setup as for ABRs (Roux et al., 2006), in response to 100 electrical impulses presented with alternating polarities (repetition rate 17 Hz). EEBR threshold was defined as the smallest electrical amplitude eliciting repeatable waves above noise background level (the same as for ABRs), labelled from E II to E IV in reference to their ABR equivalents II-IV. Controlled electrical stimulation was applied at 5 dB above EEBR detection threshold with a 200 Hz repetition rate. Occasionally, the silver electrode on the round window served for recording Compound Action Potentials (CAPs) in response to the same tone-bursts used for ABR studies (averages of 32 presentations, repetition rates 17/s), prior to EEBR data collection. These recordings served to check that CAP thresholds and ABR thresholds were within 2 dB of each other at all frequencies, and the exact position of ABR wave I could be ascertained form the larger wave N1, its equivalent on CAP recordings. This was particularly important in mice with abnormally small wave I to avoid incorrect identifications (when wave I was reduced to a very small

flattened deflection resembling a summating potential, the slightly larger wave II might have been mistakenly labelled wave I on ABR recordings, while wave N1, even when small, kept its characteristic shape).

The round-window electrode also provided access to the cochlear microphonic potential (CM), with the same setting used for CAP measurements, except that the stimulus polarity was fixed for CM recordings, instead of alternating between rarefaction and condensation tone-bursts for CAP detection. CM is a far-field potential resulting from mechanoelectrical transduction currents through the OHCs at the basal end of the cochlea, near the collecting electrode, and is an oscillating change in electric potential at the stimulus frequency. Although its shape is closely similar to that of the stimulus that activates the sound-delivering earphone, it was easily separated from a possible electric artefact radiated by the earphone by its delay of about 0.5 ms after stimulus onset, in relation to sound propagation along the tubing system that connected the earphone to the ear canal of the mouse. Its peak-to-peak amplitude was measured for a stimulus of 5 kHz (a frequency much lower than the best frequency of the responding OHCs, so that CM was independent of their electromotility status) presented at 95 dB SPL.

Recording of mouse vocalizations

The protocol was adapted from the protocol described previously by Menuet et al. (2011). In brief, mice were placed in a polyethylene cage covered by a metal wire lid. A free field microphone (type 4192, ½-inch, Brüel & Kjaer) was placed 2 cm above the metal lid, in the centre of the cage. The microphone output was preamplified (Microphone power supply type 2801, Brüel & Kjaer) and digitized by the sound card of a computer (Dell D830; Dell Inc.) at the sampling rate of 192 kHz. Acoustic vocalizations in the 5- 90 kHz frequency range were stored online by Adobe Audition 1.5 software. Their analysis was performed using software developed on Matlab (The MathWorks Inc., MA), allowing a spectrographic display of vocalizations in the time-frequency domain, from which the total time of vocalization, the average intensity of vocalizations, and the spectral complexity of vocalizations were determined.

Stabulation of mice in an acoustically quiet environment

Noting that most of the noise exposure of a young mouse comes from surrounding sound vocalizations (Ehret & Riecke, 2002), the pups were split from the same litters into three

groups placed in isolated boxes. Separation was done before P10, that is several days before the onset of hearing in the mouse. Boxes were kept in quiet booths, shielded from the sound from other cages. In the first group, only 2 mice were kept in a cage with a foster mother; in the second group, 4 mice; and in the third group, the remaining (6 to 10) pups were left with their mother.

Audiological tests and controlled sound exposure in patients

Informed consent was obtained from all the subjects included in the study. Clinical examination was carried out on the five affected subjects carrying the p.T54I mutation in *PJVK*, and 13 control patients with sensorineural hearing impairments of cochlear origin and matched auditory thresholds and extant otoacoustic emissions. Pure-tone audiometry was performed using air- and bone-transmitted tones. Hearing impairment was objectively assessed by means of ABRs and transient-evoked otoacoustic emissions (TEOAEs). To test the hearing hypervulnerability to sound in these patients, a minimal sound exposure eliciting ABRs was used. ABRs were first recorded in response to 250 impulse stimuli – clicks (at a repetition rate of 20/s) at 99 dB above normal detection threshold (the maximum level with this equipment, a Vivosonic Integrity™ Version 4.50), that is, 20-30 dB above the ABR threshold in the tested ear. Then, averaging was extended to 500 and 1000 clicks, and the three averaged ABRs were compared as regards wave identification, amplitudes and latencies post click-onset. In control patients, averaging was prolonged until about 4000 responses to clicks had been collected. After a 10-min pause with no sound stimulus, the procedure was done all over again. TEOAEs were averaged just before the first ABR procedure, then just after, in response to 260 series of clicks presented at 40 dB above normal detection threshold (i.e., they were inaudible in patients). The so-called nonlinear TEOAE recording procedure was used (derived from the ILO88 system, Kemp, 2002), allowing genuine TEOAEs to be extracted from linear reflection artefacts from the middle ear and background noise to be evaluated. TEOAE responses were analysed in 1-kHz-wide bands centred on 1, 2, 3 and 4 kHz.

Acoustic overexposure for quantification of cochlear transcripts in mice

Three-week old C57Bl/6 wild-type mice were used. The sound stimulation episode to which the animals were exposed consisted, in a first set of experiments, of a 1-hour pure tone overstimulation at 5-20 kHz with an intensity of 105 dB SPL. In the second set of experiments, the mice were submitted to a so-called "preconditioning sound exposure" that consisted of a bandpass-filtered white noise (BPWN) whose spectrum covered the interval 5-20 kHz, with a

lower intensity of 90 dB SPL for 1 hour. The BPWN signal was generated using custom Matlab software (The Mathworks), and delivered by an amplifier to a set of four Ultrasonic Vifa speakers (Avisoft Bioacoustics). The speakers were attached to the tops of four custom-made, cylindrical sound-isolation chambers (15 cm in radius) in which the mice were enclosed. The noise intensity delivered by the speakers was calibrated with a BK4812 probe (Bruel & Kjaer) placed centrally at the bottom surfaces of the isolation chambers. The sound field inside each chamber varied by less than 10 dB over its bottom surface.

Generation of an anti-pejvakin monoclonal antibody

The coding sequence of the *Pjvk* cDNA (accession no. NM_001080711.2) 3'-end was amplified and cloned into a pGST-parallel-2 vector (*derived* from *pGEX-4T-1*; Amersham). The resulting construct, encoding the C-terminal region of pejvakin (residues 290-352; accession no. NP_001074180.1) fused to a N-terminal glutathione *S*-transferase (GST) tag, was transformed into *E. coli* BL21-Gold (DE3) competent cells (Stratagene). The pejvakin protein fragment was purified using a glutathione Sepharose 4B column, followed by size-exclusion chromatography and used as the antigen for immunization. Young (4-6 weeks old) *Pjvk*$^{-/-}$ mice were immunized with 15–50 mg of antigen by subcutaneous injection. Mice were bled from eye vein after 3 injections, and presence of the antibody in the plasma was tested by ELISA and western blot. Once plateau of antibody production was detected, hybridoma fusion was performed. Antibody titre was determined by ELISA.

Treatment of mouse embryonic fibroblasts with H_2O_2

Fibroblasts were isolated from mouse embryos at embryonic day 13.5 and cultured as described by Xu (2005). The cells were incubated in DMEM (Gibco) supplemented with 0.1 mM β-mercaptoethanol, and 0.5 mM H_2O_2 for 4 hours at 37 °C, under normoxic conditions (95% air). The culture medium was then replaced with H_2O_2-free medium. Cell viability was checked 18 hours after H_2O_2 treatment, by measuring mitochondrial reductase activity with the MTT (3-(4,5-dimethylthiazol-2-yl)-2,5-diphenyl tetrazolium bromide) (Sigma M2128) assay. A polyclonal antibody against peroxisome membrane protein 70 (PMP70, Abcam ab3421) was used to label peroxisomes.

Plasmids and DNA transfections

The full-length *Pjvk* cDNA was obtained by RT-PCR on a double-strand cDNA library prepared

from organs of Corti of postnatal day 7 (P7) C57BL/6 mice, and then was cloned into the pIRES2-EGFP vector (Clontech). The mutant *Pjvk* clones (missense mutations) were prepared from the wild-type clone using QuikChange™ Site-Directed Mutagenesis kit (Stratagene). HeLa, COS-7, HEK293 cells were transiently transfected using lipofectamine™ 2000 (Invitrogen), according to the manufacturer's instructions.

Immunofluorescence studies

For cryosections, inner ears were dissected in PBS and fixed by immersion in 4% paraformaldehyde (PFA) in PBS for 2 hours at 4°C. The samples were decalcified in 10% EDTA in PBS, pH 7.4 for 4 days at 4°C, fixed again in 4% PFA in PBS for 1 hour, rinsed twice in PBS for 10 min, and immersed in 20% sucrose in PBS for 12 hours. They were embedded in Tissue Freezing Medium (Triangle Biomedical Sciences, USA). Cryostat sections (12 µm thick) were used for immunohistochemistry. An antibody against 4-hydroxy-2-nonenal (HNE) (Calbiochem) was used to detect the lipid oxidation products.

For whole-mount immunolabelling analyses, the inner ears were fixed in 4% PFA in PBS, and the cochlear sensory areas (organ of Corti) were microdissected. The tissues were rinsed twice in PBS, then permeabilized and blocked by incubation in PBS containing 20% normal goat serum and 0.3% Triton X-100 for 1 hour at room temperature. For GFP detection, whole-mount cochleas were incubated with a mixture of rabbit anti-GFP antibody (Invitrogen) and chicken anti-GFP antibody (Abcam) in 1% bovine serum albumin (BSA) in PBS. A monoclonal antibody against parvalbumin (Sigma) was used to label auditory neurons. A polyclonal antibody against peroxisome membrane protein 70 (PMP70, Abcam) was used to label peroxisomes. Anti-myosin VI (Roux et al., 2009), anti-ribeye/CtBP2 (Santa Cruz), and anti-glutamate receptor 2 (GluR2, Invitrogen) antibodies were used to delimit the contours of IHCs, to label and count IHC ribbons, and to label post-synaptic glutamate receptors on the dendritic ends of cochlear ganglion neurons, respectively.

For immunocytochemistry, HeLa, COS-7, HEK293, and HepG2 cells were fixed in 4% PFA for 15 min, washed in PBS, and incubated in NH_4Cl 50 mM – Triton X-100 0.2% solution for 15 min at room temperature (RT). After washing, cells were incubated in PBS - Normal Goat Serum 20% solution for 1 hour. Cells were incubated with the primary antibody in PBS-BSA 1% solution for 1 hour. Peroxisomes were labelled using a rabbit polyclonal antibody against peroxisome membrane protein 70 (PMP70, Abcam). Antibodies against mitochondrial import receptor subunit TOMM22 (Sigma) and *lysosomal-associated membrane protein 1,* LAMP1 (Abcam) were used to label mitochondria and lysosomes, respectively. The mouse monoclonal antibody

against pejvakin (Pjvk-G21) was used to detect the subcellular location of pejvakin. Cells were then washed in PBS and incubated with the appropriate secondary antibody for 1 hour at RT. For immunofluorescence, the antibodies Atto-488- or Atto-647-conjugated goat anti-rabbit IgG, Atto-594-conjugated goat anti-mouse IgG (Sigma) and Alexa-Fluor-488-conjugated goat anti-chicken IgG (Invitrogen) were used. TRITC-conjugated phalloidin (Sigma) and DAPI (Sigma) were used to label actin and cell nuclei, respectively. Images were collected using a Zeiss LSM700 Meta confocal microscope (Carl Zeiss MicroImaging, Inc.). Automated quantification of peroxisomes was realised using the Particles Analysis plugin of ImageJ software (Collins, 2007). Data were expressed as a number of peroxisomes per 100 μm^2, and enlarged peroxisomes were measured in two perpendicular directions using ImageJ software.

Morphological analyses and peroxisome staining

For scanning electron microscopy studies, inner ears from adult mice were fixed by perfusion of the perilymphatic compartment with 2.5% phosphate-buffered glutaraldehyde, and rinsed in PBS. Cochleae were then microdissected, dehydrated in graded ethanol solutions, and dried up to critical point. Processed specimens were then mounted on aluminium stubs with colloidal silver adhesive and sputter-coated with gold palladium before imaging in a JSM-6700 F Jeol scanning electron microscope. Inner ears from a total of 10 *Pjvk*$^{+/+}$ mice (three at P15, four at P30, three at P60), and 12 *Pjvk*$^{-/-}$ mice (three at P15, five at P30, four at P60) were analysed by scanning electron microscopy.

For transmission electron microscopy studies, the cochleas were prepared as previously described (Thelen et al., 2009). They were fixed in 2.5% glutaraldehyde in 0.1 M Sörensen's buffer pH 7.4 for 2 hours at 4°C. After several washes in 0.1 M Sörensen's buffer pH 7.4, the samples were postfixed at 4 °C with 2% osmium tetroxide in Sörensen's buffer for 60 min. The selective staining of peroxisomes is adapted from (Angermüller & Fahimi, 1981). Briefly, the cochleas were fixed at 4°C in 1% glutaraldehyde in 0.1 M cacodylate buffer pH 7.2 for 1 hour. After several washes in the same buffer, the samples were immersed in 2 mg/ml 3,3'-*Diaminobenzidine* (*DAB*) and 0.15% H_2O_2 in 0.05 M Teorell-Stenhagen buffer (T/S: 57 mM boric acid, 50 mM phosphoric acid, 35 mM citric acid, 345 mM NaOH) pH 10.5 for 45 min at 30°C. After several washes in T/S, the samples were postfixed at 4 °C with 2% osmium tetroxide in H_2O for 60 min. All the cochleas were then washed in deionized water, dehydrated in graded ethanol solutions, and embedded in Epon (Epon-*812,* Electron Microscopy Sciences) for 48 hours at 60 °C.

Ultrathin sections (70 nm thick) were obtained using an ultramicrotome (Reichert Ultracut E) equipped with a diamond knife (Diatome), and mounted on copper grids coated with collodion. Sections for the morphological analysis were contrasted with uranyl acetate and lead citrate for 15 min each. Sections stained with DAB were contrasted with lead citrate for 15 min. The ultrathin sections were observed under a JEM-1400 transmission electron microscope (Jeol) at 80 kV and photographed with an 11 MegaPixel bottom-mounted TEM camera system (Quemesa, Olympus). The images were analysed via iTEM software (Olympus). The quantitative data were obtained using the same software.

Microarray analysis and real-time quantitative PCR

Total RNA was extracted from dissected organs of Corti of *Pjvk*$^{-/-}$ and wild-type P15 mice (an age at which no cellular defect could be detected in the organ of Corti of *Pjvk*$^{-/-}$ mice) using TRIzol reagent (Invitrogen), purified on Rneasy columns (Qiagen, Valencia, CA), and tested on an Agilent (Waldbronn, Germany) 2100 Bioanalyzer. Three biological replicates were run for each genotype. cRNAs obtained from 100 ng of RNA were amplified by using the GeneChip Expression Two-Cycle 3' amplification system (Affymetrix, High Wycombe, U.K.). Fragmented biotin-labeled cRNA samples were hybridized to Affymetrix Mouse Gene ST 1.0 arrays. Following hybridization, the array was washed and stained according to the Affymetrix protocol. The stained array was scanned at 532 nm using an Affymetrix GeneChip Scanner 3000, producing CEL files for each array. Gene-level expression values were derived from the CEL file probe-level hybridization intensities using the model-based Robust Multichip Average algorithm (RMA) (Bolstad et al. 2003). Arrays were compared using the Local Pool Error test (Jain et al., 2003), and the P values were adjusted by using the Benjamini–Hochberg algorithm (Benjamini & Hochberg, 1995). The fold differences reflect the relative expression levels of the genes in the organs of Corti of *Pjvk*$^{-/-}$ mice normalized to the expression levels of the same genes in the organs of Corti of *Pjvk*$^{+/+}$ mice.

The fold changes of *Mpv17*, *Dct*, *Gpx2*, *CypA*, *c-Fos*, and *Hsp70* transcripts between sound-exposed and unexposed cochleas were analysed by quantitative PCR. Cochleas were collected from unexposed and sound-exposed mice at 1 hour, 3 hours, 6 hours, and 18 hours after sound exposure. RNA was extracted from dissected organs of Corti using NucleoSpin® RNA II (Macherey-Nagel). Real-time quantitative PCR was performed using the Universal Probe Library (UPL) system from Roche. UPL probes were labelled with FAM, and the fluorescence was read with the Applied Biosystems 7500 Real-Time PCR System. The thermocycling conditions were 50°C for 2 min followed by 95°C for 2 min, and then 40 cycles at 95°C for 15 s

and 60°C for 30 s. Three independent experiments were performed for each exposed or unexposed cochlea. Each assay was conducted for target transcript probe-set in a multiplex reaction in which glyceraldehyde-3-phosphate dehydrogenase (*Gapdh*) probe-set was used as an internal control. Relative levels of target transcript dosage were determined using the comparative CT method. The relative transcript copy number for each target transcript was calculated as $2^{-\Delta\Delta CT}$. UPL probes and primers were indicated in the table below. To compare the transcription level of each gene in the organ of Corti of exposed and unexposed mice, statistical significance was assessed using the unpaired, Student's t-test.

List of primers and probes used for quantitative PCR.

Gene	**UPL probe (Roche)**	**Forward primer (5'-3')**	**Reverse primer (5'-3')**
Pjvk	#60 (cat. 04688589001)	CCAGTGCTCTCTGTCAGTGC	TCTGTTCATCCATAAAATGAAACC
Mpv17	#75 (cat. no 04688988001)	CGCACTCTGACCATGGTATC	CCCGGGATTAAGTGGTCTAAA
Dct	#6 (cat. no. 04685032001)	GGCTACAATTACGCCGTTG	CACTGAGAGAGTTGTGGACCAA
Gpx2	#2 (cat. no. 04684982001)	GTTCTCGGCTTCCCTTGC	TTCAGGATCTCCTCGTTCTGA
CypA	#46 (cat. 04688066001)	ACGCCACTGTCGCTTTTC	GCAAACAGCTCGAAGGAGAC
c-Fos	#26 (cat. 04687574001)	GGCTCTCCTGTCAACACACA	GACCAGAGTGGGCTGCAC
Hsp70	#80 (cat. 04689038001)	GAAGACATATAGTCTAGCTGCCCAGT	CCAAGACGTTTGTTTAAGACACTTT
Gadph	(cat. no. 050462	ATGGTGAAGGTCGGTGTGA	AATCTCCACTTTGCCACTGC

Measurement of total GSH and GSSG

Total glutathione (GSH + GSSG) and oxidized glutathione (GSSG) levels were measured by the method of Rahman et al. (2006). Three independent experiments were performed. Cochleas and livers were collected from *Pjvk*$^{+/+}$ and *Pjvk*$^{-/-}$ mice at 3 weeks of age. The tissues were quickly removed and placed in ice-cold 0.1 M potassium phosphate buffer with 5 mM EDTA disodium salt, pH 7.5 (KPE), and homogenized on ice-cold extraction buffer (0.1% Triton-X, 0.6% sulfosalicylic acid and 5% metaphosphoric acid in KPE). The homogenate was centrifuged at 8,000 x g for 10 min at 4°C. The supernatant was used as lysate for assay. To measure GSSG only, reduced GSH was derivatized with 2-vinylpyridine. Measurement of GSH/GSSG levels was done by adding 5,5′ -dithio-bis (2-nitrobenzoic acid) (DTNB) to the lysate. Both GSH and GSSG react with DTNB and form a yellow derivate 5′ -thio-2-nitrobenzoic acid (TNB). The rates of TNB formation were calculated by spectrometry at 405 nm. The total GSH and GSSG concentrations in the samples were measured by using linear regression to calculate the values obtained from the standard curve. The GSH concentration was calculated by subtracting the GSSG concentration from the total GSH concentration.

TBARS assay for quantification of lipid peroxidation

To test the level of MDA, a by-product of lipid peroxidation, the TBARS assay kit was used (Cayman Chemical Company, Ann Arbor, MI, USA). Three independent experiments were performed. For each assay, cochlear sensory areas were microdissected from 30 *Pjvk*$^{+/+}$ and 30 *Pjvk*$^{-/-}$ mice. Cochlear tissue was homogenized on ice in RIPA buffer (50 mM Tris-HCl, pH 7.6, containing 150 mM NaCl, 1% NP-40 (Igepal), 0.5% sodium deoxycholate, and 0.1% SDS). Cochlear homogenate was used for the assay. The prescribed TBARS protocol was applied, in addition to the triplicate pipeting of MDA aliquots of known concentration to produce a standard curve. Fluorescence was read at excitation and emission wavelengths of 530 and 590 nm, respectively, using a Synergy 2 thermoregulated spectrophotometer plate reader (BioTek). The averaged values were used to determine MDA concentration from the MDA standard curve graph.

AAV-*Pjvk* viral constructs and intracochlear viral transduction

To obtain AAV2/8-Pjvk-IRES-EGFP, the mouse *Pjvk* cDNA flanked by an IRES-EGFP reporter cDNA sequence was subcloned into the multiple cloning site of vector pENN.AAV.CB7.CI.RBG (PennVector P1044, Penn Medicine Vector Core - University of Pennsylvania School of Medicine). The virus production and titration were performed by Penn Medicine Vector Core. To product AAV8-Pjvk, mouse *Pjvk* cDNA was subcloned in a single promoter Ad.MAX™ shuttle vector (ITR-CAG-Dfnb59-WPRE-PolyA-ITR; SignaGen Laboratories). The virus packaging and titration were done by SignaGen Laboratories.

Intracochlear viral transduction was carried out as described by Akil et al. (2012). Three-day old *Pjvk*$^{-/-}$ pups were anesthetized by hypothermia, and the left ear was approached through a dorsal incision. A small hole was made in the bulla with an 18G needle, and the round window membrane was gently punctured with a borosilicate capillary pipette. A fixed volume of AAV8-Pjvk or AAV2/8-Pjvk-IRES-EGFP (0.5 µl of a 1 x 10^{13} vg/ml) was then gently injected (during 1–2 min) into the perilymphatic compartment of the cochlea. After pulling out the pipette, the round window niche was quickly sealed with fascia and adipose tissue, and the bulla was sealed with dental cement. Auditory function was tested at P21 in treated and untreated ears by recording of ABR, DPOAEs, and EEBR.

Antioxidant treatment

N-acetyl-L-cysteine (L-NAC; Sigma) or taurine (Sigma) was administrated to pregnant *Pjvk*$^{-/-}$ mice in the drinking water. A daily dose of 1% L-NAC or 2% taurine was given to the mother during and after pregnancy, so that pups received them from birth on by feeding on the mother's milk. The treatment was continued until P21, and the auditory function of the treated *Pjvk*$^{-/-}$ pups was tested at P21.

Statistical analyses

After checking for data normality and homoscedasticity, statistical differences were evaluated using the Student's t-test and one-way ANOVA. A p value < 0.05 was set for statistical significance.

II. Results

1. Extreme heterogeneity in hearing sensitivity in *Pjvk*$^{-/-}$ mice

Pejvakin-null mice, *Pjvk*$^{-/-}$, carrying a deletion of exon 2 resulting in a frameshift at codon position 71 (p.G71*fs*X9) (Fig. 1) were analysed at postnatal day 30 (P30), for hearing sensitivity by ABR thresholds. ABR thresholds at 10 kHz ranged from 35 to 110 dB SPL in *Pjvk*$^{-/-}$ mice (n= 50), whilst they never exceeded 30 dB SPL in *Pjvk*$^{+/+}$ and *Pjvk*$^{+/-}$ littermates (n= 50) (Fig. 2A). This broad range in hearing sensitivity, from near-normal to near-totally absent, extended across the whole frequency spectrum. OHC activity was tested by the thresholds of the distortion-product otoacoustic emissions (DPOAEs). The DPOAEs thresholds were affected, establishing OHC dysfunction, and differ widely, from 30 to 75 dB SPL in 30 *Pjvk*$^{-/-}$ mice up to undetectable DPOAEs regardless of stimulus intensity in 20 Pjvk$^{-/-}$ mice (Fig. 2B). A puzzling degree of variability of the hearing phenotype results from the absence of pejvakin.

2. Hypervulnerability to natural acoustic environment in *Pjvk*$^{-/-}$ mice

To gain insight into the origin of the considerable variations of *Pjvk*$^{-/-}$ auditory phenotypes, the ABR thresholds of the *Pjvk*$^{-/-}$ littermates were first examined from different crosses. Large variations were detected from one cross to another, which contrasted with only marginal differences between the *Pjvk*$^{-/-}$ littermates of individual crosses. This observation might be consistent with a phenotypic heterogeneity of genetic origin. However a careful observation pointed to an alternative explanation. ABR thresholds elevations tended to vary according to the number of pups in the litter (6 to 10); the larger this number, the more elevated ABR thresholds. This suggested that the natural acoustic environment resulting from pups' calls might have a deleterious effect on hearing of *Pjvk*$^{-/-}$ mice. Indeed pups are vocally very active from birth to about P20, when crowding around the mother, at the feeding time (Ehret & Riecke, 2002). To directly evaluate whether hearing of *Pjvk*$^{-/-}$ pups could be compromised by their vocalizations, large litters were randomly split in groups of 2, 4, 6 and 10 pups per cage kept with a foster mother, from P10 (i.e. before onset of hearing which occurs at P14). ABR thresholds at P21 showed a highly significant correlation ($p < 0.001$) with the number of pups present in a given cage (Fig. 2C). The coefficient of determination, $R^2 = 0.51$, indicates that 51% of ABR threshold variations was described by the independent variable, number of pups per cage.

Acoustic measurements showed that the most energetic pup calls, in a 12-pup litter, are harmonics of about 5 kHz that reach 105 ± 5 dB SPL from P0 to P21, at the entrance of the ear canals of the pups. A 1-hour exposure is energetically equivalent to a continuous exposure of 42-50 s to the sound of a call. To directly test the effect of sound stimulation and evaluate its possible deleterious consequences on hearing in a controlled manner, 10-kHz 105 dB SPL tone-bursts (2-ms plateau stimulation separated by 60-ms silent intervals) were used, such that one thousand presentations of this stimulus are energetically equivalent to a 3-min stay in the natural environment of a 12-pup litter, whilst allowing ABRs to be monitored during exposure. This is referred as "controlled sound exposure" henceforth. ABR tests performed before and after controlled sound exposure to assess its effects negligibly contributed to the exposure, as they were limited to 50 repetitions each. Indeed, alone, they had no effect on *Pjvk*$^{-/-}$ mice hearing threshold (data not shown).

In a sample of P30 old *Pjvk*$^{-/-}$ mice (n = 8) with initial ABR thresholds inferior to 65 dB SPL, "controlled sound exposure" resulted in increased ABR thresholds in the 12-20 kHz frequency interval (corresponding to cochlear places where intense 10-kHz sound induces the largest hair-cell stimulations (Cody & Johnstone, 1981)). The ABR threshold increase was 21.7 ± 10.3 dB ($p < 0.001$) in *Pjvk*$^{-/-}$ mice whilst producing no effect in *Pjvk*$^{+/+}$ mice (n = 12) (2.2 ± 2.4 dB, p = 0.3) (Fig. 2D). *Pjvk*$^{-/-}$ mice immediately transferred in a silent environment after "controlled sound exposure", displayed a further elevation of their ABR threshold, reaching 33.7 ± 16.0 dB (n = 8), 2 days after exposure. It decreased to 23.7 ± 18.0 dB after 7 days and disappeared after 14 days. ABR threshold elevations of *Pjvk*$^{-/-}$ mice with initial ABR thresholds larger than 65 dB SPL (n = 8) showed a similar yet smaller trend, due to the ceiling effect of their already large initial hearing loss. The lack of pejvakin thus results in an inordinate vulnerability to very low acoustic energy, slowly reversible.

3. Hair cells, afferent auditory neurons and neurons of auditory brainstem pathways are targets of the pejvakin defect.

Which cells are the targets of the pejvakin defect, and are they all hypervulnerable to sound exposure? To address this issue, the outcomes of functional tests specific of various types of auditory cell were compared among *Pjvk*$^{-/-}$, hair-cell conditional knock-out for *pjvk* (*Pjvk*$^{fl/fl}$*Myo15*-cre$^{+/-}$) and *Pjvk*$^{+/+}$ 2-3 weeks old mice, at baseline and after "controlled sound exposure". Moreover, Electrically-Evoked Brainstem Responses (EEBR) to a direct electric stimulation of the auditory neurons, which test the response of the auditory pathway beyond

the cochlea, was also analysed. A "controlled electric exposure" (as it will be named henceforth), an electric-impulse stimulation rate of 200/s for a 1-min duration was delivered, as compared to 16/s and 10-s duration of the stimulus used for the pre and post-exposure EEBRs.

The inner hair cells (IHCs) are the genuine auditory sensory cells. Their responses to vibrations produced by tone bursts and amplified by the mechanical activity of OHCs trigger action potentials in the auditory neurons, which make up the auditory nerve. Synchronized action potentials in the peripheral part of this nerve generate ABR wave-I. In *Pjvk*$^{fl/fl}$*Myo15*-cre$^{+/-}$, as a result of pejvakin absence from the hair cells only, and stimulation condition in which the IHCs' response is made independent of the OHC activity by a sound stimulation intensity exceeding 90 dB SPL (Robles & Ruggero, 2001), ABR wave-I amplitude and latency specifically reflect IHC function. An increase of wave-I latency (1.58 ms in *Pjvk*$^{fl/fl}$*Myo15*-cre$^{+/-}$ (n=20), vs. 1.32 ms in *Pjvk*$^{+/+}$ littermates (n = 30); $p < 0.001$) and a decrease of wave-I amplitude (37% of the amplitude in control littermates; $p < 0.001$), incriminate IHC dysfunction in the hearing impairment caused by pejvakin defect. "Controlled sound exposure" induced further decreases of ABR wave-I amplitude in *Pjvk*$^{-/-}$ and *Pjvk*$^{fl/fl}$*Myo15*-cre$^{+/-}$ (48% and 55% of pre-exposure amplitude respectively compared to 108% in *Pjvk*$^{+/+}$ mice, $p < 0.001$; Fig. 3A). Pejvakin-lacking IHCs are thus defective and hypervulnerable to sound.

As shown above, OHCs, are also target cells of the pejvakin-defect. In *Pjvk*$^{-/-}$ mice with persisting DPOAEs (n=8), the "controlled sound exposure" produced an average increase in DPOAE threshold of 17.1 ± 6.7 dB in the 12 to 20 kHz frequency interval ($p < 0.0001$) whilst *Pjvk*$^{+/+}$ mice (n = 9) were unaffected ($p = 0.5$) (Fig. 3B). Pejvakin-lacking OHCs are thus also hypervulnerable to sound.

To investigate the influence of the absence of pejvakin on neural conduction whilst excluding any confounding effect of cochlear damage, we compared EEBR waves E II and E IV (easiest to reliably measure owing to their sharpness) between *Pjvk*$^{-/-}$ and *Pjvk*$^{fl/fl}$*Myo15*-cre$^{+/-}$ mice. The amplitudes of these waves did not differ (for wave E IV for example, average amplitudes were 2.6 ± 1.8 µV in *Pjvk*$^{-/-}$ mice (n = 18) as against 2.2 ± 1.2 µV in *Pjvk*$^{fl/fl}$*Myo15*-cre$^{+/-}$ mice (n = 11); t-test, $p = 0.13$). However upon controlled electric exposure, EEBR waves E II and E IV were reduced in amplitude by 41% and 47% respectively for at least 3 min, in *Pjvk*$^{-/-}$ mice (n = 10; $p = 0.02$ and $p = 0.012$ respectively) (Fig. 3D for E IV; E II not shown), in contrast with

Pjvk$^{fl/fl}$*Myo15*-cre$^{+/-}$ mice (n = 10), which were insensitive to controlled electric exposure even prolonged 10 min (Fig. 3D, 3G-3I). The interwave E II-E IV interval differed between *Pjvk*$^{-/-}$ mice and *Pjvk*$^{fl/fl}$*Myo15*-cre$^{+/-}$ (n = 10 for each group), by 0.41 ms (unpaired t-test; p = 0.003). Controlled electric exposure induced a further increase of interwave E II-E IV interval, of 0.15 ms, in *Pjvk*$^{-/-}$ mice (paired t-test, p = 0.001), whilst being ineffective in *Pjvk*$^{fl/fl}$*Myo15*-cre$^{+/-}$ mice (Fig. 3G-3I). Neural activity evoked by sound can also be assessed independent of OHC and IHC function by measuring the neuronal conduction time between ABR wave I and wave IV (the counterpart of wave E IV), which was increased beyond the normative interval in about one third of tested *Pjvk*$^{-/-}$ mice (n = 25) (Fig. 3C, 3E) and further increased in all *Pjvk*$^{-/-}$ mice in response to 'controlled sound exposure' (n = 16 ears with an ABR threshold < 95 dB SPL, average increase 0.16 ms relative to their pre-exposure value; p < 0.001, paired t-test) whilst both *Pjvk*$^{+/+}$ and *Pjvk*$^{fl/fl}$*Myo15*-cre$^{+/-}$ mice maintained normal interwave I-IV intervals (p = 0.5, paired t-test, for the two genotypes) (Fig. 3C, 3F). So as to clarify whether these anomalies are of neuronal or glial origin, a rescuing experiment was performed in *Pjvk*$^{-/-}$ mice using the murine pejvakin cDNA vectorised by the adenoviral associated vector 8, AAV8, which transduces exclusively neurons in the auditory pathway, from the auditory neurons to the brainstem, upon direct injection into the cochlea. All *Pjvk*$^{-/-}$ mice (n = 7) injected on P3 by AAV8-PjvkcDNA tested at P21, displayed normal ABR interwave I-IV intervals (Fig. 3J), and EEBR wave-E IV amplitude insensitivity to controlled electric stimulation (Fig. 3K, 3L, 1.91 ± 0.97 µV before and 1.87 µV ± 1.07 after; paired t-test, p = 0.5).

4. Redox metabolism anomalies in the absence of pejvakin

To address the pathogenesis of the hearing impairment of *Pjvk*$^{-/-}$ mice, it was first proceeded with the morphological analysis of their cochlea, by light microscopy on semithin sections and scanning (SEM) and transmission electron microscopy (TEM). On P15, hair cells and auditory neurons showed normal morphology and numbers. Notably, the OHC and IHC hair bundles, the mechanoreceptive structures to sound of the hair cells, analysed from P15 to P60 by SEM, and the ribbon synapses of the IHCs and their afferent auditory neurons studied by TEM, were unmodified (Fig. 4A and data not shown). On P30, a loss of a few OHCs (16 %), restricted to the base of the cochlea, tuned to high frequency sounds, was observed. From P30 onwards, OHCs and cochlear ganglion neurons, then IHCs, disappeared, and the sensory epithelium (organ of Corti) progressively degenerated.

Since the above-described physiological anomalies were already present in a broad range of frequencies in *Pjvk*$^{-/-}$ mice at P15, i.e. well before any morphologically abnormal features could be detected, the hearing impairment of young *Pjvk*$^{-/-}$ mice can be attributed to functional defects.

Possible changes in gene expression in *Pjvk*$^{-/-}$ organ of Corti, the cochlear sensorineural epithelium, were then investigated by microarrays in P15 old mice. Eighteen genes showed changes of their expression levels in *Pjvk*$^{-/-}$ mice above or below 1.5-fold relative to *Pjvk*$^{+/+}$ mice. Major changes were found in four genes involved in redox metabolism, specifically, *CypA*, *Gpx2, c-Dct*, and, *Mpv17*, which encode cyclophilin A, glutathione peroxidase 2, c-dopachrome tautomerase and Mpv17, respectively. All these genes displayed a down-regulated expression in *Pjvk*$^{-/-}$ mice, a result confirmed by quantitative RT-PCR (qRT-PCR), and all encode proteins with antioxidant function. Glutathione peroxidase 2 and cyclophilin A are involved in the reduction of hydrogen peroxide (H_2O_2) into H_2O, directly and indirectly *via* the activation of several peroxiredoxins, respectively (Lee et al., 2001; Evans & Halliwell, 1999). Although Mpv17 has a yet unknown activity, Mpv17-defect in both human and mouse results in a hepatocerebral mitochondrial DNA depletion syndrome with profound deafness (Binder et al., 1999) reported in the mutant mice and reactive oxygen species (ROS) accumulation (Meyer zum Gottesberge et al., 2001). Finally, c-dopachrome tautomerase decreases cell sensitivity to oxidative stress by increasing reduced glutathione (GSH) level, the major small antioxidant molecule of the cell (Michard Q et al, 2008a; 2008b). The antioxidant defence in the cochlea of 3 weeks old *Pjvk*$^{-/-}$ mice was then assessed by measuring the level of oxidized glutathione (GSSG) and the ratio between reduced and oxidized glutathione (GSH:GSSG). GSSG content was increased about 3 fold in *Pjvk*$^{-/-}$ cochlea compared to *Pjvk*$^{+/+}$ (1.80 ± 0.57 nmole/mg protein and 0.57 ± 0.12 nmole/mg protein, respectively; unpaired t-test, $p = 0.01$), whilst GSH level was moderately decreased in *Pjvk*$^{-/-}$ cochlea compared to *Pjvk*$^{+/+}$ (4.91 ± 0.80 nmole/mg protein and 6.42 ± 0.92 nmole/mg protein, respectively; unpaired t-test, $p = 0.05$). The ratio of GSH:GSSG decreased in *Pjvk*$^{-/-}$ cochlea compared to *Pjvk*$^{+/+}$ cochlea (3.45 ± 1.77 and 11.74 ± 1.90 in *Pjvk*$^{-/-}$ and *Pjvk*$^{+/+}$ cochlea, respectively; unpaired t-test, $p < 0.001$) (Fig. 5A). Increase in GSSG and decrease of the GSH:GSSG are markers of oxidative stress; taken together these results show that lack of pejvakin results in oxidative stress in the *Pjvk*$^{-/-}$ cochlea. Since Ca^{2+}-activated potassium (BK) channels are well known as target of ROS (Tang et al., 2004), we investigated whether the number of these channels is altered in *Pjvk*$^{-/-}$ IHCs. The mean number of spots immunolabelled for the BK α-subunit per IHC was much lower in *Pjvk*$^{-/-}$ mice (5.0 ± 1.4,

n = 283 IHCs from 7 mice) than in *Pjvk*$^{+/+}$ mice (13.9 ± 2.6, n = 204 IHCs from 9 mice; t-test, p < 0.001) (Fig 5B).

The presence of possible ROS damage in *Pjvk*$^{-/-}$ mice was thus tested. Lipids are natural targets of oxidation by ROS; 4-hydroxy-2-nonenal (4-HNE), a by-product of lipid peroxidation, was not immunodetected in P15 *Pjvk*$^{-/-}$ cochlea but both the hair cells and cochlear ganglion neurons were labelled in P30 *Pjvk*$^{-/-}$mice with a marked increase at P60 (Fig. 4B). We quantified lipid peroxidation in cochlear lysates from P30 *Pjvk*$^{-/-}$ and *Pjvk*$^{+/+}$ mice using the thiobarbituric acid-reactive substances (TBARS) colorimetric assay, which detects malondialdehyde (MDA), another end product of lipid peroxidation (Janero DR et al., 1990). Cochlea tested independently, gave consistent results, specifically, a 16% average increases in MDA content in *Pjvk*$^{-/-}$ (2.15 ± 0.14 µM) compared to *Pjvk*$^{+/+}$ (1.84 ± 0.11 µM) mice (unpaired t-test, p = 0.04). These results suggested that *Pjvk* defect results in an antioxidant metabolism failure progressively leading to ROS cellular damages.

5. Pejvakin is a peroxisomal protein

In order to assess the subcellular localization of pejvakin, HeLa cells were transfected with recombinant vectors expressing the GFP-tagged C-terminal or N-terminal regions of mouse pejvakin and obtained a diffuse labelling throughout the cytoplasm. Pejvakin detection by immunolabeling also turned out to be unsuccessful, as none of the antibodies (commercially available or generated in the lab), specifically recognized this protein. Considering the very limited sequence divergence of pejvakin amino-acid sequence among vertebrates, it was attempted to elicit an antibody response in *Pjvk*$^{-/-}$ mice. A monoclonal antibody (Pjvk-G21) was obtained, that revealed a punctate immunostaining throughout the cytoplasm of transfected HeLa cells expressing pejvakin, absent in non-transfected cells. Co-staining with a marker of peroxisomes (peroxisome membrane protein 70, PMP70) revealed a strict colocalisation between pejvakin and peroxisomes (Fig. 7A). Our observations were extended to transfected HEK cells and COS-7 cells (not shown). Finally, in the human hepatoblastoma cell line HepG2, particularly rich in peroxisomes, a strong endogenous pejvakin-immunolabelling was detected, strictly localised at the peroxisomes (Fig. 6A and 6B). The specificity of the Pjvk-G21 antibody was demonstrated by the immunolabelling of peroxisomes in the hair cells of *Pjvk*$^{+/+}$, but not *Pjvk*$^{-/-}$ and *Pjvk*$^{fl/fl}$Myo15-*cre*$^{+/-}$ mice (Fig. 7B).

6. Pejvakin role in peroxisome proliferation

In HepG2 cells, protrusions emerging from some peroxisomes, the first step of peroxisome biogenesis from pre-existing peroxisomes, were immunoreactive for pejvakin. String-of-beads structures corresponding to elongated and constricted peroxisomes, preceding final fission (Smith and Aitchison, 2013), were also pejvakin-immunoreactive, suggesting a role of this protein in peroxisome proliferation (Fig. 7C). HeLa cells were transfected with constructs encoding either GFP alone (GFP), or the normal form (Pjvk-GFP) or one of the six mutated forms (mutPjvk-GFP) of mouse pejvakin, carrying the causative mutations of *DFNB59* reported so far, p.T54I, p.R183W, p.C343S, and p.V330L*fs*X7. Thirty hours later, the peroxisomes labelled by PMP70 were analysed in GFP expressing cells. A 27.2 % increase of the peroxisome density was observed in Pjvk-GFP expressing cells as compared to GFP cells ($p < 0.001$; Fig. 6D and 8). In contrast, cells expressing the mutated forms of pejvakin, whatever the mutation, displayed a significant decrease in peroxisome density compared to cells expressing the normal form of pejvakin ($p < 0.001$ for each mutation ; Fig. 6D and 8). No difference in the number of elongated peroxisomes (measuring less than 0.4 µm in one dimension and more than 0.4µm in the perpendicular dimension (< 0.4 µm x > 0.4µm)) per cell was observed, ($p > 0.05$ for each mutation; Fig. 6D). In contrast, the percentage of transfected cells containing enlarged peroxisomes, that is with an area exceeding 0.4 x 0.4µm in two perpendicular dimensions (>0.4 µm x >0.4µm) was 3 to 4 fold higher among mutpjvk-GFP cells expressing any of the four mutations tested than in GFP or Pjvk-GFP expressing cells for every mutation (Fig. 6D); the number of these enlarged peroxisomes per cell displayed a modest (32%-40%) but significant increase in mutPjvk-GFP expressing cells compared to non-transfected cells or GFP or pjvk-GFP cells (p.R183W, p.C343S and: $p < 0.05$, p.T54I and p.V330LfsX7; $p < 0.01$), whatever the mutation (Fig. 6D).

Both the decrease of peroxisome density and the development of enlarged peroxisomes in cells expressing the mutated forms of pejvakin suggested that mutation in pjvk results in a defect of peroxisome proliferation.

Based on these results, peroxisome distribution and morphology in *Pjvk*$^{-/-}$ mice were investigated. Peroxisomes in *Pjvk*$^{-/-}$ and *Pjvk*$^{+/+}$ cochlea were labelled using *catalase* detection by *3,3'-diaminobenzidine (DAB)* and analysed in transmission electron microscopy (TEM ; Fig. 6E). It was focused on OHCs, the cells that display the earliest dysfunctioning. In P15 mice, no

differences regarding the distribution and the shape of peroxisomes were detected in *Pjvk*$^{-/-}$ and *Pjvk*$^{+/+}$ mice. In contrast at P30, the peroxisome subcellular distribution and morphology were clearly distinct in *Pjvk*$^{-/-}$ and *Pjvk*$^{+/+}$ mice. The total number of peroxisomes per cell remained similar in *Pjvk*$^{-/-}$ and *Pjvk*$^{+/+}$ mice (*Pjvk*$^{+/+}$ = 2.45 vs. *Pjvk*$^{-/-}$ = 2.12 ; Fig. 6E). In *Pjvk*$^{+/+}$ mice, peroxisomes were strictly localized just beneath the cuticular plate, a rigid network of actin filaments immediately below the apical surface of the hair cells. Strikingly, in *Pjvk*$^{-/-}$ mice, peroxisomes were observed underneath the cuticular plate and irregular catalase labelled structures were observed with no visible membrane in the perinuclear region. The catalase positive (catalase^{+}) area of such perinuclear peroxisomes is significantly larger compared the one of peroxisomes present at the cuticular plate from either *Pjvk*$^{+/+}$ or *Pjvk*$^{-/-}$ mice (catalase^{+} area of perinuclear peroxisomes from *Pjvk*$^{-/-}$ mice: 0.11µm^2 vs catalase^{+} area of peroxisomes present at the cuticular plate from *Pjvk*$^{+/+}$ mice: 0.04µm^2, vs catalase^{+} area of peroxisomes present at the cuticular plate from *Pjvk*$^{-/-}$ mice: 0.05µm^2, $p < 0.001$ in both cases). Such structures were never observed in *Pjvk*$^{+/+}$ mice (Perinuclear peroxisomes /cell: *Pjvk*$^{+/+}$ 0.00 vs. *Pjvk*$^{-/-}$ 1.54, $p < 0.001$) (Fig. 6E). Moreover peroxisomes just below the cuticular plate were slightly but significantly larger and also less numerous in *Pjvk*$^{-/-}$ compared to *Pjvk*$^{+/+}$ mice (peroxisome area *Pjvk*$^{+/+}$ 0.125 vs. *Pjvk*$^{-/-}$ 0.16 µm^2, $p < 0.05$, and peroxisomes at the cuticular plate /cell *Pjvk*$^{+/+}$ = 2.45 vs *Pjvk*$^{-/-}$ = 1.91) (Fig. 6E). No mitochondria ultrastructural anomaly was observed; their morphology and localisation were indistinguishable in P30 *Pjvk*$^{+/+}$ and *Pjvk*$^{-/-}$ mice.

Because *Pjvk*$^{-/-}$ mice displayed features of marked oxidative stress in the cochlea, we investigated the possible role of pejvakin in peroxisome proliferation in response to oxidative stress induced by H_2O_2 (Lopez-Huertas et al., 2000). Embryonic fibroblasts derived from *Pjvk*$^{+/+}$ and *Pjvk*$^{-/-}$ mice were exposed to H_2O_2 (see Extended Experimental Procedures). In unexposed cells, the number of peroxisomes was similar between the two genotypes (t-test, $p = 0.82$). After H_2O_2 treatment, it increased by 46% in *Pjvk*$^{+/+}$ fibroblasts ($p = 0.004$), but remained unchanged in *Pjvk*$^{-/-}$ fibroblasts ($p = 0.83$), resulting in a statistically significant difference between the two genotypes ($p < 0.001$; Figures 6C).

The lack of pejvakin thus results in an *in vivo* peroxisomal morphological defect that occurs after hearing onset.

7. Pjvk transcriptional regulation belong to the adaptative response to sound

It was then asked whether this pathological condition was relevant to the cochlear physiological response to sound. Noise overexposure is known to induce oxidative stress due to the overproduction of oxygen species resulting from cellular hyperactivity that overwhelm the antioxidant defence of the cells. Could transcription of the *pjvk* gene be modulated by sound exposure? The level of *Pjvk* transcripts and of *CypA*, *Gpx2, c-Dct*, and *Mpv17* transcripts, the down regulated genes observed in *Pjvk*$^{-/-}$ mice, were first measured in microdissected organs of Corti from non-stimulated and over-stimulated by sound (5-40 kHz, 105 dB SPL for 1 hour) P21 wild-type mice, at various times (1, 3, 6, and 18 hours) after the sound exposure, by qRT-PCR (Fig. 9A). *Pjvk* transcripts increased 2-fold after 1hr, reaching 4-fold after 6 hours. *CypA*, *c-Dct*, and *Mpv17* also showed an up regulation, as well as *c-Fos* and *Hsp70* used as a positive control, but not *Gpx2*. This increase reached up to 6.26 and 8.71-folds for *c-Dct* and *CypA*, respectively, but was only 2 fold for *Mpv17*.

In contrast to sound overexposure that produces a permanent auditory thresholds shift (PTS), exposure to low acoustic energy can result in a temporary thresholds elevation (TTS), which indicates a reversible stress of the cochlea. A TTS is evoked by sound preconditioning, which refers to a low energy sound stimulation that exerts a protective effect against a subsequent sound overexposure (Roy et al., 2013). To test whether pejvakin transcriptional up-regulation could also be implicated in sound-preconditioning, P21 mice were exposed to standard preconditioning sound stimulation (5-40 kHz at 90 dB SPL for 2 hours) (Roy et al., 2013), and the expression level of *Pjvk, c-Dct, CypA* was measured after 6 hours by qRT-PCR. Sound preconditioning up regulated the expression of *Pjvk* and *CypA* (2.69 ± 0.42 fold and 3.99 ± 1.32 fold, respectively) but not of *c-Dct* (Fig. 9B). These results showed that *Pjvk* and *CypA* transcriptional regulation belongs to the physiological response to noise and are likely involved in the early antioxidant protective pathway.

8. Hypervulnerability to sound of DFNB59 affected patients

Finally, it was asked whether hearing of DFNB59 patients was also hypervulnerable to sound exposure. Five patients carrying the p.T54I mutation who were living in Iran were tested (Delmaghani et al., 2006). Transient-evoked OAEs (TEOAEs) testing OHC function over a broad range of frequencies were analysed. All patients had bilateral broadband TEOAEs despite pure-

tone audiograms showing severe hearing impairment (from 66 dB HL at 250 Hz to 84 dB at 8 kHz).

To test their possible hearing hypervulnerability to sound, a minimal sound exposure eliciting ABRs was used. ABR waves were clearly identified in response to 250 impulse stimuli –clicks- at 99 dB above normal detection threshold. Extending sound exposure to 1000 stimulus presentations (the standard clinical procedure for ABR recording), spectacularly affected ABR waves. The equivalent of mouse ABR-wave IV, wave V, the most reliably spotted wave after the shortest sound exposure, 250 clicks, exhibited after 500 then 1000 clicks, a progressive decrease in amplitude (to 39 ± 30% of its initial amplitude, Fig. 10C, left boxplot, and Fig. 10A) and an increase in latency (of 0.30 ± 0.15 ms, right panel of Fig. 10D, left boxplot, and Fig. 10A). The interwave latency I-V also increased by 0.30 ± 0.15 ms. Full recovery of wave-V amplitude and latency was obtained after 10-min in silence (Fig. 10B). In a control group of patients with matched ABR thresholds and sensorineural hearing impairments of cochlear origin, the same sound stimulation, even extended to 4000 clicks, had no influence on ABR wave amplitude (105 ± 14% of its initial amplitude after exposure; n = 13) or latency (-0.02 ± 0.07 ms post-exposure change; Fig. 10C and 10D, right boxplots).

Therefore, in DFNB59 patients as in pejvakin-deficient mice, IHC, OHC, and neuronal responses are affected by abnormally low energy sound-exposure.

These results predicted that sound-exposure would lead to peroxisome proliferation in the auditory system of wild-type mice. Six hours after exposure (5-40 kHz, 105 dB SPL for 1 hour), the numbers of peroxisomes were unchanged (34.5 ± 0.8 and 35.9 ± 1.0, mean ± SEM, per IHC from unexposed and sound-exposed mice, respectively, n = 75 cells from 6 mice; t-test, p = 0.25). However, at 48 hours, they had markedly increased, by a factor of 2.3, in both IHCs and OHCs (84.7 ± 5.0 per IHC and 16.5 ± 1.0 per OHC, n = 90 cells and n = 150 cells from 6 mice, respectively) compared to unexposed mice (36.8 ± 3.0 per IHC and 7.3 ± 0.4 per OHC, n = 90 cells and n = 150 cells from 6 mice, respectively; t-test, $p < 0.0001$ for both comparisons). The number of peroxisomes had also increased, by 35%, in the dendrites of primary auditory neurons (1.7 ± 0.1 and 2.3 ± 0.2 peroxisomes per µm of neurite length, n = 40 neurites from 5 unexposed and 5 sound-exposed *Pjvk*$^{+/+}$ mice, respectively; t-test, p = 0.003 ; Fig. 11).

9. Therapeutic approaches of the DFNB9 form of deafness

The above results validate *Pjvk*$^{-/-}$ mice as a model to investigate therapeutic approaches for human deafness. Based on these results, the effect of antioxidants was tested on the auditory function of *Pjvk*$^{-/-}$ mice. N-acetyl cysteine, the most common antioxidant, and taurine, were ingested by mothers during and after pregnancy so that pups received them from birth on by feeding on the mother's milk. When tested around P21, treated *Pjvk*$^{-/-}$ pups (n = 21) raised in batches of about 10, i.e., maximally exposed to natural sound exposure, had for most of them, no DPOAE, thus N-acetyl cysteine and taurin had no beneficial effect on OHCs. The ABR thresholds were however slightly improved only in NAC-treated *Pjvk*$^{-/-}$ pups compared to those of untreated *Pjvk*$^{-/-}$ pups (n = 24) (e.g. at 10 kHz, 72.2 ± 9.3 dB SPL, as against 84.4 ± 6.3 dB SPL, $p < 0.001$) (Fig. 12A). The amplitude of ABR wave I in response to 105 dB SPL (which bypasses OHC activity) was similar to age-matched *Pjvk*$^{+/+}$ mice (n = 18) in NAC-treated *Pjvk*$^{-/-}$ mice, in contrast with untreated mice (4.35 ± 1.16 μV, as against 4.36 ± 1.15 μV in *Pjvk*$^{+/+}$ mice, but only 1.88 ±1.07 μV in untreated *Pjvk*$^{-/-}$ mutants, ANOVA, $p < 0.001$; Fig. 12B). ABR wave I latencies did not significantly shorten under treatment (1.55 ± 0.18 ms as against 1.62 ± 0.34 ms in untreated mutants, both being similarly longer than controls, 1.30 ± 0.08 ms; ANOVA, $p < 0.001$ between controls and mutants; Fig. 12C). Likewise, ABR interwave I-IV latencies hardly responded to treatment (2.91 ± 0.32 ms in treated pups, 2.68 ± 0.13 ms in controls, as against 2.98 ± 0.35 ms in untreated mutants; Fig. 12D). The EEBRs of N-acetyl cysteine treated animals resisted to high-rate electric stimulation of auditory pathways better than untreated *Pjvk*$^{-/-}$ mice (Fig. 12E). Full recovery of neuronal function was obtained 5 min after high-rate exposure in treated mice. (Fig. 12F), as opposed to an absence of recovery at that time in untreated mice. This suggests a moderate protective effect of IHCs and neurons by N-acetyl cysteine.

Because a full recovery of the neural phenotype was obtained by intracochlear injection of AAV8 expressing the murine *Pjvk* cDNA, the potential of AAV2/8, which transduces hair cells exclusively, to rescue the hair-cell phenotype was tested in *Pjvk*$^{-/-}$ mice (n= 7). Auditory function of *Pjvk*$^{-/-}$ mice injected on P3 by this vector expressing the pejvakin cDNA (mPjvk-IRES-GFP) were examined at P21 and the percentage of transduced by IHC and OHC in every cochlea was evaluated by the fluorescence of GFP. A partial reversion of OHC function with detectable DPOAEs was obtained, with a decrease in DPOAE thresholds (from 80 dB in untreated ears, to 57.1 ± 14.7 dB in treated ears), with a highly significant linear correlation ($R^2 = 0.72$, $p < 0.001$)

with the number of GFP-tagged OHCs in the treated ear (Figures 13A and 13B). Its linear extrapolation suggests that the DPOAE threshold might be normalized if more OHCs could be treated. As a result of improved OHC function, ABR thresholds improved, e.g. at 10 kHz, from 85.7 ± 9.3 dB SPL in the contralateral ears, to 51.1 ± 15.3 dB SPL in the treated ears. The amplitude of ABR wave I in response to 105 dB SPL stimulations fell within the normative range in treated ears (7.0 ± 2.3 μV (n = 6) compared to the contralateral ears (2.3 ± 1.1 μV)) (Fig. 13C), and a highly significant correlation was observed (R^2 = 0.89, p < 0.001) with the number of GFP-tagged IHCs in the treated ears (Fig. 13D), which indicates reversion to a normal phenotype in transduced IHC.

Finally, the effect of the transduction of *Pjvk*$^{-/-}$ IHCs by AAV2/8-Pjvk-IRES-EGFP on their peroxisomes was investigated. Before sound-exposure, the numbers of peroxisomes in IHCs of P21 *Pjvk*$^{-/-}$ and AAV2/8-Pjvk-IRES-EGFP injected *Pjvk*$^{-/-}$ mice did not differ from that of *Pjvk*$^{+/+}$ mice (30.5 ± 1.9, 32.3 ± 2.1, and 36.8 ± 3.0 peroxisomes, mean ± SEM per IHC, n = 60 cells from 4 *Pjvk*$^{-/-}$ and 4 AAV2/8-Pjvk *Pjvk*$^{-/-}$ mice, and n = 90 cells from 6 *Pjvk*$^{+/+}$ mice, respectively; t-test, p = 0.11 and p = 0.30, respectively). By contrast, 48 hours after sound-exposure (5-40 kHz) at 105 dB SPL for 1 hour, the number of peroxisomes had decreased by 63% in *Pjvk*$^{-/-}$ IHCs (30.5 ± 1.9 and 11.2 ± 1.3 peroxisomes per IHC, n = 75 cells from 5 unexposed and 5 sound-exposed *Pjvk*$^{-/-}$ mice, respectively; t-test, p < 0.0001), and enlarged PMP70-labeled structures were present close to the nucleus (Fig. 14). In response to the same sound but of a lower intensity, i.e. 97 dB SPL for 1 hour, the number of peroxisomes was unchanged in *Pjvk*$^{-/-}$ IHCs (30.5 ± 1.9 and 34.6 ± 2.3 peroxisomes per IHC, n = 60 cells from 4 unexposed and 4 sound-exposed *Pjvk*$^{-/-}$ mice, respectively; t-test, p = 0.17), and no enlarged PMP70-stained structures were detected (data not shown). The absence of pejvakin thus resulted in defective sound-induced peroxisomal proliferation (both at 105 dB SPL and 97 dB SPL), and even, in peroxisome degeneration (at 105 dB SPL) in IHCs. In *Pjvk*$^{-/-}$ mice injected with AAV2/8-Pjvk-IRES-EGFP on P3 and exposed to 105 dB SPL for 1 hour on P21, enlarged PMP70-labeled structures were no longer detected in transduced IHCs, and the number of peroxisomes increased by 35% (32.3 ± 2.1 and 43.7 ± 3.0 peroxisomes per IHC, n = 60 cells from unexposed and exposed transduced *Pjvk*$^{-/-}$ IHCs, respectively; t-test, p = 0.002) (Fig. 14). We conclude that pejvakin re-expression fully protects *Pjvk*$^{-/-}$ IHCs from the degeneration of peroxisomes, and partially restores their impaired adaptive proliferation.

These results show that gene therapy approaches could provide protective or therapeutic opportunities in DFNB59 affected patients.

DISCUSSION

Noise overexposure is a major and increasingly prevalent cause of hearing loss accounted for by the overcrowding of the towns and the overuse of portable music players by younger children, worldwide. Noise-induced hearing loss (NIHL), considered as the most preventable and treatable/remediable hearing impairment, currently does not benefit of efficient therapeutic intervention. This situation echoes the still limited information regarding its underlying pathogenic processes as well as its genetic susceptibility. The above-disclosed results uncovered a new origin of NIHL by showing that pejvakin defect in mouse and human (DFNB59 patients) leads to a hypervulnerability to sound due to a peroxisomal deficiency. No such a hypersensitivity to sound has ever been reported. This study introduces the peroxisome as a key regulatory organelle of the redox homeostasis of the auditory system, pivotal to cope with ROS overproduction induced by high acoustic energy. It shows that pejvakin is involved in peroxisome proliferation. This understanding pinpoints hearing impairment in DFNB59 patients as calling for a specific management and suggests that pejvakin and the proteins of its associated networks may be useful for preventing and curing NIHL.

Acoustic energy is the main factor that determines the damaging effects of exposure to loud sounds. The so-called Lex index for workplace noise exposure has been introduced to calculate the energies delivered by sounds of different levels and time courses in order to evaluate and compare their detrimental potential (see material and methods). The legal limit in western countries varies from 80 to 90 dBA Lex, an acoustic energy not leading to a permanent threshold shift (PTS). In *Pjvk*$^{-/-}$ mice a single exposure to a 63 dBA Lex produces an about 30 dB hearing threshold elevation. As the dB scale is a logarithmic one, a 3-dB increase translates in a two-fold increase in energy, and a 10-dB increase in a ten-fold increase in energy. Up until now, the lowest dBA Lex reported as producing an elevation of the hearing threshold in wild type mice of the same background strain as *Pjvk*$^{-/-}$ mutants was 73 dB (10 times fold more energetic) (Housley G, 2013). Moreover it was a temporary threshold shift (TTS) of only 18 dB with a recovery time constant of twelve hours compared to the threshold shift of 30 dB with a recovery time constant of about one week in *Pjvk*$^{-/-}$ mice. The second observation herein made, is that the natural acoustic environment of a mouse litter, due to pup cries in relation to feeding and crowding, is about 83 dBA Lex in a cage of 10 pups (100 times fold more energetic than the sound exposure affecting hearing threshold of *Pjvk*$^{-/-}$ mice) during the few days from the onset of hearing to weaning. This possible effect of this natural exposure to high acoustic

energy has been overlooked so far in the studies carried out on NIHL. Based on the present results, it should be systematically taken into account in future works addressing the origin of the variability of the hearing threshold in the mouse. Because transduction in hair cells begins to operate more and more efficiently with the progressive increase of the endocochlear potential from P5 to P17 (Sadanaga and Morimitsu, 1995), this raises the possibility that hearing loss in *Pjvk*$^{-/-}$ mice might be due entirely to naturally occurring sound exposure. Consistently when mouse pups are kept in small numbers (pups n=2) with foster mothers and in quiet rooms, their hearing thresholds is 30 dB lower, on average (and 60 dB lower, in some individuals) than their littermates maintained in their regular sound environment. DFNB59 patients, who carry deleterious mutations in *PJVK*, also display an astonishing sound sensitivity, since it is evidenced under the standard conditions used in clinics to record ABRs in response to impulse sounds. At a 57 dBA Lex, these sounds, routinely used for audiological diagnosis at much higher levels induced in all tested DFNB59 patients large changes in their evoked responses, with an increase in latency of all identifiable waves, which often exceeded 0.5 ms for wave V, and a two- to three-fold decrease in amplitude of these waves. Such changes are never observed in a sample of 13 patients with matched hearing thresholds and auditory profile could be exposed to at least four times as much acoustic energy without suffering any change in latency or amplitude of their auditory evoked potentials. These hearing features unique to DFNB59 patients, and akin to auditory fatigue, were reversible after 10 min in silence.

The effects of loud sound of excessive energy are two-pronged, - mechanical alterations affecting the stereocilia bundles including inter-stereociliary links and the cell-cell junctions of the auditory hair cells and - cellular hyperactivity related disturbances leading to an excessive release of glutamate by the IHC synapses that results in excitotoxicity, characterized by a swelling of the post-synaptic dendrites of their afferent neurons. A strong emphasis is increasingly placed/put on the contribution of oxidative stress to NIHL, a condition in which the production of ROS, including oxygen-based free radicals and hydrogen peroxide, H_2O_2, exceeds the capacity of the antioxidant defence systems, and subsequently creates oxidative cellular damages of DNA, proteins and lipids becoming progressively irreversible (Henderson et al., 2006). Superoxide radical ($O_2^{\cdot-}$) and the hydroxyl radical ($OH^{\cdot}$), have indeed been observed in the cochlea after noise exposure (Yamane et al., 1995; Ohlemiller et al., 1999b; Ohinata et al., 2000; Yamashita et al., 2004). Also supporting the key role of the oxidative stress in NIHL, defect in Cu/Zn superoxide dismutase, SOD1 that converts $O_2^{\cdot-}$ in H_2O_2 (Ohlemiller et al.,

1999a), and in glutathione peroxidase 1 (*Gpx1*) that reduces H_2O_2 in H_2O (Ohlemiller et al., 2000), both proposed to lead to H_2O_2 accumulation, and an increase of susceptibility to NIHL. The present work establishes that the defect in pejvakin impacts the cellular redox status of the auditory system followed by ROS induced cellular damages: *(i)* in *Pjvk*$^{-/-}$ mice already at P15, whilst no morphological anomalies can be detected, the down regulated expression of *Mpv17, CypA*, *Gpx2 and c-Dct* indicate that the organ of Corti is submitted to an oxidative stress: an increase of ROS production (*Mpv17)* and a decrease in the reduction of H_2O_2 (*CypA*, *Gpx2, c-Dct*) then converted in $OH^{\cdot}$ by the Haber-Weiss and the Fenton reactions, are indeed predicted *(ii)* at around P21, markers the oxidative stress, the increase in GSSG as well the decrease in GSH:GSSG ratio, are observed *(iii)* at P30, lipid peroxidation by $OH^{\cdot}$ in hair cells and auditory neurons reveals ROS induced cellular damage *(iv)* hair cell and auditory neuron loss present throughout the cochlea but the apical region from P60 onwards (data not shown). OHCs, display an especially high vulnerability to noise, whilst IHCs are also susceptible but to a lesser degree (Wang et al., 2002). Sound vulnerability is well known to extend to the primary auditory neurons (that compose the spiral ganglion nerve) (Kujawa and Liberman, 2009), as well as the central auditory pathways including the cochlear nucleus, the inferior colliculus and even the auditory cortex (Imig and Durhan, 2005; Basta et al., 2005; Pienkowski and Eggermont, 2009). Of note *Pjvk*$^{-/-}$ mice, *Pjvk*$^{fl/fl}$*Myo15*-cre$^{+/-}$ mice and rescuing targeted to auditory neurons or hair cells, unambiguously show that all the cells here explored, the sensory hair cells (with a more pronounced effect on the OHCs), the primary auditory neurons and neurons of the brainstem, are indeed hypervulnerable to sound in the absence of pejvakin.

Noise exposure highly solicits the mitochondrial activity to generate large amount of ATP through aerobic respiration which in parallel produces ROS (Ohlemiller et al., 1999b) and its intermediate of formation, H_2O_2. In particular, $O_2^{\cdot-}$, a by-product of the mitochondrial oxidative phosphorylation, is generated through the capture of an electron (derived from the activity of complex I and complex III) by molecular oxygen, O_2. Recent results further documented this ROS production by showing that the decrease of mitochondrial NAD^+ induced by noise exposure, reduces the activity of sirtuin 3, a mitochondrial NAD^+-dependent deacetylating/deacylating enzyme which is essential to the functioning of numerous mitochondrial enzymes (He et al., 2012; Han and Someya, 2013).

The association of pejvakin with peroxisomes and the structural alterations of peroxisomes in *Pjvk*$^{-/-}$ mice, including the presence peroxisome-derived matrix in the perinuclear region, reminiscent of the translocation of damaged mitochondria at the same emplacement (Okatsu et al., 2010), unveiled the first peroxisomal origin of an isolated form of inherited deafness. This peroxisomal deficiency in addition underlies an auditory phenotypic variability that has no equivalent so far, and that can be attributed to a hypersensitivity to natural environmental noise. No attention has been payed to this organelle in the auditory system so far, with the exception of a recent report indicating that cultured organ of Corti in the presence of a proteasome inhibitor leads to hair cell degeneration associated with peroxisome dysfunction (Lee et al., 2015). In the various forms of Zellweger syndrome, the most severe peroxisome biogenesis disorders (peroxisomes can be undetectable), sensory hearing impairment has been reported. Probably due to the focus on the associated impaired vital functions which includes a ubiquitous failure of neuronal conduction, auditory tests have not been extended beyond ABRs threshold measurements. The defective neuronal conduction has been attributed to the faulty synthesis of two essential components of the myelin sheaths, plasmalogens and DHA (docosahexaenoic acid), which is critically dependent on peroxisomes, and this conclusion extended to the pathogenesis of the hearing defect. Our results suggest that this hypothesis should be revisited. Contrary to peroxins defective in Zellweger syndrome, our results point to an essential role of pejvakin, restricted to cells of the auditory pathway. This is in line with the well-known extreme diversity of the peroxisomes in shape, density and protein/enzyme equipment and concentration, from one cell type to another, which may explain that, although expressed in a large variety of cells, pejvakin may be essential only in a few. Also contrary to peroxins, pejvakin is dispensable for the constitutive biogenesis of peroxisomes, and the structural failures of this organelle become apparent only in the context of the redox stress elicited by sound. In principle, sound hypervulnerability of *Pjvk*$^{-/-}$ mice may be the manifestation of an exacerbation by sound of pre-existing redox homeostasis failure, with at ultimate stage, perinuclear inclusions containing catalase and probably other factors too, contributing to cell degeneration. However *Pjvk* transcriptional up-regulation in wild type mice, immediately upon a sound exposure, whether being traumatic (leading to PTS) or protective (leading to PTS) that is likely involving in the immediate adaptive antioxidant response to noise, pinpoints the existence of a peroxisomal response as part of the physiological response to high acoustic energy. The ability of the peroxisomes to rapidly adapt to the demand created by changes in environmental and physiological conditions, thanks to a

panel of possible adjustments (dynamic shape and size changes, proliferation, degradation, and modification of their molecular content), grants them with an amazing functional plasticity. These organelles, actively contribute to cellular redox homeostasis by producing (by its rich content in oxidases, SOD1, and SOD2) and degrading H_2O_2 ($O2^{\cdot-}$ being possibly also involved in this transduction) by peroxidases (Schrader and Fahimi, 2006; Bonekamp and Schrader, 2009; Fransen et al., 2012).

Transfection experiments indicate that pejvakin is involved in peroxisome proliferation. Although its exact role in this process cannot be directly inferred from the changes of peroxisome shapes observed upon expression of mutated forms of pejvakin, the observed enlarged and spherical-like PMP70 positive structures, indicates the involvement of pejvakin in the pathway leading to the formation of new peroxisomes from pre-existing peroxisomes. This pathway, referred to as growth and fission cycle, is faster than the other one, the *de novo* formation in which peroxisomes form from endoplasmic reticulum derived vesicles (for a review see Smith and Aitchison, 2013). The growth and fission cycle involves the emergence of an elongation from pre-existing spherical peroxisomes. This elongation process is mediated by Pex11β and Pex11α (Delille et al., 2010; Koch et al., 2010; Li et al., 2002; Schrader et al., 1998), which consistently were associated with 70% and 55% of the pejvakin stained peroxisomes in HepG2 cells. Moreover, stress-induced peroxisome formation pathway, involves the recruitment of COP1, which promotes membrane protrusion at the elongation initiation site (Lay et al., 2006; Passreiter et al., 1998), where pejvakin colocalises. Altogether the present results provide evidence that sound-stress evokes a pejvakin-dependent peroxisomal response that leads to the generation of new peroxisomes from pre-existing ones. They also involve the peroxisome in redox signalling pathway elicited by sound, that likely uses H_2O_2, as signal molecule. In coherence, H_2O_2 has been shown to up-regulate the expression of peroxisome biogenesis genes (Lopez-Huertas et al., 2000) and induced elongation of the peroxisomes has been blocked by antioxidants (Schrader et al., 1999). Other roles could be ensured by this pejvakin-dependent stress-induced proliferation of peroxisomes, such as a matrix import of ROS degrading or scavenging molecules within peroxisomes (Motley, 2007) or a regulation of the activity of their redox enzymes by their changes in shape (Lizana, 2008). Of note, whilst peroxisome proliferation has been reported either to induce oxidative stress (Reddy et al., 1980) or to reduce ROS production (Santos et al., 2005; Diano et al., 2011), the rapid transcriptional up regulation response already set up one hour after sound exposure and in

addition observed under PTS generating conditions, as well as the early massive oxidative stress detected in *Pjvk*$^{-/-}$ mice, argue for an antioxidant role of pejvakin-dependent peroxisomal proliferation in the context of noise-induced oxidative stress. Finally, the transcriptional down-regulation of *CypA* encoding cyclophilin A and *c-Dct* encoding the dopachrome tautomerase, in *Pjvk*$^{-/-}$ mice and conversely, their transcriptional up-regulation (limited to the highest energy sound tested for *c-Dct*) associated with the transcriptional up-regulation of *Pjvk* in response to sound exposure in wild type mice, indicates that these proteins may belong to the same redox homeostasis pathway.

The conclusion is that as a result of peroxisomal deficiency, ROS metabolism is perturbed enough, so that sound of normally harmless energy can become harmful, has never been brought forward or tested, as done here in DFNB59 patients and *Pjvk*$^{-/-}$ mice. In patients, conventional intervention in case of sensorineural hearing impairment includes sound amplification by hearing aids and cochlear implant fitting, depending on the degree of impairment. However, conventional hearing aids, routinely used in severely hearing-impaired patients, might have harmful results in DFNB59 patients, as exposure to amplified sound is expected to lead to long-lasting damage to cochlear sensory cells and auditory neurons. Cochlear implant, an acoustico-electronic device that bypasses the cochlea and delivers a direct electrical stimulation to the primary auditory neurons, which is particularly beneficial for patients affected by profound deafness of cochlear origin, should similarly increase ROS in these neurons, thereby threatening their long-term survival. In both cases, specific protection against the production or the effects of the ROS is anticipated to be mandatory. However, used alone in the absence of pejvakin, N-acetyl cysteine, the most effective antioxidant drug here observed, had only a limited impact on the sensory hair cells although it reduces some adverse effects of controlled sound exposures in *Pjvk*$^{-/-}$ mice, restoring in particular the number of auditory neurons able to respond in synchrony to a loud tone-burst. Molecules targeting ROS metabolism might thus provide some benefice to DFNB59 patients. Moreover, our results on AAV-mediated Pjvk-cDNA transfer in *Pjvk*$^{-/-}$ mice clearly show that gene therapy has the potential to fully protect all these cells. Finally, after an acoustic trauma, subjects often experience protracted worsening of their hearing lesions in relation to disrupted ROS cellular homeostasis, which *Pjvk* gene therapy could improve.

GENE THERAPY FOR TREATING USHER SYNDROME

BACKGROUND OF THE INVENTION

As yet described above, hearing impairment – herein defined as referring to any hearing defect that can either be congenital or not – is a major concern and a serious burden for Public health.

The early-onset forms of severe deafness are mostly genetic in origin and are frequently due to sensory hair cells defect.

In particular, Usher syndrome (USH) is an autosomal recessive disease that affects both the inner ear and the retina. It is the most frequent cause of hereditary deaf-blindness, affecting 1 child in 25,000.

The following three USH clinical subtypes have been defined:

- USH type I (USH1), the most severe, involves severe to profound congenital sensorineural deafness, constant vestibular dysfunction and retinitis pigmentosa with prepubertal onset;
- USH2 differing from USH1 mainly in the deafness being less severe, the absence of vestibular dysfunction and the onset of retinitis pigmentosa after puberty; and
- USH3 differing from USH1 and USH2 in the progressiveness of hearing loss and the occasional presence of vestibular dysfunction.

USH1 is genetically heterogeneous. Seven loci responsible for this disease have been defined and called *USH1A-G*, with four of the corresponding genes having been identified: *USH1B, C, D* and *F*. *USH1B* encodes the actin-based motor protein myosin VIIa. *USH1C* encodes harmonin which is a PDZ domain-containing protein. Mutations in the genes encoding two cadherin-related proteins, cadherin 23 and procadherin 15, have been shown to cause USH1D and USH1F, respectively.

Studies of USH1G-affected families allowed to identify *SANS*, the human orthologue of the gene defective in Jackson shaker (*js*) mutant mice, as the causative gene (Mustapha et al., 2002; Weil et al., 2003).

Current clinical approaches to remedy hearing impairment, in particular USH, include hearing aids for mild to moderate impairments and cochlear implants for severe to profound impairments. These existing solutions are however not curative treatments and are not adapted to noisy environments.

There is thus a need in the art for therapeutic approaches to cure genetic forms of human deafness with or without balance defects, in particular USH, yet in particular USH1G.

In this aim, the present inventors studied *Ush1g* knock-out mice (*Ush1g*$^{-/-}$ model as described in Caberlotto et al., 2011). This study allowed them to provide a virally-mediated gene therapy for restoring genetically-impaired auditory and vestibular functions. More precisely, their results show that it is possible to efficiently target hair cells and to restore the normal morphology of both cochlear and vestibular hair bundles, which is shown to be critical for auditory and balance functions.

These findings have major therapeutic implications, as described below.

DETAILED DESCRIPTION OF THE INVENTION

In vivo administration of a USH1 gene product: vectors

According to the present invention, an *USH1* gene product, preferably the SANS protein, is administered to a subject in need thereof by *in vivo* gene therapy wherein the gene product/protein of interest is produced *in situ* in the appropriate auditory cells.

Two alternative strategies for gene therapy can be contemplated for treating subjects in need thereof. One strategy is to administer a vector encoding the gene of interest directly to the subject. The second is to use cells that have been i) removed from the subject and ii) treated *ex vivo* with a vector expressing the gene of interest; these cells are then re-administered to the same subject.

As used herein, the term "**subjects**" is intended to mean humans or non-human mammals such as primates, cats, dogs, swine, cattle, sheep, goats, horses, rabbits, rats, mice and the like. In a preferred embodiment, said subjects are human subjects. This definition applies to all aspects and embodiments of the present invention.

Thus, in an aspect, the present invention relates to vectors expressing at least one *USH1* gene product, in particular AAV2/8 vectors expressing at least one *USH1* gene product, preferably expressing at least the *SANS* gene product.

In one embodiment, the AAV2/8 vector of the invention comprises a nucleic acid sequence encoding at least one *USH1* gene product, preferably encoding at least the *SANS* gene product.

In another embodiment, the AAV2/8 vector of the invention comprises at least one nucleic acid sequence of an *USH1* gene, preferably at least the *SANS* gene.

According to the present invention, the vector is of interest as it is capable of expressing a functional protein.

As indicated, the vector of the invention is a viral vector that is able to transfect the cells of the auditory pathway and, more specifically, to target hair cells.

Among well-known viral vectors, adeno-associated viruses (AAV) vectors display several advantages such as i) a long lasting expression of synthesized genes (Cooper et al, 2006), ii) a low risk for pathogenic reactions (because they are artificially manufactured and not ototoxic), iii) they trigger low immunogenic response, and iv) they do not integrate the human genome (Kaplitt et al., 1994). AAV is therefore preferred to produce *in situ* a functional *USH1* gene product in order to efficiently cure USH1 syndrome.

The Inventors could show that AAV serotypes have different cell tropism in the cochlea. Accordingly, they could select an AAV2/8 configuration (i.e., vectors having the nucleotide sequence of an AAV2 genome that is modified so as to encode AAV8 capsid proteins) as being the most efficient to target hair cells (Fig. 1).

Thus, in the context of the present invention, the vector expressing an *USH1* gene product, preferably expressing the SANS protein, yet preferably expressing the SANS protein of amino acid sequence SEQ ID NO:49, is an AAV2/8 vector, preferably comprising a viral nucleic acid sequence SEQ ID NO:47 and/or SEQ ID NO:48.

In one embodiment, the AAV2/8 vector of the invention comprises a viral nucleic acid sequence of SEQ ID NO:47 and/or SEQ ID NO:48.

Advantageously, the AAV2/8 vector of the invention comprises both viral nucleic acid sequences SEQ ID NO:47 and SEQ ID NO:48, both of them forming an empty AAV2/8 vector, wherein a *USH1* gene is in turn incorporated.

In one embodiment, said *USH1* gene is the *SANS* gene product having the amino acid sequence SEQ ID NO:49.

In another aspect, the present invention also relates to a vector as described above, for use as a medicament.

In vivo administration of a USH1 gene product: viral particles

In another aspect, the present invention relates to viral particles comprising at least one vector as described above.

Advantageously, the viral particles of the invention are infectious viral particles.

In yet another aspect, the present invention relates to such viral particles, for use as a medicament.

Pharmaceutical compositions

Vectors and/or viral particles of the invention as described above can be incorporated into pharmaceutical compositions suitable for an administration to a subject.

Accordingly, another aspect of the present invention concerns a pharmaceutical composition comprising at least one vector of the invention and/or at least one viral particle of the invention, and a pharmaceutically acceptable carrier.

As used herein, the term "**pharmaceutically acceptable carrier**" refers to any and all solvents, dispersion media, coatings, antibacterial and antifungal agents, isotonic and absorption delaying agents, and the like that are physiologically compatible. Examples of pharmaceutically acceptable carriers include one or more of water, saline, phosphate buffered saline, dextrose, glycerol, ethanol and the like, as well as combinations thereof. In many cases, it can be preferable to include isotonic agents, for example, sugars, polyalcohols such as mannitol,

sorbitol, or sodium chloride in the composition. Pharmaceutically acceptable carriers can further comprise minor amounts of auxiliary substances such as wetting or emulsifying agents, preservatives or buffers, which enhance the shelf life or effectiveness of the vector(s) and/or viral particle(s) or of the pharmaceutical compositions containing same. This definition applies to all aspects and embodiments of the present invention.

The pharmaceutical compositions of the invention may be in a variety of forms. These include, for example, liquid, semi-solid and solid dosage forms, such as liquid solutions (e.g., injectable and infusible solutions), dispersions or suspensions, tablets, pills, powders, liposomes and suppositories. The form used depends on the intended mode of administration and therapeutic application. Typical compositions are in the form of injectable or infusible solutions.

Pharmaceutical compositions typically must be sterile and stable under the conditions of manufacture and storage. The pharmaceutical composition of the invention is preferably formulated as a solution, microemulsion, dispersion, liposome, or other ordered structure suitable to high drug concentration. Sterile injectable solutions can be prepared by incorporating the vector(s) and/or the viral particle(s) of the invention in the required amount in an appropriate solvent optionally with one or a combination of ingredients enumerated above, as required, followed by filtered sterilization. Generally, dispersions are prepared by incorporating the vector(s) and/or the viral particle(s) of the invention into a sterile vehicle that contains a basic dispersion medium and optionally other ingredients from those enumerated above, as required. In the case of sterile lyophilized powders for the preparation of sterile injectable solutions, the preferred methods of preparation are vacuum drying and spray-drying that yields a powder of the active ingredient plus any additional desired ingredient from a previously sterile-filtered solution thereof. The proper fluidity of a solution can be maintained, for example, by the use of a coating such as lecithin, by the maintenance of the required particle size in the case of dispersion and by the use of surfactants. Prolonged absorption of injectable compositions can be achieved by including an agent in the compositions that delays absorption, for example, monostearate salts and/or gelatine.

In the context of the invention, the typical mode of administration of the composition of the invention is a local administration, or intratympanic (in the middle ear) or intracochlear, or parenteral (e.g., intravenous, subcutaneous, intraperitoneal, intramuscular, intrathecal). In one example, the pharmaceutical composition of the invention is delivered to a specific location

using stereostatic delivery, particularly through the tympanic membrane or mastoid into the middle ear of a subject. In one example, the pharmaceutical composition of the invention is injected in the cochlea of a subject. In another example, the pharmaceutical composition of the invention is administered by intravenous infusion or injection. In another example, the pharmaceutical composition of the invention is administered by intramuscular or subcutaneous injection. In another example, the composition of the invention is administered perorally.

Preferably, the pharmaceutical composition of the invention is injectable, yet preferably it is injectable in the cochlea of a subject.

The pharmaceutical compositions of the invention include a "**therapeutically effective amount**" of the vectors and/or the viral particles of the invention. A "therapeutically effective amount" refers to the amount of the vectors and/or the viral particles of the invention that is effective, at dosages and for periods of time necessary, to achieve the desired therapeutic result in a subject in need thereof, in this case to efficiently treat hearing impairment, preferably USH1 syndrome, yet preferably USH1G syndrome, without unacceptable toxicity or undesirable side effects.

A therapeutically effective amount of the vectors and/or the viral particles of the invention can vary according to factors such as the disease state, age, sex, and weight of the subject, and the ability of said vectors and/or said viral particles to elicit a desired response in same. A therapeutically effective amount can also be one in which any toxic or detrimental effects of the vectors and/or the viral particles are outweighed by the therapeutically beneficial effects.

Dosage regimens can be adjusted to provide the optimum desired response (e.g., to cure USH1G syndrome). For example, a single bolus can be administered, several divided doses can be administered over time or the dose can be proportionally reduced or increased as indicated by the exigencies of the therapeutic situation. It can be especially advantageous to formulate injectable compositions in dosage unit form for ease of administration and uniformity of dosage. Dosage unit form as used herein refers to physically discrete units suited as unitary dosages for the subjects to be treated; each unit containing a predetermined quantity of the vector(s) and/or the viral particle(s) of the invention calculated to produce the desired therapeutic effect in association with the required pharmaceutical carrier. The specification for the dosage unit forms can be dictated by and directly dependent on (a) the unique

characteristics of the vector(s) and/or the viral particle(s) and the particular therapeutic effect to be achieved, and (b) the limitations inherent in the art of formulating such vector(s) and/or the viral particle(s) for treating Usher syndrome, in particular USH1 syndrome, preferably USH1G syndrome, in a subject in need thereof.

Use for treating USH1 hearing impairment

A further aspect of the present invention relates to vectors and/or viral particles and/or pharmaceutical compositions as described above, for use in a method for treating Usher syndrome in a subject in need thereof.

In other words, the present invention relates to the use of a vector and/or a viral particle and/or a pharmaceutical composition, in a method for treating Usher syndrome in a subject in need thereof.

These methods preferably comprise an injection, preferably a cochlear injection, of said vector.

Yet in other words, the present invention relates to a method for treating Usher syndrome in a subject in need thereof, comprising administering to said subject, preferably by injection, a vector and/or a viral particle and/or a pharmaceutical composition. In a particular embodiment, said injection is a cochlear injection.

In another aspect, the present invention relates to the use of the vectors and/or the viral particles of the invention for manufacturing pharmaceutical compositions intended to treat subjects suffering from Usher syndrome, in particular from USH1 syndrome, preferably from USH1G syndrome.

Preferably, said pharmaceutical compositions are as described above.

Kit

In another aspect, the present invention relates to a kit comprising, in one or more containers in a single package, at least one vector and/or at least one viral particle and/or at least one pharmaceutical composition as described above, and means for injecting said vector(s) and/or viral particle(s) and/or pharmaceutical composition(s).

Accordingly, the vector(s) and/or the viral particle(s) and or the pharmaceutical composition(s) in the kit are capable of expressing at least one *USH1* gene product, preferably of expressing the *SANS* gene product, advantageously for use in a method for treating Usher syndrome, in particular USH1 syndrome, preferably USH1G syndrome in a subject in need thereof.

In one embodiment, the means for injecting said vector(s) and/or viral particle(s) and/or pharmaceutical composition(s) as provided in the kit of the invention include or are means for a cochlear injection of said vector(s) and/or viral particle(s) and/or pharmaceutical composition(s).

Particular kits according to the present invention further comprise a means for communicating information and/or instructions and/or recommendations to allow a proper use of the kits' elements.

BRIEF DESCRIPTION OF THE DRAWINGS

Figure 15 describes different expression and efficiency, in cochlear hair cell, of AAV based on their serotype and promoter efficiency. Wild type mice were injected at P2 with AAV containing GFP as a gene reporter. Organs of Corti were harvested at P8, and immunolabelled for GFP (in light grey) and otoferlin (in dark grey) (**A**) AAV2/1-CAG mainly transduced supporting cell, and some neurons. (**B**) AAV2/8-CAG (SignaGen Laboratories) transduced neurons and afferent fibers. (**C**) AAV2/8-CAG (Penn Vector Core) transduced 85% of auditory hair cells. (**D**) ABR thresholds measured in a left injected cochlea did not differ from ABR thresholds of right non-injected cochlea.

Figure 16 describes MDCK cells transduced by AAV2/8-SANS-IRES-GFP. MDCK cells were plated on coverslips and infected with AAV2/8-sans-IRES-GFP. 24h after cells were immunolabelled for GFP (in light grey). 90% of MDCK cells were e-GFP positive

Figure 17 represents AAV2/8-Sans transduced cochlear hair cells, and restored sans expression. Wild type mice were injected by AAV2/8-sans at P2. Organs of Corti were harvested at P8, and immunolabelled for GFP (in light grey), and sans (dark grey). A) Tonotopic gradient was observed for viral transduction of AAV2/8-sans, with more eGFP-positive cells in IHCs than OHCs, and at the apex than at the base. B) Sans expression and distribution was restored.

Figure 18 shows that AAV2/8-Sans restored the morphology of cochlear hair cells. Scanning electron microscopy of cochlear hair cells shows degeneration of the hair bundle, abnormal staircase pattern and no prolate shape in *Ush1g*$^{-/-}$ mice (**A**) compared to and *Ush1g*$^{+/+}$ mice (**B**). Restore of the staircase pattern and the prolate shape is observed in *Ush1g*$^{-/-}$ mice treated with AAV2/8-Sans (**C**).

Figure 19 shows that AAV2/8-Sans rescued the mechanoelectrical transduction currents in cochlear hair cells. *Ush1g*$^{-/-}$ mice were injected at P2 with AAV2/8-Sans. Measurements of MET currents were realized at P8.

Figure 20 shows that AAV2/8-Sans delivery restored the auditory function. *Ush1g*$^{-/-}$ and *Ush1g*$^{f/f}$ *Myo15-Cre*$^{+/-}$ mice were injected at P2 with AAV2/8-sans, and ABR measurements were recorded between P17 and P37, in response to 5 to 40 kHz tone bursts, and for sounds level between 10 and 115 dB. ABR thresholds measured in *Ush1g*$^{-/-}$ mice. ABR thresholds of *Ush1g*$^{-/-}$ mice were elevated at 100 dB. ABR thresholds of *Ush1g*$^{-/-}$ treated mice showed a partial restore of 20-25 dB for low-frequencies, and 5-10 dB for high-frequencies. Variability of restore in *Ush1g*$^{-/-}$ injected mice. ABR thresholds measured in *Ush1g*$^{f/f}$ *Myo15-Cre*$^{+/-}$ mice. ABR thresholds of *Ush1g*$^{f/f}$ *Myo15-Cre*$^{+/-}$ mice were elevated at 100 dB. ABR thresholds of *Ush1g*$^{f/f}$ *Myo15-Cre*$^{+/-}$ treated mice showed a partial restore of 30-40 dB for low-frequencies.

Figure 21 represents AAV2/8-sans transduced vestibular hair cells, and restored Sans expression. Wild type mice were injected by AAV2/8-sans at P2. Vestibules were harvested at P8, and immunolabeled for GFP (in light grey), and sans (dark grey). A) A high rate of transduction (90 %) was observed for viral delivery of AAV2/8-sans in vestibular hair cells. Sans expression and distribution was also restored.

Figure 22 shows that AAV2/8-Sans restored the morphology of vestibular hair bundles - *Ush1g*$^{-/-}$ mice were injected at P2 with AAV2/8-sans, and structure of hair bundles were assessed by scanning electron microscopy at P8. (**A**) Characteristic staircase pattern of vestibular hair bundles observed in not treated heterozygous mice. (**B**) No difference of morphology in treated heterozygous mice, showing that injection did not alter the bundle structure. (**C**) Vestibular hair bundles of not treated *Ush1g*$^{-/-}$ mice showed not organized hair bundles with fused stereocilia, with irregular diameters and heights. Treated *Ush1g*$^{-/-}$ mice presented heterogeneous organized vestibular hair bundles, with normal shape and the characteristic staircase pattern. Some stereocilia observed had a prolate shape. Smaller hair bundles with a kinocilium, were also frequently observed, showing that these young cells were transduced since the beginning of their development. In contralateal vestibule less hair cells were restored.

Figure 23 shows AAV2/8-Sans restored the vestibular function. The circling behavior in an open-field chamber was evaluated at P40 in treated or untreated *Ush1g*$^{-/-}$ mice *Ush1g*$^{+/-}$ mice using a tracking software system. Turns in clockwise and counter clockwise were counted : treated *Ush1g*$^{-/-}$ mice did not show any circling behavior, like heterozygous mice (3 turns during 2min for treated *Ush1g*$^{-/-}$ mice *vs.* 23 turns for uninjected *Ush1g*$^{-/-}$ mice).

EXAMPLES

I. Material and Methods

Animals

Experiments on mice were carried out according to Institut National de la Santé et de la Recherche Médicale and Institut Pasteur welfare guidelines.

Animals were housed in the Institut Pasteur animal facilities accredited by the French Ministry of Agriculture to perform experiments on live mice.

Knockout sans mice (*Ush1g*$^{-/-}$) were generated, as described in Caberlotto *et al.*, 2011, in C57BL/6-129/Sv strain mice. Intracochlear injections were achieved on P2-P3 aged-mice.

Viral construction

Recombinant AAV vectors were obtained from Penn Vector Core (Perelman, Philadelphia, Pennsylvania, USA) and SignaGen Laboratories (Bethesda, Maryland, USA) containing a CMV or CAG promoter driving expression of eGFP. AAV2/1-CAG-GFP and AAV2/1-CMV-GFP were produced at a titer of 1,2 x 10^{12} genome copies (gc)/mL by SignaGen Laboratories. AAV2/1-CAG-GFP-rhodopsine at a titer of 1,4 x 10^{13} gc/mL by Penn Vector Core. The AAV2/2-CAG-GFP was produced at a titer of 6,4 x 10^{13} gc/mL, by Penn Vector Core. The AAV2/5-CMV=-GFP was produced at a titer of 1,13 x 10^{13} gc/mL, by Penn Vector Core. The AAV2/8-CAG produced by SignaGen Laboratories at a titer of 1,6 x 10^{12} gc/mL. And the AAV2/8-CAG from Penn Vector Core had a titer of 1,4 x 10^{13} gc/mL.

Murine *Sans* cDNA flanked by an IRES eGFP reporter cDNA sequence was subcloned into the multiple cloning site of the pENN.AAV.CB6.PI.rBG vector (Penn Vector p1045, Penn Medicine Vector Core).

Vectors were generated by transient transfection of HEK293 cells using three plasmids : the cis ITR-containing plasmid, the trans plasmid encoding AAV replicase and capsid genes and the adenoviral helper plasmid. The recombinant vectors were purified by tangential flow filtration followed by iodixanol gradient purification and buffer exchange (*Upenn website*).

Concentrated AAV2/8-mSANS-IRES-eGFP titer was 1,47 x 10^{13} genomes copies per mL.

Virus aliquots were stored at −80°C and thawed prior to surgery.

Transfection in MDCK cells (p1045 SANS IRES GFP, AAV2/8 SANS IRES GFP)

MDCK cell lines were cultured in Dulbecco' s modified Eagle medium (DMEM, Gibco) supplemented with 10% fœtal bovine serum, 1% penicillin-streptomycin antibiotics and 1% fungizone antimycotic.

Both plasmid and virus forms containing mSANS.IRES.eGFP in MDCK cells were tested. For the plasmid, cells were transfected with Lipofectamine 2000 (Invitrogen). For the vector form cells were directly transfected without reagent. Cells were fixed 24h after transfection with 4% paraformaldehyde (PFA) in phosphate buffered saline (PBS) for 20 minutes. Cells were rinsed three times for 10 minutes in PBS, permeabilized in PBS containing 0,3 TritonX-100 supplemented with NH_4Cl, and blocked with PBS contaning 20% normal goat serum (NGS).

Then cells were processed for immunochemistry with chicken anti-GFP (Abcam, 1:250) in PBS containing 1% of bovine serum albumin (BSA) overnight. After washing three times for 10 minutes in PBS, cells were incubated 1 hour in ATTO-488 conjugated goat anti-chicken IgG antibody (Sigma-Aldrich, 1:500 dilution). Actin was labelled with ATTO-647N–conjugated phalloidin (Sigma-Aldrich, 1:200 dilution). Samples were then mounted in Fluorsave (Calbiochem, USA).

Intracochlear injection

Animal protocols were approved by animal care and use of committee of Pasteur Institute.

Intracochlear viral transduction was carried out as described by Akil *et al*. (2012). After anesthesia on ice, a left postauricular incision was made, and using two landmarks including the cochlear basal turn and the stapedia artery, the otic bulla was exposed and then opened. Next, a glass micropipette of 10µm outer tip diameter containing 2µl of the viral vector was inserted into the round window membrane (RWM). The viral preparation was then gently injected through the round window. After pulling out the pipette, the hole in the RWM was plugged with connective tissue and the incision sealed with biological glue (3M Vetbond).

Immunofluorescence

After dissection, mice cochleae were perfused with 4% PFA in PBS for 45 minutes at 4°C. Cochleae were further microdissected, rinsed three times for 10 minutes, incubated 1 hour at room temperature in PBS containing 20% NGS and 0.3% Triton X-100, and incubated overnight with the primary rabbit antibody anti-Sans (Caberlotto et al., 2011), and/or chicken anti-GFP (Abcam, 1:250) in PBS containing 1% of NGS. Cochleae were rinsed three times for 10 minutes in PBS, and then incubated for 1 hour in ATTO-550 conjugated goat anti-rabbit IgG antibody (Sigma-Aldrich, 1:500 dilution) and ATTO-488 conjugated goat anti-chicken IgG antibody (Sigma-Aldrich, 1:500 dilution). Actin was labelled with ATTO-647N–conjugated phalloidin (Sigma-Aldrich, 1:200 dilution). Samples were then mounted in Fluorsave (Calbiochem, USA). The z-stack images were captured with a x63 Plan Apochromat oil immersion lens (NA 1,4) using a Zeiss LSM-700 confocal microscope and processed using Zeiss LSM image browser.

Hair cell counting

To evaluate the rate of transduction, the expression of eGFP used as a gene reporter was analysed in mice injected with the viral construction. For counting, the total number of inner or outer hair cells positive for eGFP was divided by the total number of inner or outer hair cells existing in the tissue, detectable by rhodamine phalloidin staining. For mature stages, rate of transduction was calculated in middle turn and apex of each cochlea.

Electrophysiological recordings

Electrophysiological cell recordings were performed on cochlear and utricular explants from mice at P8 as previously described (Michalski, 2009). Cochlea and utricule were finely dissected, placed under nylon meshes and observed under a x40 water-immersion Olympus objective mounted on an Axioscope Zeiss microscope.

Extracellular and dissecting solutions were identical and composed of 146 mM NaCl, 5.8 mM KCl, 1.5 mM CaCl2, 0.7 mM NaH2PO4, 2 mM Na-pyruvate, 10 mM glucose and 10 mM N-2-hydroxyethylpiperazine-N-2-ethanesulfonic acid (HEPES; pH = 7.4, 305 mosmol/kg). Intracellular solution contained 130 mM KCl, 10 mM NaCl, 3.5 mM MgCl2, 1 mM ethyleneglycoltetraacetic acid (EGTA), 5 mM K2ATP, 0.5 mM GTP and 5 mM HEPES (pH =7.3, 290 mosmol/kg). Borosilicate patch pipettes (2–3 MΩ) were approached parallel to the hair cell rows through a hole in the reticular lamina. During this step, extracellular solution was abundantly perfused to avoid contact between EGTA and the transduction apparatus, which is sensitive to calcium chelators. Hair cells were whole-cell voltage clamped at room temperature (20–25°C) at −80 mV using an EPC-9 patch clamp amplifier and the Patchmaster software (HEKA, Lambrecht, Germany). No correction was made for liquid junction potential. Series resistance was always below 10 MΩ and was compensated to 70%. Data were sampled at 100 kHz and filtered at 10 kHz (8-pole Bessel). Each hair bundle was mechanically stimulated by applying axial step displacements with a rigid glass rod that had been fire-polished prior to the experiment to yield a tip diameter of 2–3 µm. The probe was systematically positioned against the top of the hair bundle in the bundle's plane of bilateral symmetry towards the tallest row of stereocilia at an angle of ~30° relative to the cell apical surface. The probe used for mechanical stimulation of the hair bundles was secured to a stacktype piezo-electric actuator (PA8/12; Piezosystem Jenas) driven by a low-voltage power supply (30V300, Piezosystem Jena). As measured offline with a displacement monitor containing photodiodes, the first two

milliseconds of the time course of probe motion were well described by an exponential rise with a time constant of 100 ms. Data were analyzed in Matlab, version 7.0 (MathWorks). Po(X) curves were fitted with a three-state Boltzmann relation. For sensitivity measurements, the mean value of the three-state Boltzmann relation derivative was calculated for displacements corresponding to P0 values between 0.2 and 0.8.

Audiological tests

Auditory Brainstem Responses (ABR) were recorded and analysed as described previously (Le Calvez *et al.*, 1998). Mice were anesthetized with xylazine and ketamine, and places in a sound-attenuated room. Three electrodes were placed at the vertex and ipsilateral mastoid, with the lower back as the earth. Pure tone stimuli at 5, 10, 15, 20, 32 and 40 KHz were used. Sounds level between 10dB and 100dB in 10dB steps were tested. ABR thresholds were determined about 20 days after injection. Thresholds were determined as the lowest stimulus level resulting in recognizable waves.

Distortion product otoacoustic emissions (DPOAEs) were collected in the ear canal using a microphone. Two simultaneous pure tone stimuli, at frequencies f1 and f2, were used with the same levels, from 30 to 75 dB SPL in 5 dB steps. The f2 frequency was swept from 5 to 20 kHz in $1/8^{th}$ octave steps, with f1 chosen such that the frequency ratio f2/f1 was 1.20. Only the cubic difference tone at 2f1-f2, the most prominent one from the ear, was measured (Le Calvez *et al.*, 1998). Statistical significance was tested by the two-tailed unpaired t test with Welch's correction.

Cochlear microphonic (CM) responses to a 5 kHz pure tone stimulus at 105 dB SPL were collected between an electrode inserted in the round window and the vertex. The response from the electrodes was amplified (gain 10 000), filtered, digitally converted and averaged using a comprised-data acquisition system.

Behavioral analysis

Firstly, mice were observed in cage to evaluate signs like circling or head bobbing. Then various tests were performed on mice, to assess the vestibular function before and after intracochlear injection, as described in Hardisty-Hughes et al., 2010. The trunk curl test was performed by holding the mouse by the tail and observing whether the mouse reached a horizontal surface or curls its trunk toward its tail. Mice's equilibrium was also evaluated with

the platform test, were mice are positioned upon a platform (height: 29cm, platform: 7cm x 7cm) and the number of fells of the mouse was counted over a period of 1min.

The contact righting test was realized by placing the mouse into a closed clear tube and observing if the mouse re-orientates when the tube was rotated through 180°. The swimming ability of each mouse in a container filled of 24-26°C water was also scored. Finally, the circling behavior was evaluated with a tracking software system (Ethovision de Noldus Information Technology, Wageningen, The Netherlands + Lentz et al., 2013). Turns in clockwise and counter clockwise were counted.

Scanning Electron Microscopy

Scanning electron microscopy (SEM) analyzes were realized to assess the morphology of cochlear and vestibular hair bundles after intracochlear injections. Organs of Corti were finely dissected and fixed in 2,5% glutaraldehyde in 0,1M aqueous sodium cacodylate solution at room temperature. Then samples were rinsed in cacodylate 0,1M three times for 1-2 minutes, and incubated alternatively in 1% osmium tetroxide and 0,1M thiocarbohydrazide (OTOTO), with water washing between each incubation. Cochleae were then dehydrated in graded series of ethanol and critical point dried. Observations were done by field emission scanning electron microscopy with Jeol JSM6700F operating at 3 kV.

II. Results

Evaluation of AAV mediated transgene expression, tropism and promoters efficiency in cochlear hair cell

The AAV are on the top of a list of promising gene delivery carrier for gene therapy for human diseases. The main advantages of the AAV virus are their capacity to infect non-dividing cells, the absence of immune response and long-term transgene expression. The AAV serotypes identified up to date display variable cell tropism. The ability of several AAV to transduce sensory hair cell in odor was evaluated to determine which AAV would best transduce the inner ear sensory cells.

To this end, transgene expression and cellular distribution of several AAV pseudotypes were investigated after intracochlear injection. Wild type mice were subjected to the viral cochlear

delivery, through the round window membrane (RWM), at postnatal day 2-3 (P2-3). Left cochleae were injected with either AAV1, AAV2/1, AAV2/2, AAV2/5 or with AAV2/8, encoding the green fluorescent protein (GFP) as a gene reporter, at titers ranged from 1,2 x 10^{12} to 6,4 x 10^{13} genome copies (gc)/mL. Six days after the injection, organs of Corti were microdissected and immunolabelled for otoferlin, a protein highly expressed in IHCs, and for GFP. All the tested AAVs were able to transduce cells within the cochlea, but with different cochlear cell tropism and transduction rates. Interestingly, two AAV with the same serotype and promoter (CAG or CMV) but from different suppliers did not transduce the same cell within the cochlea. In fact, while the AAV2/1 from SignaGen Laboratories mainly transduced supporting cells, (Fig.15A) the one from Penn Vector Core, transduced primarily IHCs (40%) but only in 1 out of 5 mice (Fig. 15A). The AAV2/2 serotype with CAG promoter (Penn Vector Core) transduced only supporting cells. The AAV2/5 with the CMV as promoter did not transduced any cochlear cell types. The AAV2/8-CAG serotype (SignaGen Laboratories) transduced predominantly primary neurons (Fig.15B). On the contrary, in the present experimental tests, the AAV2/8 with CAG as promoter (Penn Vector Core) transduced mainly the hair cells (Fig.15C). A tonotopic gradient viral transduction for AAV2/8-GFP establishes, with more eGFP-positive hair cells at the apex (70%), than at the base (40%). Thus, the AAV2/8-CAG from Penn Vector Core was chosen for this study, as it was the most efficient to transduce sensory auditory hair cells.

Next, the effects of surgery and of the cochlear injection of the viral preparation through the round window membrane on the development of auditory function were assessed. The auditory brainstem responses (ABRs) were examined at different frequencies (from 4kHz to 40kHz), fourteen days after the injection. In the twelve treated mice, ABR hearing thresholds of the injected ear recorded at the frequencies tested did not differ significantly from those of the control ear (Fig. 15D), suggesting that surgery and viral injection did not interfere with the normal development and maturation of the auditory system.

AAV2/8-SANS-IRES-GFP transduced MDCK cells

The coding sequence for the murine sans cDNA was subcloned into AAV2 genome downstream of internal ribosome entry sites (IRES) eGFP cDNA sequence. The expression cassette was flanked with AAV2 inverted terminal repeats (ITRsp) and pseudotyping strategy was used to produce AAV2 vectors packaged with AAV8. To evaluate the relative expression efficiencies of this viral particle and to assess specificity of sans protein expressed, MDCK cells were plated on coverslips and infected with AAV2/8-sans-IRES-GFP using MOI (Multiplicity Of Infection) of

10,000. Sans expression was then probed by immunohistochemistry using a specific anti sans antibody, and the transduced cell were quantified. The results show that all cells expressing GFP also expressed sans, and that AAV2/8-sans-IRES-GFP transduced an average of 90 % of MDCK cells (Fig. 16).

Gene therapy restored sans expression and targeting in inner ear hair cells of *Ush1g*$^{-/-}$ mice

Having established the efficiency of the AAV2/8-sans *in vitro*, the expression of AAV2/8-sans was investigated in the cochlea *in vivo*. To this end, 2µL of AAV2/8-sans were injected through the round window membrane into one ear of wild type mice. Eight days after inoculation, organs of Corti, from the injected and the contralateral cochlea, were microdissected, immunolabelled for GFP. Positive eGFP-hair cells were then counted. The transduction rate of both IHCs and OHCs upon cochlear injection of the AAV2/8-sans was comparable to that observed for AAV2/8-GFP. Indeed, the hair cell transduction efficacy of AVV2/8-sans displayed a basoapical gradient higher at the apex than at the base. In addition the number of the transduced IHCs was much greater than OHC regardless of the cochlear region. The viral transduction efficiency tended to be higher in the apical turn. The rate of the transduced IHC was about 87% at the apex and gradually declined to 45% at the base. The rate of the transduced OHCs was about 33% at the apex and gradually declined to 25% at the base (Fig. 17). Transduced hair cells were also observed in the contralateral ear although at a lower rate (IHCs: 66 % at the apex, 30% in the mid turn, 32% at the base; OHCs: around 10% all along the cochlea). Interestingly the vestibular sensory hair cells of the treated and untreated ear were also transduced at a rate of 90% and 80% respectively (Fig. 21). These data show that the efficiency of inner ear hair cell transduction with AAV2/8-sans vectors qualifies this AAV pseudotype to carry out sans gene therapy in Ush1g$^{-/-}$ mice.

The ability of AAV2/8-sans to restore the normal expression and targeting of the protein in cochlear and vestibular hair cell of the Ush1g-/- mice was tested. To this end, several Ush1g-/- mice were subjected to cochlear injection of the AAV2/8-sans viral particle as described above. To monitor vector-mediated sans expression, the mice were sacrificed 5 days after injection and the organ of Corti and the vestibule were subjected to double immunostaining for GFP and sans, using previously characterized antibodies (Caberlotto, 2011). A widespread expression of GFP was observed in both IHC and OHCs of the injected cochleas. Remarkably, in all GFP positive cells, sans immuolabelling was evident in both IHC and OHC where it was readily localized at the tip of the hair cell stereocilia. These observations are consistent with what has

been reported for the native protein. These observations demonstrate that GFP and sans protein are transduced independently, enabling the normal targeting the later to the stereocilia.

Sans Gene therapy prevents cochlear and vestibular hair cell stereocilia degeneration in *Ush1g*$^{-/-}$ mice

The Ush1g-/- mice are characterized by profound congenital sensorineural deafness and severe balance defect. In these mice, the sensory hair cell of both the vestibule and the cochlea displayed abnormal hair bundle, including fused and decreased numbers of stereocilia, dissociation of hair bundles fragmented or flat stereocilia, and the kinocilia misposition. The most striking feature is the loss of the staircase pattern due to the loss the middle and the short rows of inner and outer hair cell. Therefore, it was verified whether the normal expression and targeting of the protein sans in the inner ear hair cell of the *Ush1g-/-* mice prevents the abnormal morphological features of their stereocilia and kinocilia to take place. On P8, organs of Corti and utricules of the *Ush1g*$^{-/-}$ mice treated ear were microdissected and processed for scanning electron microscopy to closely scrutinized stereocilia morphology at high resolution. The bundle architecture of hair cells was preserved in all transduced hair cell at a degree reminiscent of the transduction rate observed using GFP expression as proxy (Figure.18C). The hair bundles of the transduced cochlear hair cells retained their typical staircase pattern with the three rows. The stereocilia of all transduced hair cells of both vestibule and cochlea retained their typical staircase pattern including the short, middle and tall row of cochlear (Fig. 18C and 22C). Remarkably the tallest row displayed a characteristic oblate tip and the stereocilia of the lower and the middle rows typically displayed a prolate tip that points toward its taller neighbors (Fig. 18C). These prolate shapes are believed to be a hallmark of the presence of functional tip links. The vestibular hair bundles of utricle hair cells appear nearly normal and displayed staircase tenting at stereocilia tips suggesting that tip links were also present. Finally, using a custom MATLAB (MathWorks) interface, stereocilium numbers, projected heights, and distances between stereocilia were estimated. No differences were found that there were in the number, the form or the height of the vestibular hair bundles in the *Ush1g-/-* treated mice relative to those observed and measured in the *Ush1g+/-* mice. Of note the morphology of cochlear and vestibular hair bundles of treated wild type mice did not differ from the untreated ones, suggesting that the injection through the round window membrane did not impaired the development of the morphology of hair bundles.

These data show that sans gene therapy restored nearly to normal the stereocilia structure in transduced inner ear hair cell, including thickness, length and number in sans deficient mice.

Sans gene therapy rescue the mechanosensory transduction of *Ush1g-/-* mice hair cells in vivo.

To evaluate if the restored hair bundle by sans gene therapy are functional, mechanoelectrical transduction (MET) currents were recorded from both IHCs and OHCs of *Ush1g*$^{-/-}$ mice, five days after treatment. In untreated *Ush1g*$^{-/-}$ mice, MET currents were nearly absent in both cochlear hair cells (Caberlotto, 2011) (111 ± 31 pA for IHCs (n= 5), and 47 ± 6 pA for OHCs (n= 4)). However, maximal amplitudes of MET currents of treated *Ush1g*$^{-/-}$ mice were comparable to currents observed in wild type mice (763 ± 128 pA for IHCs (n= 3), and 721 ± 97 pA for OHCs (n= 4)). The average (±SEM) peak sensory transduction current for rescued IHCs was 424 ± 70 pA (n= 11), and 641 ± 35 pA for OHCs (n= 12) (Fig. 19). Given the high rate of transduction in IHCs, MET currents were measured in cells randomly. Although for OHCs, in which less transduced cells were observed, currents were observed and measured in GFP-transduced cells. No difference of sensitivity to the hair bundle displacement between treated *Ush1g*$^{-/-}$ and heterozygous mice were observed (Fig. 19). Moreover, MET currents measured in treated wild type mice showed no significant difference, suggesting that the injection did not damage the mechanoelectrical machinery. These results demonstrated that single intracochlear injection of sans in *Ush1g*$^{-/-}$ mice, completely restored the auditory hair cell-MET.

Sans gene therapy rescued the auditory function

To evaluate if sans-transduced cells can rescue auditory function, AAV2/8-sans was injected in *Ush1g*$^{-/-}$ mice, and hearing was probed by in vivo audiometric tests: auditory brainstem responses (ABR), which explore activities of IHCs and OHCs, distortion-product otoacoustic emissions (DPOAEs), which involve OHC MET channel function (Avan *et al*, 2013), and cochlear microphonics (CM), which record phasic extracellular potentials reflecting MET currents in the OHCs of the basal region of the cochlea. These auditory tests were recorded between 15 to 35 days after treatment.

According to early studies, uninjected *Ush1g*$^{-/-}$ mice showed a lack of identifiable ABR waves for all sound frequencies, indicating profound deafness (Caberlotto, 2011). Moreover, DPOAEs and CM were not detected in these mice. However, injection of AAV2/8-sans in *Ush1g*$^{-/-}$ mice led to a significant hearing recovery. Indeed, a partial restore of hearing was observed mainly

for low-frequencies of 20-25 dB (5-15 kHz), and a lower restore 5-10 dB for high-frequencies (20-32 KHz) (Fig. 20), in the injected ear. These results were obtained in all treated mice, with variability between each animal.

Thus, a single intracochlear injection of AAV2/8-sans is sufficient to restore a hearing function in *Ush1g*$^{-/-}$ mice.

To circumvent the early morphogenetic defect present in the hair bundles of *Ush1g*$^{-/-}$ mice, ABR of *Ush1g*$^{f/f}$ *Myo15-Cre*$^{+/-}$ mice was also probed (Caberlotto, 2011). In these mice, *Ush1g* is deleted postnatally, under the control of the *Myo15* promoter, specific for auditory hair cells. Thus, the viral particle is injected before the deletion of sans. Caberlotto *et al.*, showed that these mice are profoundly deaf from P13, for all sound frequencies. Nonetheless, the delivery of AAV2/8-sans through the RWM at P2, resulted in higher ABR thresholds, of about 30-40dB for low-frequencies (5-15 kHz), than in *Ush1g*$^{-/-}$ rescued mice.

Sans gene therapy completely corrected the vestibular defect

After having evaluated the morphological restore of vestibular hair bundles, the vestibular function, i.e. the behavior of treated *Ush1g*$^{-/-}$ mice was studied. In fact, *Ush1g*$^{-/-}$ mice are characterized by vestibular defects, which result in circling and head tossing (Caberlotto *et al.*, 2011). This phenotype was no longer observed in all treated *Ush1g*$^{-/-}$ mice at mature stages. To deepen these observations, various behavioral tests were performed. During the platform test, the heterozygous mice never fall over a period of 1 min, as the treated *Ush1g*$^{-/-}$ mice. Uninjected mice deficient for sans did not hold on platform more than few seconds. The trunk-curl test showed that treated mutant mice, as heterozygous mice, reached the surface without curling its trunk toward its tail. On the contrary, untreated *Ush1g*$^{-/-}$ mice cur the trunk and did not reach the surface. The contact righting test strengthened that treated *Ush1g*$^{-/-}$ mice, as heterozygous mice, had no vestibular dysfunction because they could re-orientates perfectly after a rotation of the tube, unlike the untreated mice deficient for sans. Finally, by scoring swim test (0 = swim ; 1 = irregular swim ; 2 = immobile floating ; 3 = underwater tumbling, Hardisty-Hughes et al., 2010) it was noted that treated *Ush1g*$^{-/-}$ mice swum with no difficulty (score 0 = swim), like heterozygous mice, while untreated *Ush1g*$^{-/-}$ mice drowned very rapidly (score 3 = underwater tumbling). Treated *Ush1g*$^{-/-}$ mice did not show any circling behavior, like heterozygous mice, as shown by videotracking mice in an open-field chamber (3 turns during 2min for treated *Ush1g*$^{-/-}$ mice *vs*. 23 turns for uninjected *Ush1g*$^{-/-}$ mice, Fig. 23).

It is important to consider that these tests were also achieved for injected heterozygous mice, and that they behaved as non-injected heterozygous mice, showing that the injection through the RWM did not impair the vestibular function.

These behavioral analyses show that sans gene therapy completely restores the vestibular function.

REFERENCES :

Akil, O., Seal, R.P., Burke, K., Wang, C., Alemi, A., During, M., Edwards, R.H., Lustig, L.R. (2012). Restoration of hearing in the VGLUT3 knockout mouse using virally mediated gene therapy. *Neuron* 75(2), 283-93.

Akino K, Toyota M, Suzuki H, Imai T, Maruyama R, Kusano M, Nishikawa N, Watanabe Y, Sasaki Y, Abe T, Yamamoto E, Tarasawa I, Sonoda T, Mori M, Imai K, Shinomura Y, Tokino T (2007). Identification of DFNA5 as a target of epigenetic inactivation in gastric cancer. Cancer Sci. 98(1):88-95.

Angermüller, S., and Fahimi, H. D. (1981). Selective cytochemical localization of peroxidase, cytochrome oxidase and catalase in rat liver with 3,3'-diaminobenzidine. *Histochemistry* 71(1), 33–44.

Basta, D., Tzschentke, B., and Ernst, A. (2005). Noise-induced cell death in the mouse medial geniculate body and primary auditory cortex. *Neuroscience letters 381*, 199-204.

Benjamini, Y., and Hochberg, Y. (1995). Controlling the false discovery rate: a practical and powerful approach to multiple testing. *J. Roy. Statist. Soc. Ser.* B. 57, 289-300.

Binder, C.J., Weiher, H., Exner, M., Kerjaschki, D. (1999). Glomerular overproduction of oxygen radicals in Mpv17 gene-inactivated mice causes podocyte foot process flattening and proteinuria: A model of steroid-resistant nephrosis sensitive to radical scavenger therapy. *Am. J. Pathol.* 154(4), 1067-75.

Bischoff AM, Luijendijk MW, Huygen PL, van Duijnhoven G, De Leenheer EM, Oudesluijs GG, Van Laer L, Cremers FP, Cremers CW, Kremer H (2004). A novel mutation identified in the DFNA5 gene in a Dutch family: a clinical and genetic evaluation. Audiol Neurootol. 9(1):34-46.

Bolstad, B.M., Irizarry, R.A., Astrand, M., Speed, T.P. (2003). A comparison of normalization methods for high density oligonucleotide array data based on variance and bias. *Bioinformatics* 19(2), 185-93.

Bonekamp, N.A., Volkl, A., Fahimi, H.D., and Schrader, M. (2009). Reactive oxygen species and peroxisomes: struggling for balance. *BioFactors 35*, 346-355.

Borck, G., Rainshtein, L., Hellman-Aharony, S., Volk, A.E., Friedrich, K., Taub, E., Magal, N., Kanaan, M., Kubisch, C., Shohat, M., Basel-Vanagaite, L. (2012). High frequency of autosomal-recessive DFNB59 hearing loss in an isolated Arab population in Israel. *Clin Genet.* 82(3), 271-6.

Caberlotto, E., Michel, V., Foucher, I., Bahloul, A., Goodyear, R.J., Pepermans, E., Michalski, N., Perfettini, I., Alegria-Prévot, O., Chardenoux, S., Do Cruzeiro, M., et al. (2011). Usher type 1G protein sans is a critical component of the tip-link complex, a structure controlling actin polymerization in stereocilia. *Proc. Natl. Acad. Sci. USA* 108(14), 5825-30.

Chai Y, Chen D, Wang X, Wu H, Yang T (2014). A novel splice site mutation in DFNA5 causes late-onset progressive non-syndromic hearing loss in a Chinese family. Int J Pediatr Otorhinolaryngol. 78(8):1265-8.

Cheng J, Han DY, Dai P, Sun HJ, Tao R, Sun Q, Yan D, Qin W, Wang HY, Ouyang XM, Yang SZ, Cao JY, Feng GY, Du LL, Zhang YZ, Zhai SQ, Yang WY, Liu XZ, He L, Yuan HJ (2007). A novel DFNA5 mutation, IVS8+4 A>G, in the splice donor site of intron 8 causes late-onset non-syndromic hearing loss in a Chinese family. Clin Genet. 72(5):471-7.

Cody, A.R., and Johnstone, B.M. (1981). Acoustic trauma: Single neuron basis for the '"half-octave shift". *J. Acoust. Soc. Am*. 70, 707–711.

Collin, R.W., Kalay, E., Oostrik, J., Caylan, R., Wollnik, B., Arslan, S., den Hollander, A.I., Birinci, Y., Lichtner, P., Strom, T.M. (2007). Involvement of DFNB59 mutations in autosomal recessive nonsyndromic hearing impairment. *Hum. Mutat*. 28(7), 718-23.

Collins, T.J. (2007). ImageJ for microscopy. *Biotechniques* 43, 25-30.

Cooper, L.B., Chan DK, Roediger FC, Shaffer BR, Fraser JF, Musatov S, Selesnick SH, Kaplitt MG. AAV-mediated delivery of the caspase inhibitor XIAP protects against cisplatin ototoxicity. *Otol Neurotol*. 2006 Jun;27(4):484-90

Delille, H.K., Agricola, B., Guimaraes, S.C., Borta, H., Luers, G.H., Fransen, M., and Schrader, M. (2010). Pex11pbeta-mediated growth and division of mammalian peroxisomes follows a maturation pathway. *Journal of cell science 123*, 2750-2762.

Delmaghani, S., del Castillo, F.J., Michel, V., Leibovici, M., Aghaie, A., Ron, U., Van Laer, L., Ben-Tal, N., Van Camp, G., Weil, D., et al. (2006). Mutations in the gene encoding pejvakin, a newly identified protein of the afferent auditory pathway, cause DFNB59 auditory neuropathy. *Nat. Genet*. 38, 770-8.

Diano, S., Liu, Z.W., Jeong, J.K., Dietrich, M.O., Ruan, H.B., Kim, E., Suyama, S., Kelly, K., Gyengesi, E., Arbiser, J.L., *et al.* (2011). Peroxisome proliferation-associated control of reactive oxygen species sets melanocortin tone and feeding in diet-induced obesity. *Nat Med 17*, 1121-1127.

Dobie, R.A. (2005) Audiometric Threshold Shift Definitions: Simulations and Suggestions, *Ear and Hearing* 26(1) 62-77

Ebermann, I., Walger, M., Scholl, H.P., Charbel Issa, P., Lüke, C., Nürnberg, G., Lang-Roth, R., Becker, C., Nürnberg, P., Bolz, H.J. (2007). Truncating mutation of the DFNB59 gene causes cochlear hearing impairment and central vestibular dysfunction. *Hum. Mutat.* 28(6), 571-7.

Ehret, G., and Riecke, S. (2002). Mice and humans perceive multiharmonic communication sounds in the same way. *Proc. Natl. Acad. Sci.* USA 99(1), 479-482.

Evans, P., and Halliwell, B. (1999). Free radicals and hearing. Cause, consequence, and criteria. *Ann. NY Acad. Sci*. 884, 19-40.

Fransen, M., Nordgren, M., Wang, B., and Apanasets, O. (2012). Role of peroxisomes in ROS/RNS-metabolism: implications for human disease. *Biochim Biophys Acta 1822*, 1363-1373.

Han, C., and Someya, S. (2013). Mouse models of age-related mitochondrial neurosensory hearing loss. *Molecular and cellular neurosciences 55*, 95-100.

Hashemzadeh Chaleshtori, M., Simpson, M.A., Farrokhi, E., Dolati, M., Hoghooghi Rad, L., Amani Geshnigani, S., Crosby, A.H. (2007). Novel mutations in the pejvakin gene are associated with autosomal recessive non-syndromic hearing loss in Iranian families. *Clin. Genet*. 72(3), 261-3.

He, W., Newman, J.C., Wang, M.Z., Ho, L., and Verdin, E. (2012). Mitochondrial sirtuins: regulators of protein acylation and metabolism. *Trends in endocrinology and metabolism*: TEM *23*, 467-476.

Henderson, D., Bielefeld, E.C., Harris, K.C., and Hu, B.H. (2006). The role of oxidative stress in noise-induced hearing loss. *Ear and hearing 27*, 1-19.

Housley, G.D., Morton-Jones, R., Vlajkovic, S.M., Telang, R.S., Paramananthasivam, V., Tadros, S.F., Wong, A.C., Froud, K.E., Cederholm, J.M., Sivakumaran, Y., et al. (2013). ATP-gated ion channels mediate adaptation to elevated sound levels. *Proc Natl Acad Sci* U S A. 110(18), 7494-9.

Imig, T.J., and Durham, D. (2005). Effect of unilateral noise exposure on the tonotopic distribution of spontaneous activity in the cochlear nucleus and inferior colliculus in the cortically intact and decorticate rat. *The Journal of comparative neurology 490*, 391-413.

Jain, N., Thatte, J., Braciale, T., Ley K., O'Connell, M., Lee, J.K. (2003). Local-pooled-error test for identifying differentially expressed genes with a small number of replicated microarrays. *Bioinformatics* 19(15), 1945-51.

Janero, D.R. (1990). Malondialdehyde and thiobarbituric acid-reactivity as diagnostic indices of lipid peroxidation and peroxidative tissue injury. *Free Radic. Biol. Med*. 9(6), 515-40.

Kaplitt, M.G., Leone P, Samulski RJ, Xiao X, Pfaff DW, O'Malley KL, During MJ. Long-term gene expression and phenotypic correction using adeno-associated virus vectors in the mammalian brain. *Nat Genet.* 1994 Oct;8(2):148-54.

Kayagaki N, Stowe IB, Lee BL, O'Rourke K, Anderson K, Warming S, Cuellar T, Haley B, Roose-Girma M, Phung QT, Liu PS, Lill JR, Li H, Wu J, Kummerfeld S, Zhang J, Lee WP, Snipas SJ, Salvesen GS, Morris LX, Fitzgerald L, Zhang Y, Bertram EM, Goodnow CC, Dixit VM (2015). Caspase-11 cleaves gasdermin D for non-canonical inflammasome signaling. Nature. Sep 16. doi: 10.1038/nature15541.

Kim MS, Lebron C, Nagpal JK, Chae YK, Chang X, Huang Y, Chuang T, Yamashita K, Trink B, Ratovitski EA, Califano JA, Sidransky D (2008). Methylation of the DFNA5 increases risk of lymph node metastasis in human breast cancer. Biochem Biophys Res Commun. 370(1):38-43.

Kim MS, Chang X, Yamashita K, Nagpal JK, Baek JH, Wu G, Trink B, Ratovitski EA, Mori M, Sidransky D (2008). Aberrant promoter methylation and tumor suppressive activity of the DFNA5 gene in colorectal carcinoma. Oncogene. 27(25):3624-34.

Kemp, D.T. (2002). Otoacoustic emissions, their origin in cochlear function, and use. *Br. Med. Bull*. 63, 223–241.

Koch, J., Pranjic, K., Huber, A., Ellinger, A., Hartig, A., Kragler, F., and Brocard, C. (2010). PEX11 family members are membrane elongation factors that coordinate peroxisome proliferation and maintenance. *Journal of cell science 123*, 3389-3400.

Kress, C., Vandormael-Pournin, S., Baldacci, P., Cohen-Tannoudji, M., Babinet, C. (1998). Nonpermissiviness for mouse embryonic stem (ES) cell derivation circumvented by a single backcross to 129/Sv strain: establishment of ES cell lines bearing the Omd conditional lethal mutation. *Mamm. Genome* 9,998-1001.

Kujawa, S.G., and Liberman, M.C. (2009). Adding insult to injury: cochlear nerve degeneration after "temporary" noise-induced hearing loss. *The Journal of neuroscience : the official journal of the Society for Neuroscience 29*, 14077-14085.

Lallemand, Y., Luria, V., Haffner-Krausz, R., Lonai, P. (1998). Maternally expressed *PGK-cre* transgene as a tool for early and uniform activation of the Cre site-specific recombinase. *Transgenic Res*. 7, 105-112.

Lay, D., Gorgas, K., and Just, W.W. (2006). Peroxisome biogenesis: where Arf and coatomer might be involved. *Biochim Biophys Acta 1763*, 1678-1687.

Lee, SP., Hwang, Y.S., Kim, Y.J., Kwon, K.S., Kim, H.J., Kim, K., Chae, H.Z. (2001). Cyclophilin A binds to peroxiredoxins and activates its peroxidase activity. *J. Biol. Chem*. 276(32), 29826-32.

Lee, J.N., Kim, S.G., Lim, J.Y., Kim, S.J., Choe, S.K., and Park, R. (2015). Proteasome inhibitors induce auditory hair cell death through peroxisome dysfunction. *Biochemical and biophysical research communications 456*, 269-274.

Li, X., Baumgart, E., Dong, G.X., Morrell, J.C., Jimenez-Sanchez, G., Valle, D., Smith, K.D., and Gould, S.J. (2002). PEX11alpha is required for peroxisome proliferation in response to 4-phenylbutyrate but is dispensable for peroxisome proliferator-activated receptor alpha-mediated peroxisome proliferation. *Molecular and cellular biology 22*, 8226-8240.

Li-Yang MN, Shen XF, Wei QJ, Yao J, Lu YJ, Cao X, Xing GQ (2015). IVS8+1 DelG, a Novel Splice Site Mutation Causing DFNA5 Deafness in a Chinese Family. Chin Med J (Engl). 128(18):2510-2515.

Lizana, L., Bauer, B., and Orwar, O. (2008). Controlling the rates of biochemical reactions and signaling networks by shape and volume changes. *Proceedings of the National Academy of Sciences of the United States of America 105*, 4099-4104.

Lopez-Huertas, E., Charlton, W.L., Johnson, B., Graham, I.A., and Baker, A. (2000). Stress induces peroxisome biogenesis genes. *The EMBO journal 19*, 6770-6777.

Matise, M.P., Auerbach, W., Joyner, A. (1999). Production of targeted embryonic stem cell clones. In: Joyner A, ed. *Gene targeting. A practical approach*. Oxford: Oxford University Press; p.101-132.

Menuet, C., Cazals, Y., Gestreau, C., Borghgraef, P., Gielis, L., Dutschmann, M., Van Leuven, F., Hilaire, G. (2011). Age-Related Impairment of Ultrasonic Vocalization in Tau.P301L Mice: Possible Implication for Progressive Language Disorders. *PloS One* 6(10), e25770.

Meyer zum Gottesberge, A.M., Felix, H., Reuter, A., Weiher, H. (2001). Ultrastructural and physiological defects in the cochlea of the *Mpv17* mouse strain. A comparison between young and old adult animals. *Hear. Res.* 156(1-2), 69-80.

Michard, Q., Commo, S., Belaidi, J.P., Alleaume, A.M., Michelet, J.F., Daronnat, E., Eilstein, J., Duche, D., Marrot, L., Bernard, B.A. (2008b). TRP-2 specifically decreases WM35 cell sensitivity to oxidative stress. *Free Radic. Biol. Med*. 44(6), 1023-31.

Michard, Q., Commo, S., Rocchetti, J., El Houari, F., Alleaume, A.M., Wakamatsu, K., Ito, S., Bernard, B.A. (2008a). TRP-2 expression protects HEK cells from dopamine- and hydroquinone-induced toxicity. *Free Radic. Biol. Med*. 45(7), 1002-10.

Motley, A.M., and Hettema, E.H. (2007). Yeast peroxisomes multiply by growth and division. *J Cell Biol 178*, 399-410.

Mujtaba, G., Bukhari, I., Fatima, A., Naz, S. (2012). A p.C343S missense mutation in *PJVK* causes progressive hearing loss. *Gene* 504(1), 98-101.

Needleman, S.B., and Wunsch, C.D. (1970). A general method applicable to the search for similaritis in the amino acid sequence of two proteins. *J. Mol. Biol.* 48(3), 443-453.

Nishio A, Noguchi Y, Sato T, Naruse TK, Kimura A, Takagi A, Kitamura K (2014). A DFNA5 mutation identified in Japanese families with autosomal dominant hereditary hearing loss. Ann Hum Genet. 78(2):83-91.

Ohinata, Y., Miller, J.M., Altschuler, R.A., and Schacht, J. (2000). Intense noise induces formation of vasoactive lipid peroxidation products in the cochlea. *Brain research 878*, 163-173.

Ohlemiller, K.K., McFadden, S.L., Ding, D.L., Flood, D.G., Reaume, A.G., Hoffman, E.K., Scott, R.W., Wright, J.S., Putcha, G.V., and Salvi, R.J. (1999a). Targeted deletion of the cytosolic Cu/Zn-superoxide dismutase gene (Sod1) increases susceptibility to noise-induced hearing loss. *Audiology & neuro-otology 4*, 237-246.

Ohlemiller, K.K., Wright, J.S., and Dugan, L.L. (1999b). Early elevation of cochlear reactive oxygen species following noise exposure. Audiol Neurootol *4*, 229-236.

Ohlemiller, K.K., McFadden, S.L., Ding, D.L., Lear, P.M., and Ho, Y.S. (2000). Targeted mutation of the gene for cellular glutathione peroxidase (Gpx1) increases noise-induced hearing loss in mice. *Journal of the Association for Research in Otolaryngology* : JARO *1*, 243-254.

Okatsu, K., Saisho, K., Shimanuki, M., Nakada, K., Shitara, H., Sou, Y.S., Kimura, M., Sato, S., Hattori, N., Komatsu, M*., et al.* (2010). p62/SQSTM1 cooperates with Parkin for perinuclear clustering of depolarized mitochondria. *Genes to cells : devoted to molecular & cellular mechanisms 15*, 887-900.

Op de Beeck K, Van Camp G, Thys S, Cools N, Callebaut I, Vrijens K, Van Nassauw L, Van Tendeloo VF, Timmermans JP, Van Laer L (2011). The DFNA5 gene, responsible for hearing loss and involved in cancer, encodes a novel apoptosis-inducing protein. Eur J Hum Genet. 19(9):965-73.

Park HJ, Cho HJ, Baek JI, Ben-Yosef T, Kwon TJ, Griffith AJ, Kim UK (2010). Evidence for a founder mutation causing DFNA5 hearing loss in East Asians. J Hum Genet. 55(1):59-62.

Passreiter, M., Anton, M., Lay, D., Frank, R., Harter, C., Wieland, F.T., Gorgas, K., and Just, W.W. (1998). Peroxisome biogenesis: involvement of ARF and coatomer. *J Cell Biol 141*, 373-383.

Pienkowski, M., and Eggermont, J.J. (2009). Long-term, partially-reversible reorganization of frequency tuning in mature cat primary auditory cortex can be induced by passive exposure to moderate-level sounds. *Hearing research 257*, 24-40.

Rahman, I., Kode, A., and Biswas, S.K. (2006). Assay for quantitative determination of glutathione and glutathione disulfide levels using enzymatic recycling method. *Nat. Protoc.* 1, 3159–3165.

Reddy, J.K., Azarnoff, D.L., and Hignite, C.E. (1980). Hypolipidaemic hepatic peroxisome proliferators form a novel class of chemical carcinogens. *Nature 283*, 397-398.

Robles, L., and Ruggero M.A. (2001). Mechanics of the mammalian cochlea. *Physiol Rev.* 81(3), 1305-52.

Roux, I., Safieddine, S., Nouvian, R., Grati, M., Simmler, M.C., Bahloul, A., Perfettini, I., Le Gall, M., Rostaing, P., Hamard, G., et al. (2006). Otoferlin, defective in a human deafness form, is essential for exocytosis at the auditory ribbon synapse. *Cell* 127(2), 277-89.

Roux, I., Hosie, S., Johnson, S.L., Bahloul, A., Cayet, N., Nouaille, S., Kros, C.J., Petit, C., and Safieddine, S. (2009). Myosin VI is required for the proper maturation and function of inner hair cell ribbon synapses. Hum. Mol. Genet. *18*, 4615-4628.

Roy, S., Ryals, M.M., Van den Bruele, A.B., Fitzgerald, T.S., Cunningham, L.L. (2013). Sound preconditioning therapy inhibits ototoxic hearing loss in mice. *J. Clin. Invest*. 123(11), 4945-9.

Sadanaga, M., and Morimitsu, T. (1995). Development of endocochlear potential and its negative component in mouse cochlea. *Hearing research 89*, 155-161.

Saeki and Sasaki (2011) « Endothelium and epithelium » ISBN 978-1-61470-874-2, Ed. J. Carrasco and M. Mota, pp 193-211, © 2012 Nova Science Publishers.

Santos, M.J., Quintanilla, R.A., Toro, A., Grandy, R., Dinamarca, M.C., Godoy, J.A., and Inestrosa, N.C. (2005). Peroxisomal proliferation protects from beta-amyloid neurodegeneration. *The Journal of biological chemistry 280*, 41057-41068.

Schrader, M., and Fahimi, H.D. (2006). Peroxisomes and oxidative stress. *Biochim Biophys Acta 1763*, 1755-1766.

Schrader, M., Reuber, B.E., Morrell, J.C., Jimenez-Sanchez, G., Obie, C., Stroh, T.A., Valle, D., Schroer, T.A., and Gould, S.J. (1998). Expression of PEX11beta mediates peroxisome proliferation in the absence of extracellular stimuli. *The Journal of biological chemistry 273*, 29607-29614.

Schrader, M., Wodopia, R., and Fahimi, H.D. (1999). Induction of tubular peroxisomes by UV irradiation and reactive oxygen species in HepG2 cells. *J Histochem Cytochem 47*, 1141-1148.

Schwander, M., Sczaniecka, A., Grillet, N., Bailey, J.S., Avenarius, M., Najmabadi, H., Steffy, B.M., Federe, G.C., Lagler, E.A., Banan, R. (2007). A forward genetics screen in mice identifies recessive deafness traits and reveals that pejvakin is essential for outer hair cell function. *J. Neurosci.* 27(9), 2163-75.

Shi J, Zhao Y, Wang K, Shi X, Wang Y, Huang H, Zhuang Y, Cai T, Wang F, Shao F (2015). Cleavage of GSDMD by inflammatory caspases determines pyroptotic cell death. *Sep 16. doi: 10.1038/nature15514.* [Epub ahead of print]

Shi P, Tang A, Xian L, Hou S, Zou D, Lv Y, Huang Z, Wang Q, Song A, Lin Z, Gao X (2015). Loss of conserved Gsdma3 self-regulation causes autophagy and cell death. Biochem J. 468(2):325-36.

Smith, J.J., and Aitchison, J.D. (2013). Peroxisomes take shape. *Nat Rev Mol Cell Biol 14*, 803-817.

Tang, X.D., Garcia, M.L., Heinemann, S.H., and Hoshi, T. (2004). Reactive oxygen species impair Slo1 BK channel function by altering cysteine-mediated calcium sensing. Nat. Struct. Mol. Biol. *11*, 171-178.

Thelen, N., Breuskin, I., Malgrange, B., Thiry, M. (2009). Early identification of inner pillar cells during rat cochlear development. *Cell Tissue Res*. 337, 1–14.

Tran, C., Hewson, S., Steinberg, S.J., Mercimek-Mahmutoglu, S. (2014). Late-onset Zellweger spectrum disorder caused by PEX6 mutations mimicking X-linked adrenoleukodystrophy. *Pediatr Neurol*. 51(2), 262-5.

Van Laer L, Huizing EH, Verstreken M, van Zuijlen D, Wauters JG, Bossuyt PJ, Van de Heyning P, McGuirt WT, Smith RJ, Willems PJ, Legan PK, Richardson GP, Van Camp G (1998). Nonsyndromic hearing impairment is associated with a mutation in DFNA5. Nat Genet. 20(2):194-7.

Wang, Y., Hirose, K., and Liberman, M.C. (2002). Dynamics of noise-induced cellular injury and repair in the mouse cochlea. *Journal of the Association for Research in Otolaryngology* : JARO *3*, 248-268.

Wang CJ, Tang L, Shen DW, Wang C, Yuan QY, Gao W, Wang YK, Xu RH, Zhang H (2013). The expression and regulation of DFNA5 in human hepatocellular carcinoma DFNA5 in hepatocellular carcinoma. Mol Biol Rep. 40(12):6525-31.

Yamane, H., Nakai, Y., Takayama, M., Iguchi, H., Nakagawa, T., and Kojima, A. (1995). Appearance of free radicals in the guinea pig inner ear after noise-induced acoustic trauma. *Eur Arch Otorhinolaryngol 252*, 504-508.

Yamashita, D., Jiang, H.Y., Schacht, J., and Miller, J.M. (2004). Delayed production of free radicals following noise exposure. *Brain research 1019*, 201-209.

Yu C, Meng X, Zhang S, Zhao G, Hu L, Kong X (2003). A 3-nucleotide deletion in the polypyrimidine tract of intron 7 of the DFNA5 gene causes nonsyndromic hearing impairment in a Chinese family. Genomics. 82(5):575-9.

Zhang, Q.J., Lan, L., Li, N., Qi, Y., Zong, L., Shi, W., Yu, L., Wang, H., Yang, J., Xie, L.Y., *et al.* (2015). Identification of a novel mutation of PJVK in the Chinese non-syndromic hearing loss population with low prevalence of the PJVK mutations. *Acta oto-laryngologica 135*, 211-216.

Avan P, Büki B, Petit C. (2013). Auditory distortions: origins and functions. Physiol Rev. Oct;93(4):1563-619.

Hardisty-Hughes RE, Parker A, Brown SD (**2010).** A hearing and vestibular phenotyping pipeline to identify mouse mutants with hearing impairment. Nat Protoc., Jan;5(1):177-90.

Le Calvez S, Avan P, Gilain L, Romand R., (1998) Hear Res. Jun;120(1-2):37-50.

Michalski N, Michel V, Caberlotto E, Lefèvre GM, van Aken AF, Tinevez JY, Bizard E, Houbron C, Weil D, Hardelin JP, Richardson GP, Kros CJ, Martin P, Petit C. . 2009, Harmonin-b, an actin-binding scaffold protein, is involved in the adaptation of mechanoelectrical transduction by sensory hair cells. Pflugers ArchNov;459(1):115-30.

Mustapha et al., 2002. Hum. Genet. Vol. 110, 348-350.

Weil et al., 2003. Human Molecular Genetics vol. 12, no. 5, 463-471.

CLAIMS

1. Gasdermin for use as a modulator of cellular redox homeostasis.

2. Gasdermin for use according to claim 1, as an antioxidant.

3. Gasdermin for use according to claim 2, for preventing and/or alleviating ROS-induced cellular damages.

4. Gasdermin for use according to claim 3, for preventing and/or reducing ROS-induced damages on cochlear cells, on afferent auditory neurons and on neurons of the auditory central pathway.

5. Gasdermin for use according to claim 4, wherein said ROS-induced damages are due to noise exposure or to ototoxic substance exposure.

6. Gasdermin for use according to any one of claims 1-5, for preventing and/or treating presbycusis, noise-induced hearing-loss, sudden sensorineural hearing impairment or auditory damages induced by acoustic trauma or by ototoxic substances, in a subject in need thereof.

7. Gasdermin for use according to claim 2, for treating patients suffering from peroxisomal disorders or mitochondrial disorders leading to ROS production or age-related diseases such as Parkinson's disease (PD), Alzheimer's disease (AD), Familial Amyotrophic Lateral Sclerosis (FALS), age-related macular degeneration (ARMD), type 2 diabetes, atherosclerosis, arthritis, cataracts, osteoporosis, hypertension, skin aging, skin pigmentation, and cardiovascular diseases.

8. Gasdermin for use according to claim 7, for restoring peroxisome and/or mitochondria mediated homeostasis in auditory cells in subjects.

9. Gasdermin for use according to claim 1, for treating cancer, preferably a hepatocarcinoma, a breast carcinoma, an esophageal or a gastric cancer, inflammatory diseases and ischemia-reperfusion injury.

10. Gasdermin for use according to claim 1 for preventing and/or reversing skin aging and/or skin pigmentation.

11. Cosmetic use of gasdermin for preventing and/or reversing skin aging and skin pigmentation.

12. Gasdermin for use according to any one of claims 1 to 10, or use of gasdermin according to claim 11, wherein said gasdermin is used in a subject normally expressing gasdermin.

13. A vector encoding a gasdermin polypeptide, for use for preventing and/or treating noise-induced or ototoxic substances-induced damages to auditory cells, peroxisomal disorders, cancer, inflammatory diseases and ischemia-reperfusion injury.

14. The vector for use according to claim 13, wherein it is a viral vector, preferably an AAV vector.

15. A vector encoding a gasdermin short hairpin RNA (shRNA), for use for treating cancer, inflammatory diseases and ischemia-reperfusion injury.

16. An antioxidant composition for use for treating congenital hearing impairment due to altered *DFNB59* gene expression or deficiency in a subject in need thereof, said composition comprising:

- a RS inhibiting compound and an antioxidant compound; or

- a RS inhibiting compound or an antioxidant compound with the exception of a gasdermin.

17. An antioxidant composition for use for treating subjects suffering from hearing impairment induced by noise or by ototoxic substance exposure in a subject in need thereof, said composition comprising a gasdermin and optionally at least one RS inhibiting compound.

18. The antioxidant composition for use according to claim 16 or 17, wherein gasdermin is normally expressed in said subjects.

19. Gasdermin for use according to any one of claims 1 to 10 or 12, or the use according to claims 11 or 12, or the vector for use according to any one of claims 13 to 15, or the antioxidant composition for use according to any one of claims 16 to 18, wherein said gasdermin is pejvakin.

20. An AAV2/8 vector expressing at least one *USH1* gene product.

21. The AAV2/8 vector according to claim 20, wherein said vector comprises the viral nucleic acid sequence SEQ ID NO:47 and/or SEQ ID NO:48.

22. The AAV2/8 vector according to claim 20 or 21, wherein said at least one *USH1* gene product has the amino acid sequence SEQ ID NO:49.

23. A viral particle comprising an AAV2/8 vector according to any one of claims 20 to 22.

24. A pharmaceutical composition comprising at least one AAV2/8 vector according to any one of claims 20 to 22, and/or at least one viral particle according to claim 23, and a pharmaceutically acceptable carrier.

25. The pharmaceutical composition according to claim 24, wherein said pharmaceutical composition is injectable.

26. The pharmaceutical composition according to claim 25, wherein said pharmaceutical composition is injectable in the cochlea of a subject.

27. The AAV2/8 vector according to any one of claims 20 to 22, or the viral particle according to claim 23, for use as a medicament.

28. The AAV2/8 vector according to any one of claims 20 to 22, or the viral particle according to claim 23, or the pharmaceutical composition according to any one of claims 24 to 26, for use in a method for treating Usher syndrome in a subject in need thereof.

29. The AAV2/8 vector or the viral particle or the pharmaceutical composition for use according to claim 28, wherein said method comprises an injection, preferably a cochlear injection, of said AAV2/8 vector or said viral particle or said pharmaceutical composition.

30. A kit comprising, in one or more containers in a single package, at least one AAV2/8 vector according to any one of claims 20 to 22 and/or at least one viral particle according to claim 23 and/or at least one pharmaceutical composition according to any one of claims 24 to 26, and means for injecting said AAV2/8 vector(s) and/or said viral particle(s) and/or said pharmaceutical composition(s).

31. The kit according to claim 30 wherein said means for injecting are means for a cochlear injection.

Figure 1

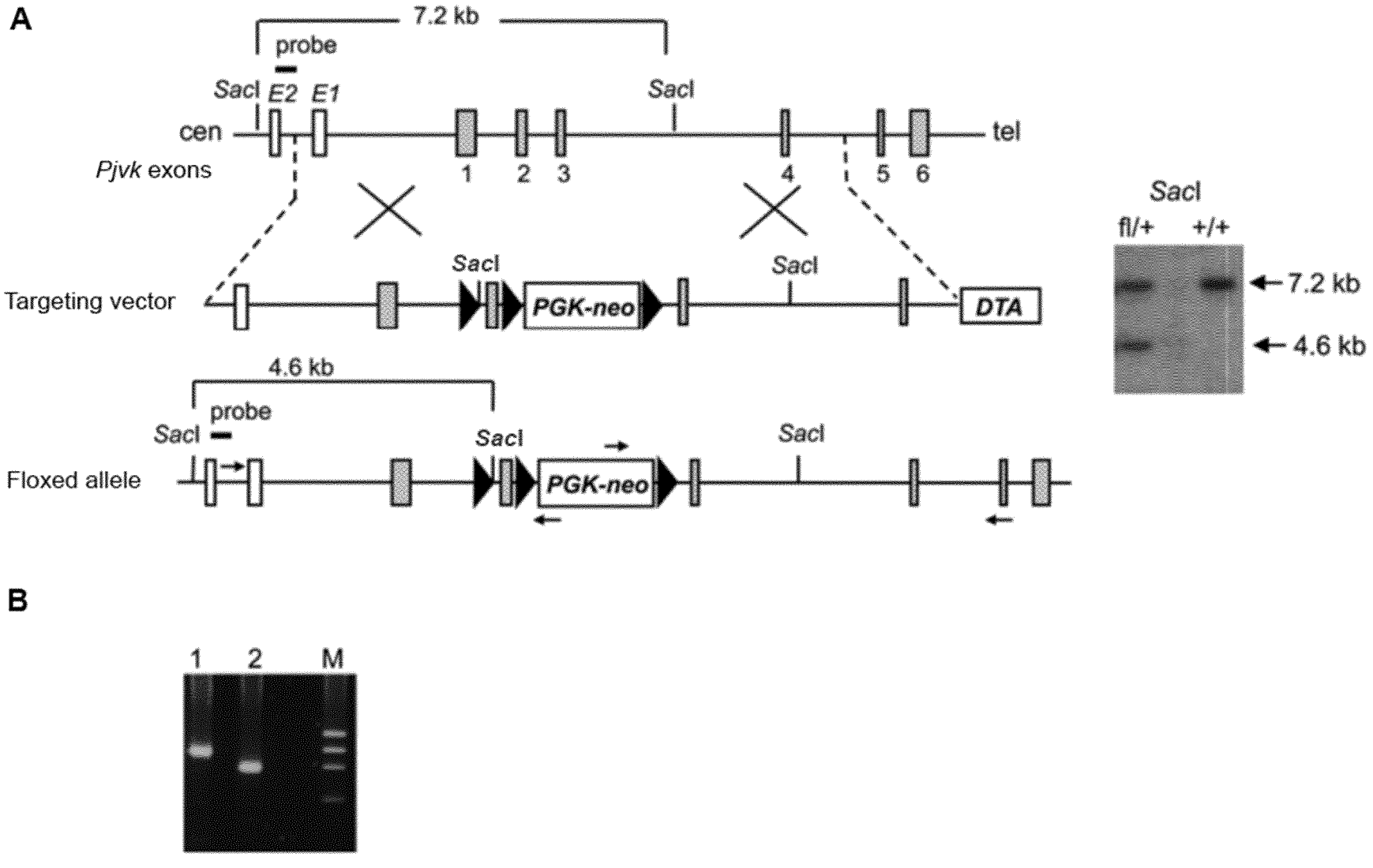
A
7.2 kb
probe
SacI
E2
E1
SacI
cen
tel
Pjvk exons
1
2
3
4
5
6
Targeting vector
SacI
PGK-neo
SacI
DTA
4.6 kb
probe
SacI
SacI
SacI
Floxed allele
PGK-neo
SacI
fl/+
+/+
7.2 kb
4.6 kb
B
1
2
M

Figure 2

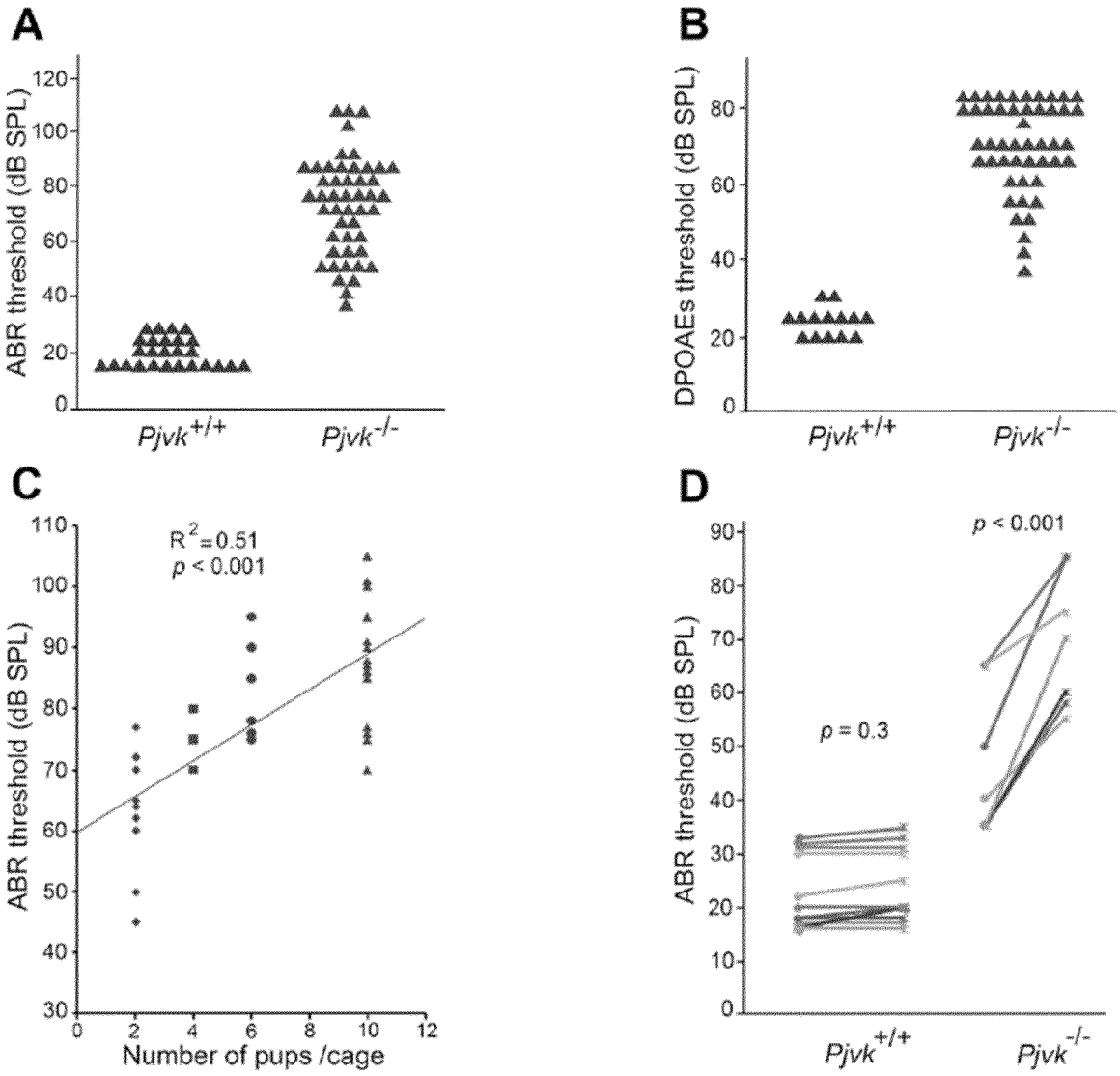
A
ABR threshold (dB SPL)
120
100
80
60
40
20
0
Pjvk+/+
Pjvk-/-
B
DPOAEs threshold (dB SPL)
80
60
40
20
0
Pjvk+/+
Pjvk-/-
C
R2=0.51
p < 0.001
ABR threshold (dB SPL)
110
100
90
80
70
60
50
40
30
0
2
4
6
8
10
12
Number of pups /cage
D
p < 0.001
p = 0.3
ABR threshold (dB SPL)
90
80
70
60
50
40
30
20
10
0
Pjvk+/+
Pjvk-/-

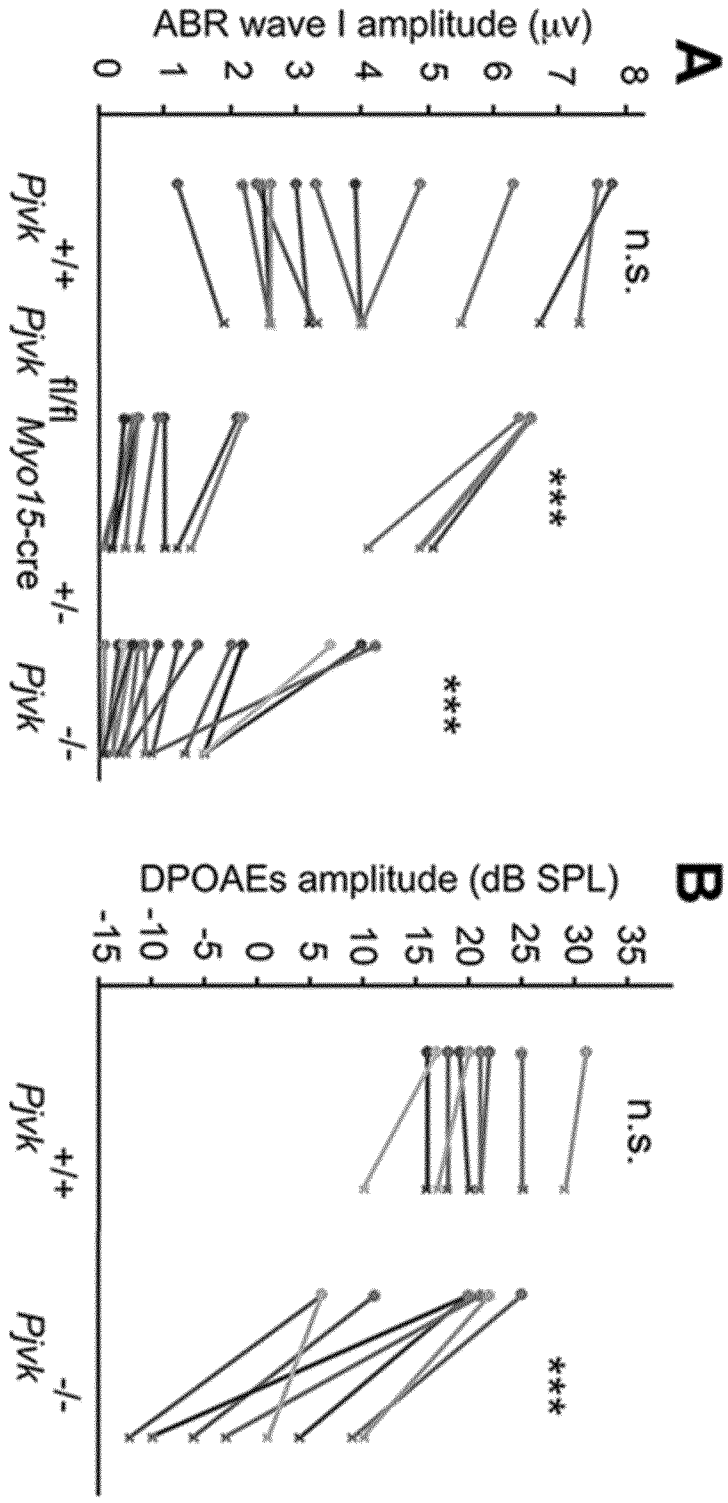
A
ABR wave I amplitude (μv)
0
1
2
3
4
5
6
7
8
n.s.
***
***
Pjvk +/+
Pjvk fl/fl Myo15-cre +/-
Pjvk -/-
B
DPOAEs amplitude (dB SPL)
-15
-10
-5
0
5
10
15
20
25
30
35
n.s.
***
Pjvk +/+
Pjvk -/-

Figure 3

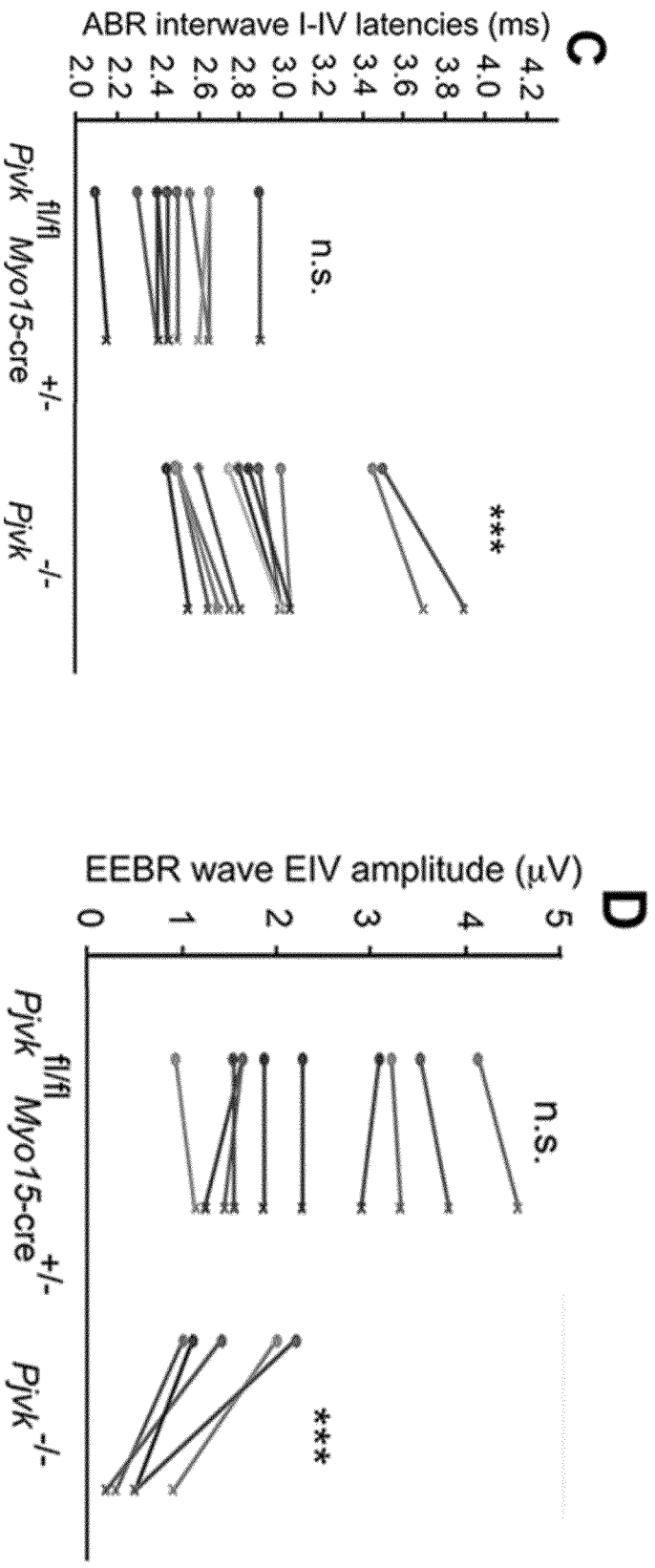

Figure 3 (continued)

Figure 3 (continued)

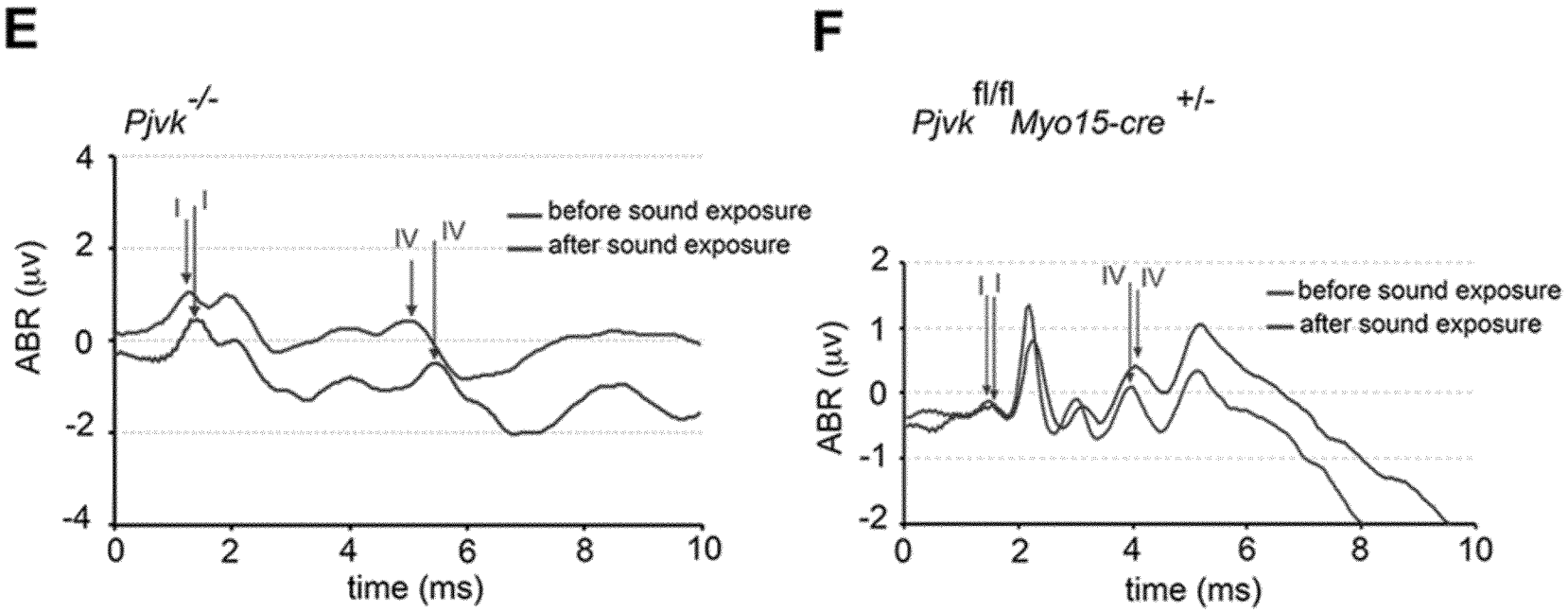

Figure 3 (continued)

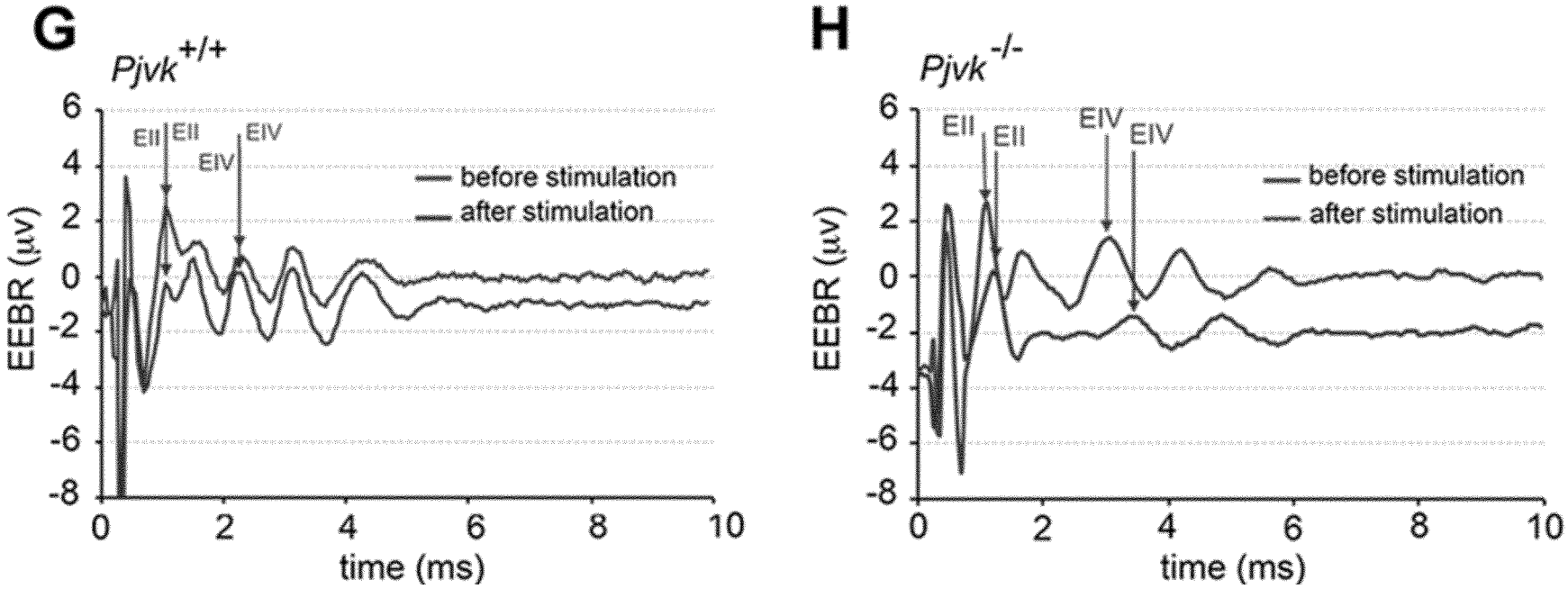

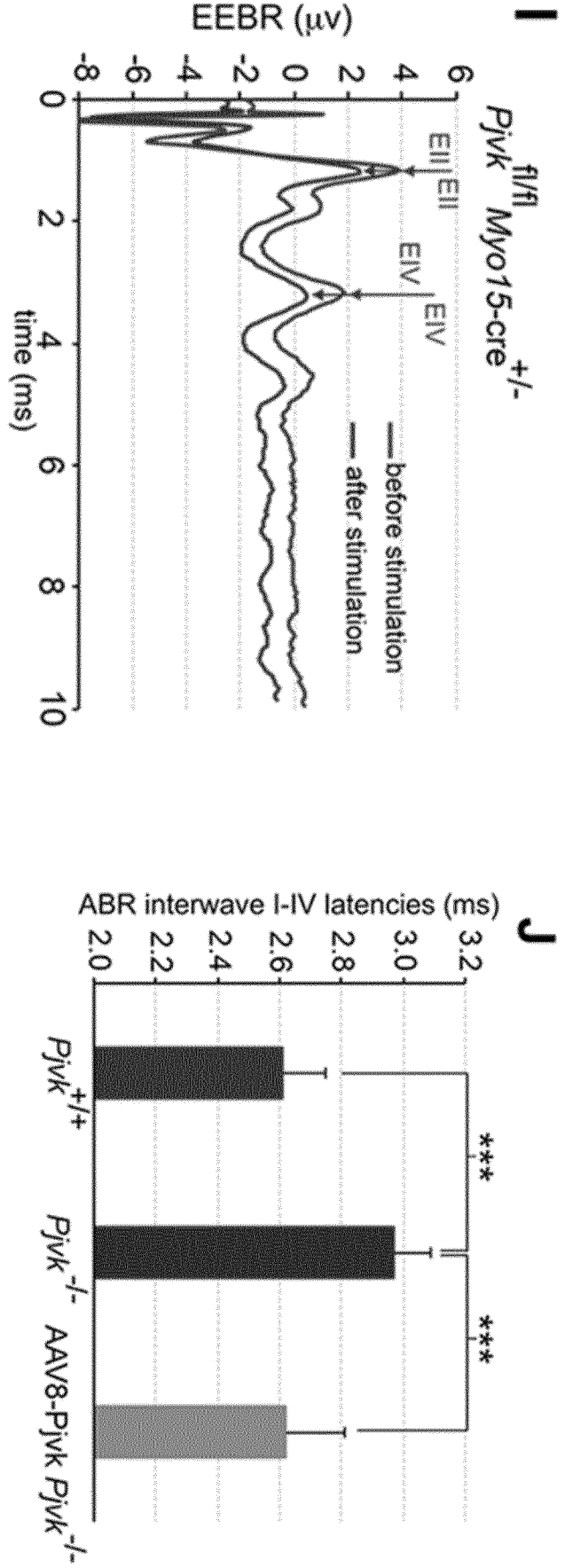

Figure 3 (continued)

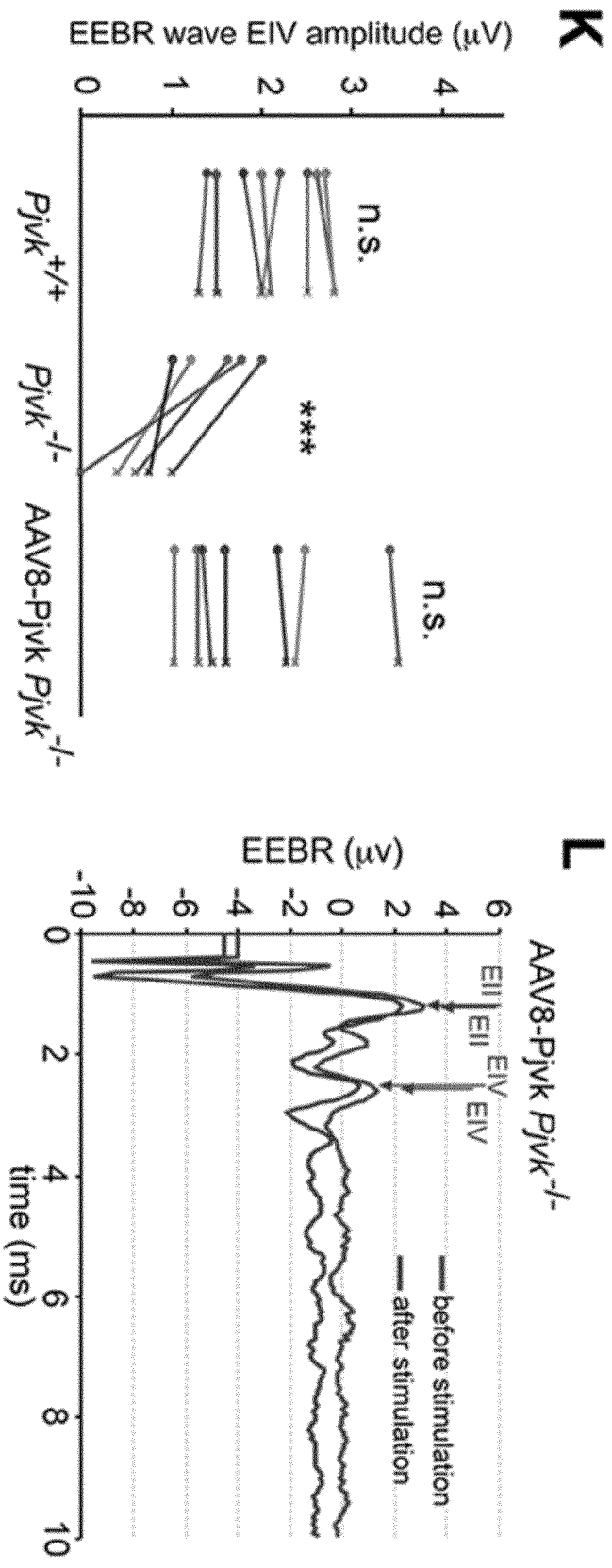

Figure 3 (continued)

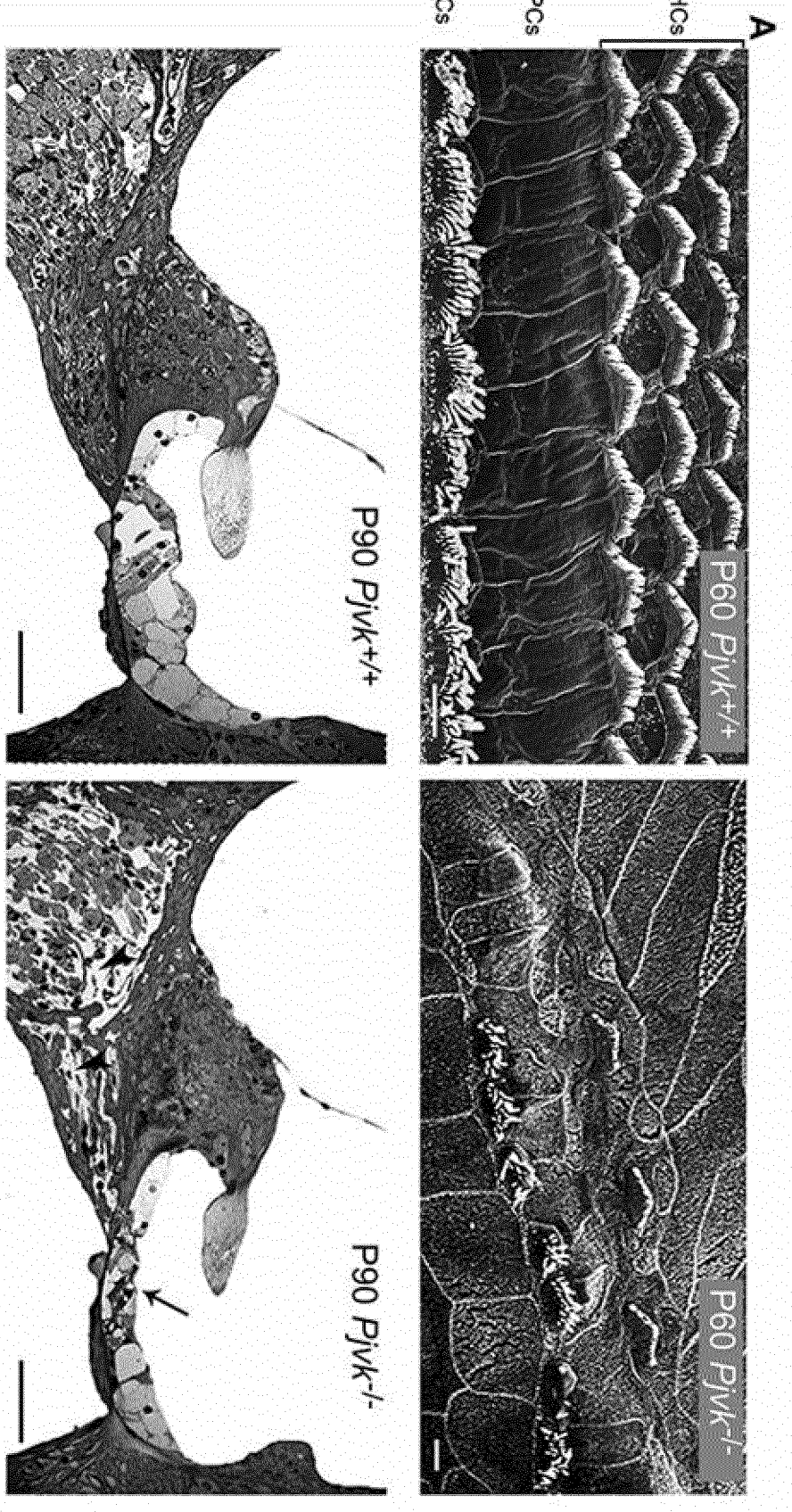

Figure 4

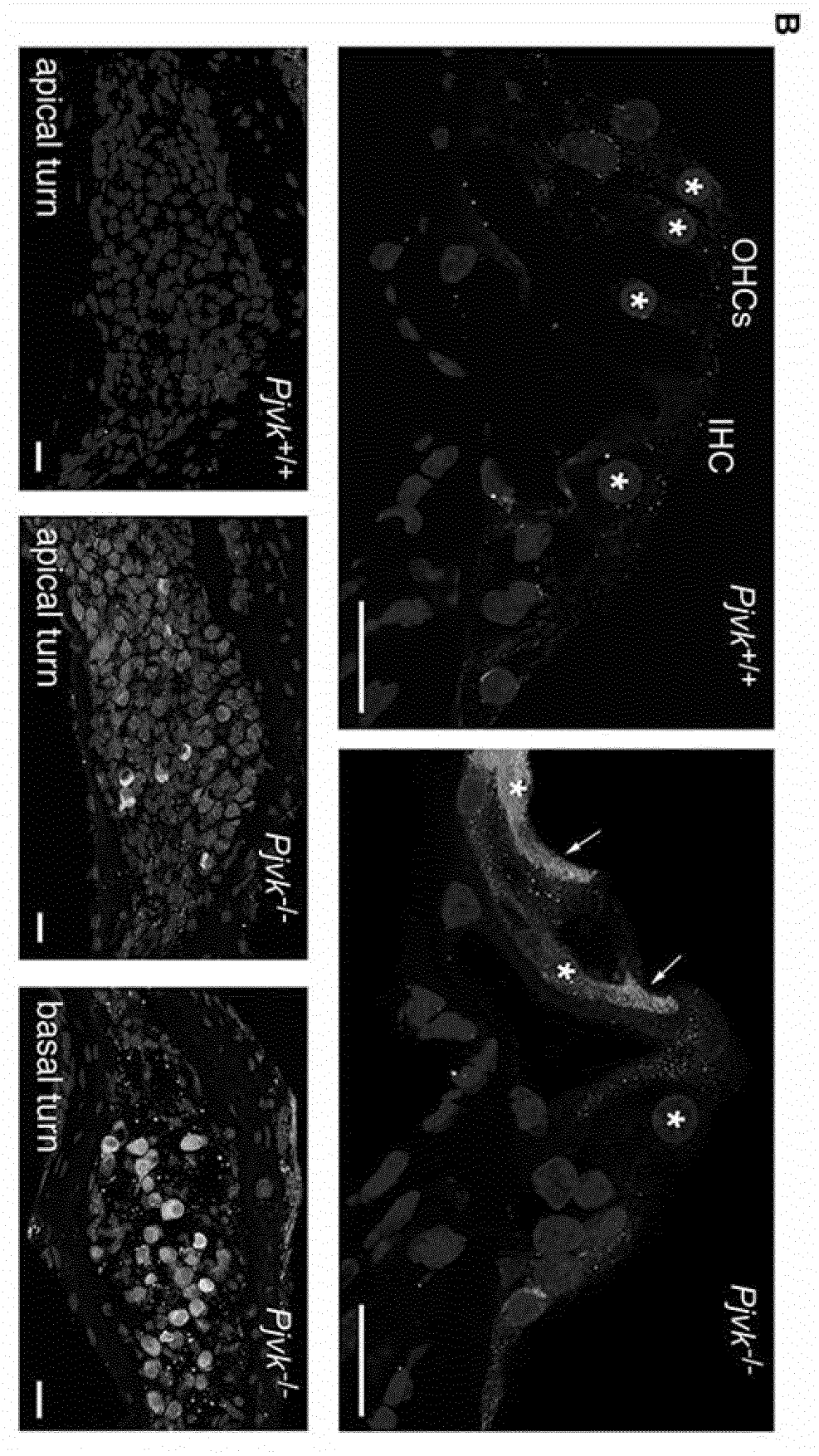

Figure 4 (continued)

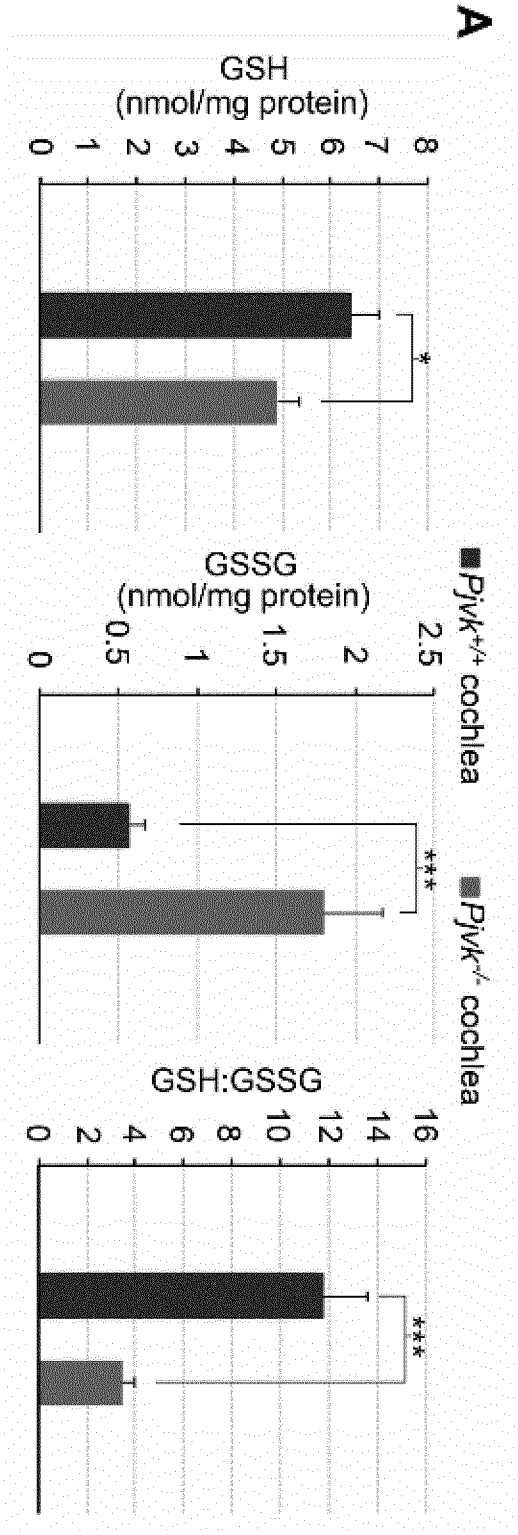
A
GSH
(nmol/mg protein)
0
1
2
3
4
5
6
7
8
*
GSSG
(nmol/mg protein)
0
0.5
1
1.5
2
2.5
***
GSH:GSSG
0
2
4
6
8
10
12
14
16
***
Pjvk+/+ cochlea
Pjvk-/- cochlea

Figure 5

Figure 5
(continued)

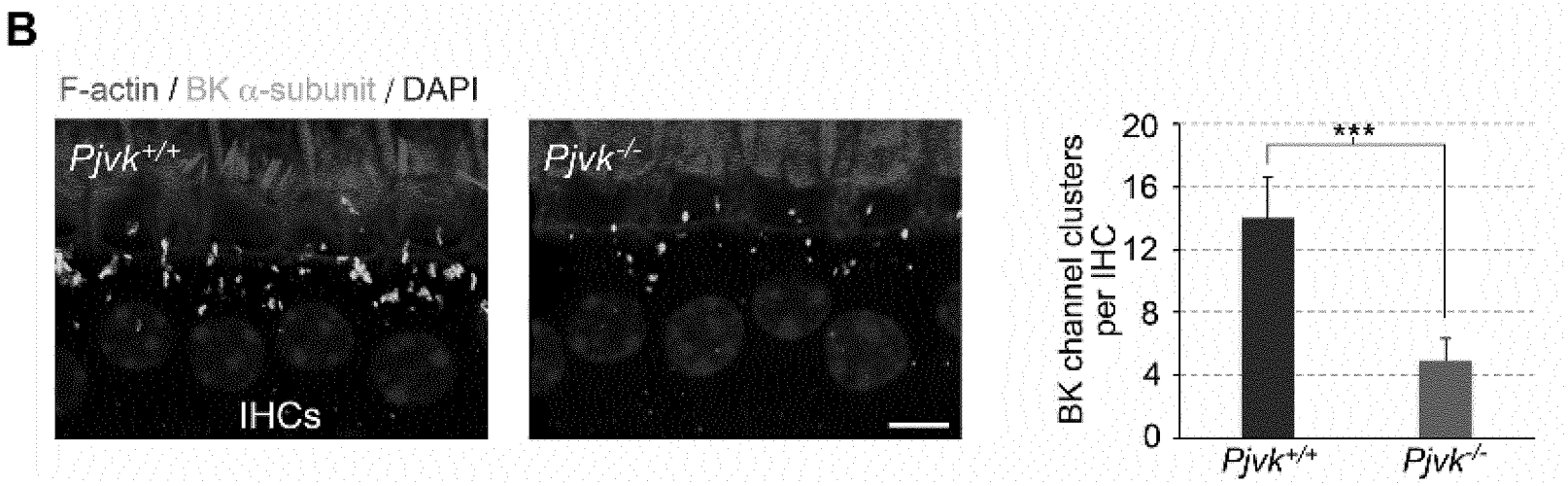

Figure 6

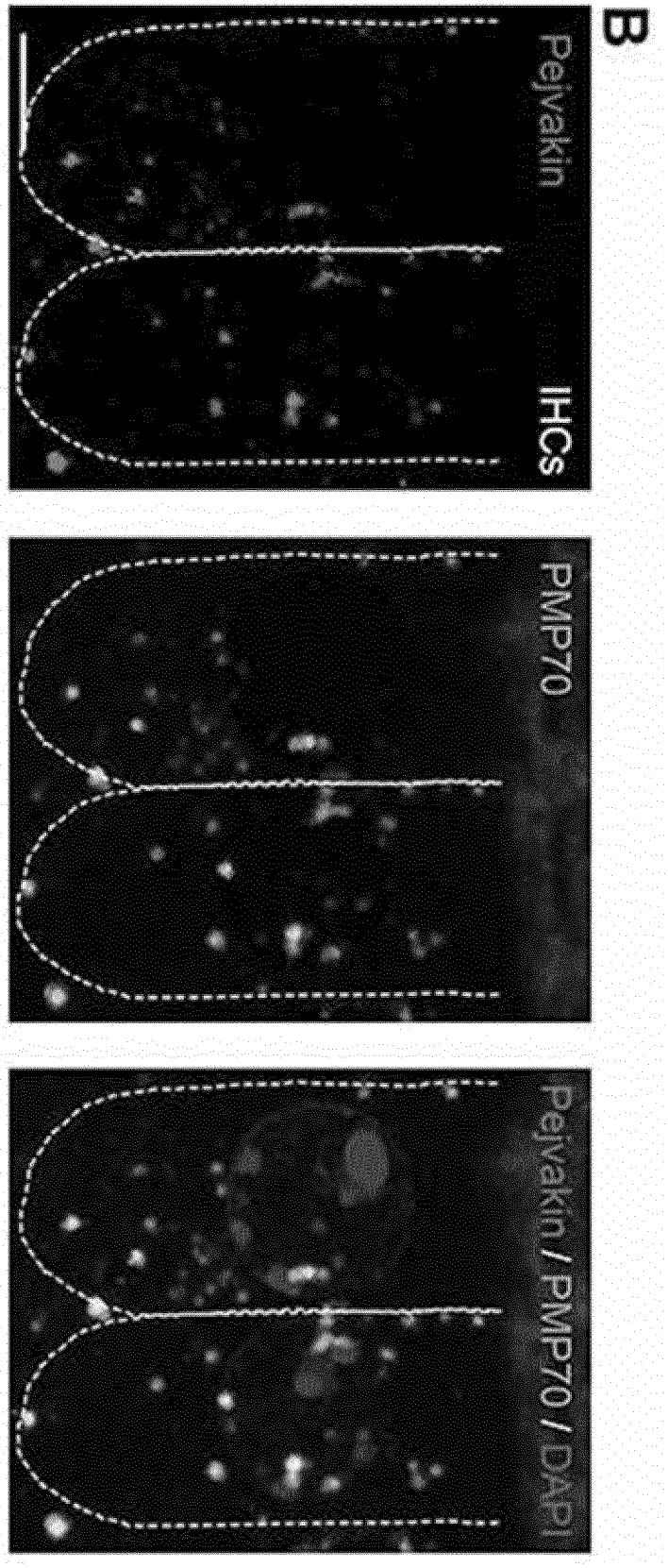

Figure 6 (continued)

Figure 6 (continued)

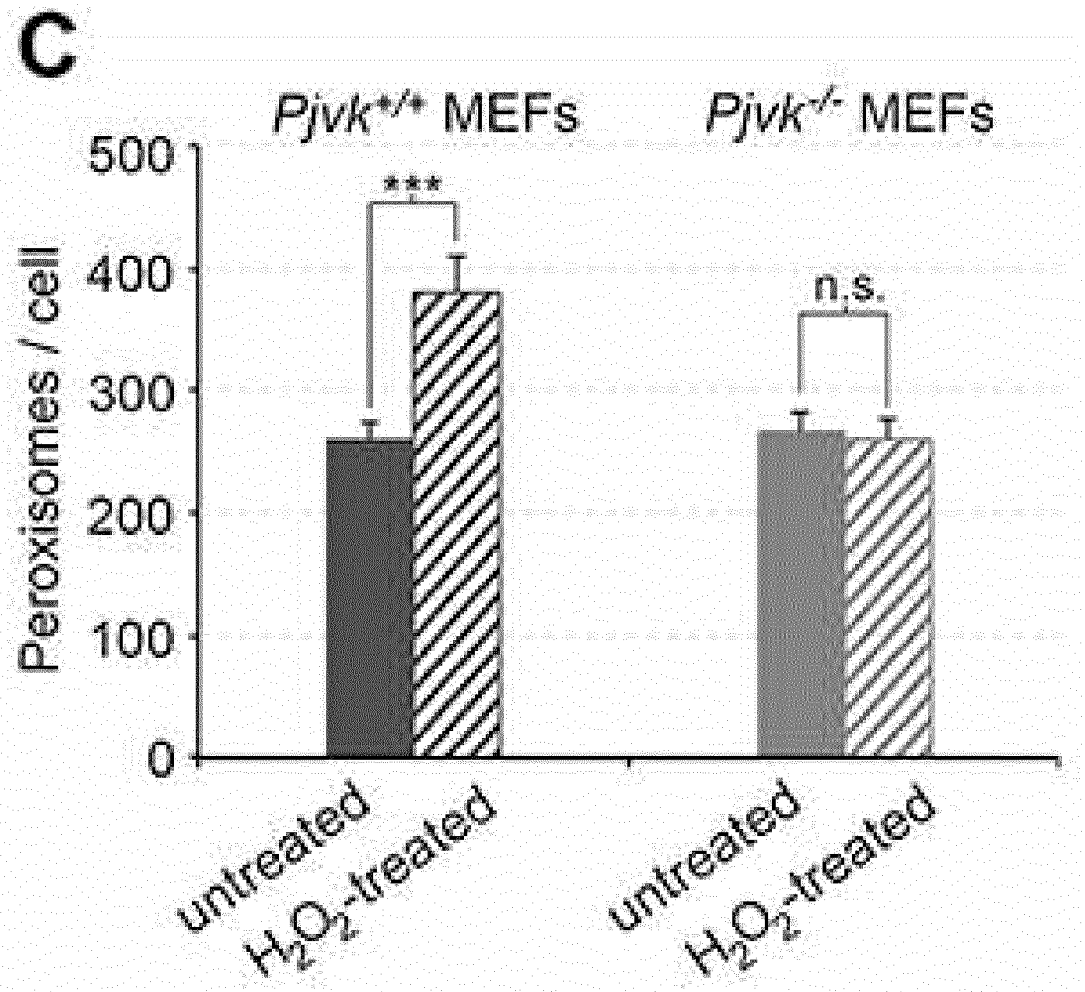

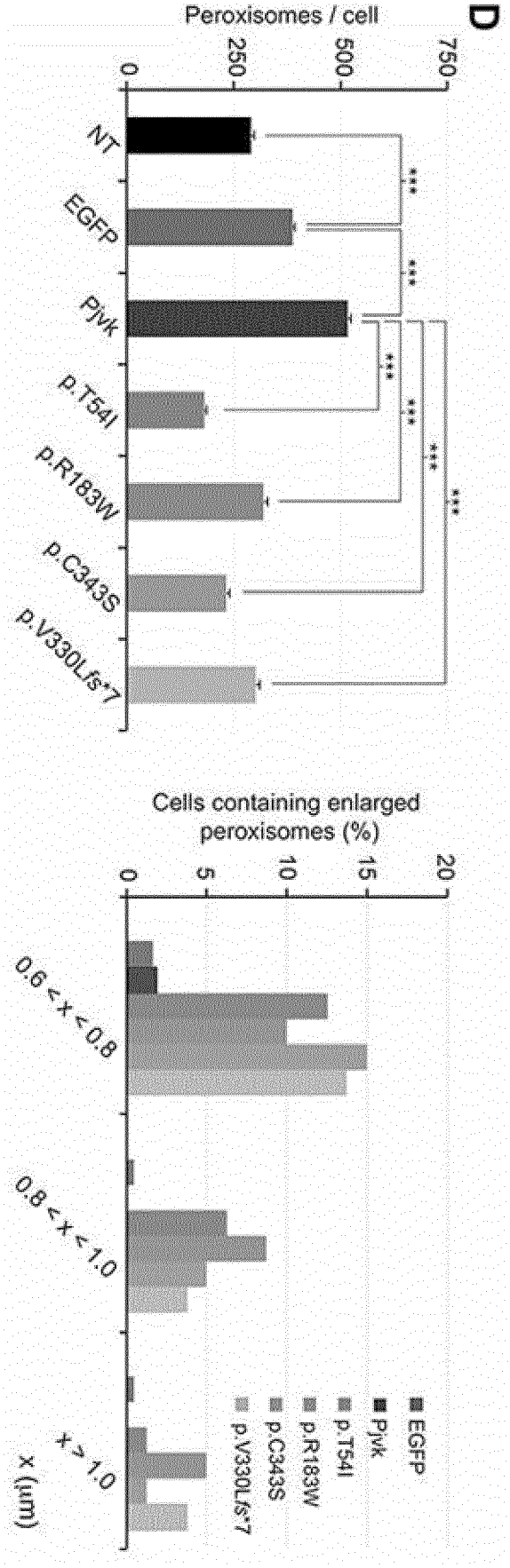

Figure 6 (continued)

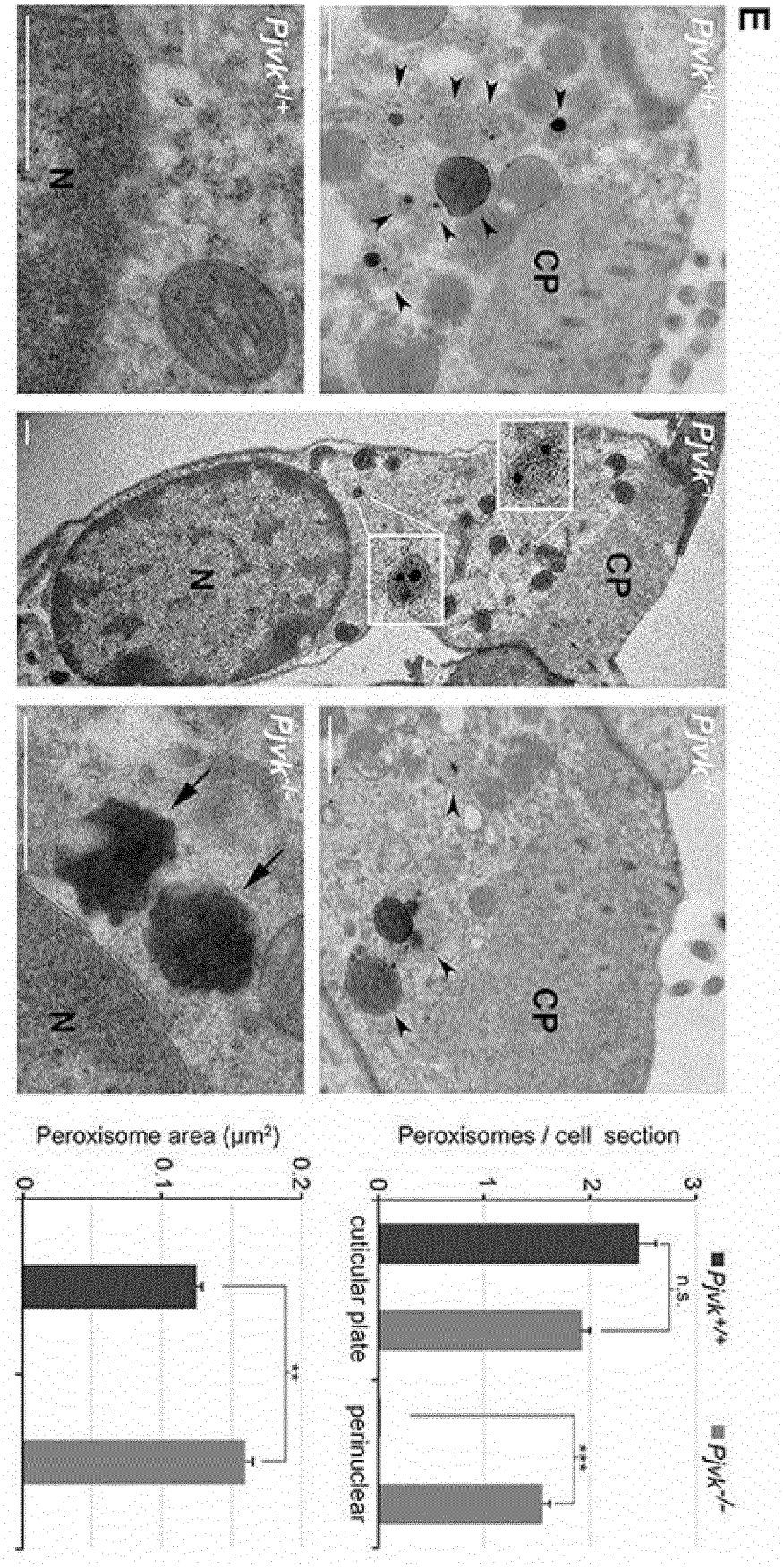

Figure 6 (continued)

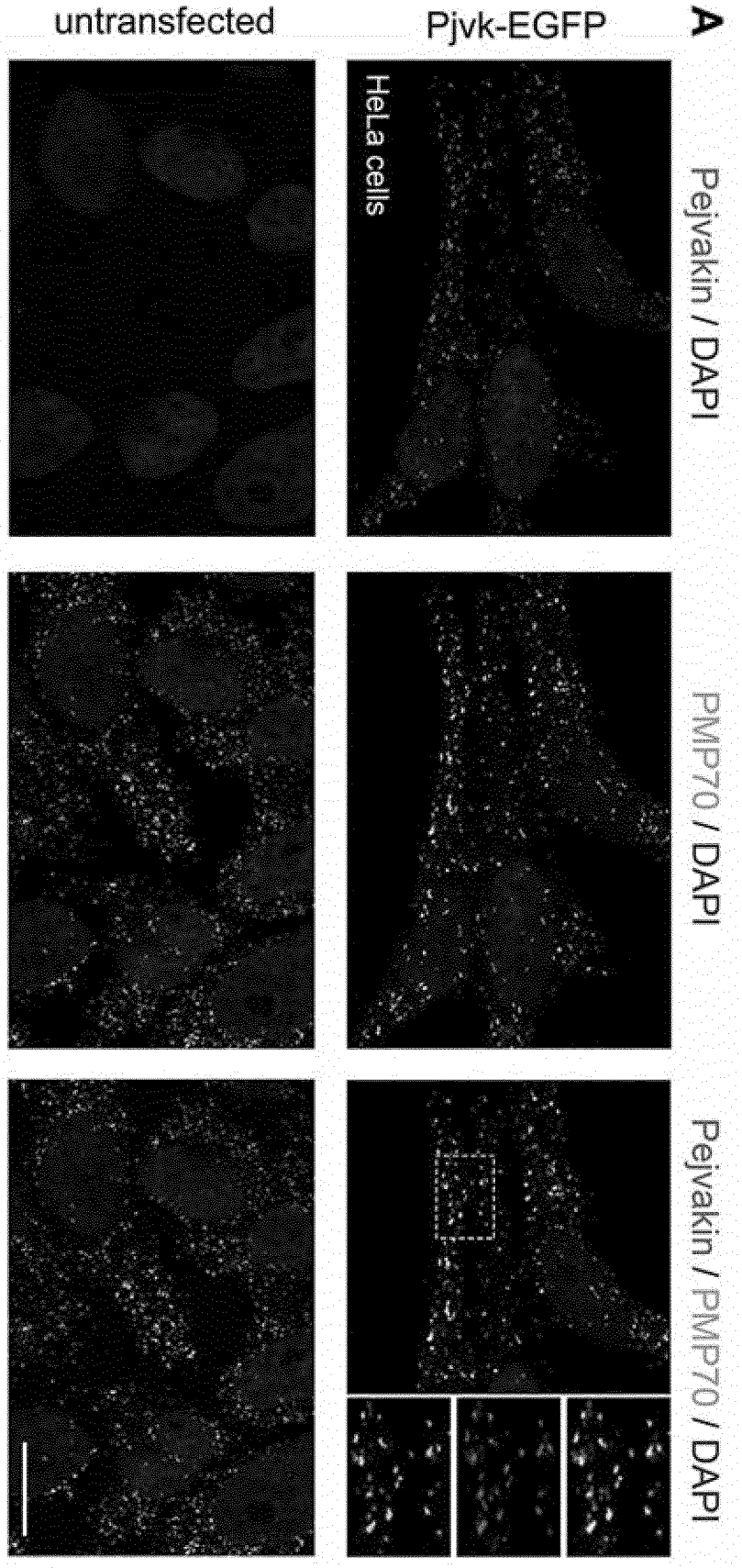
A
Pjvk-EGFP
untransfected
HeLa cells
Pejvakin / DAPI
PMP70 / DAPI
Pejvakin / PMP70 / DAPI

Figure 7

Figure 7 (continued)

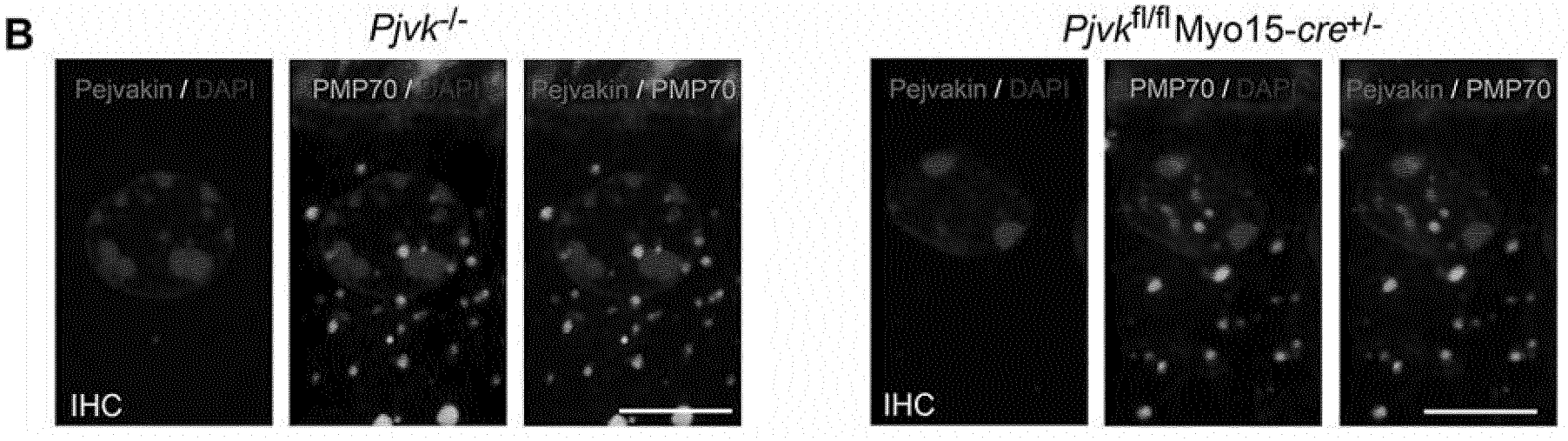

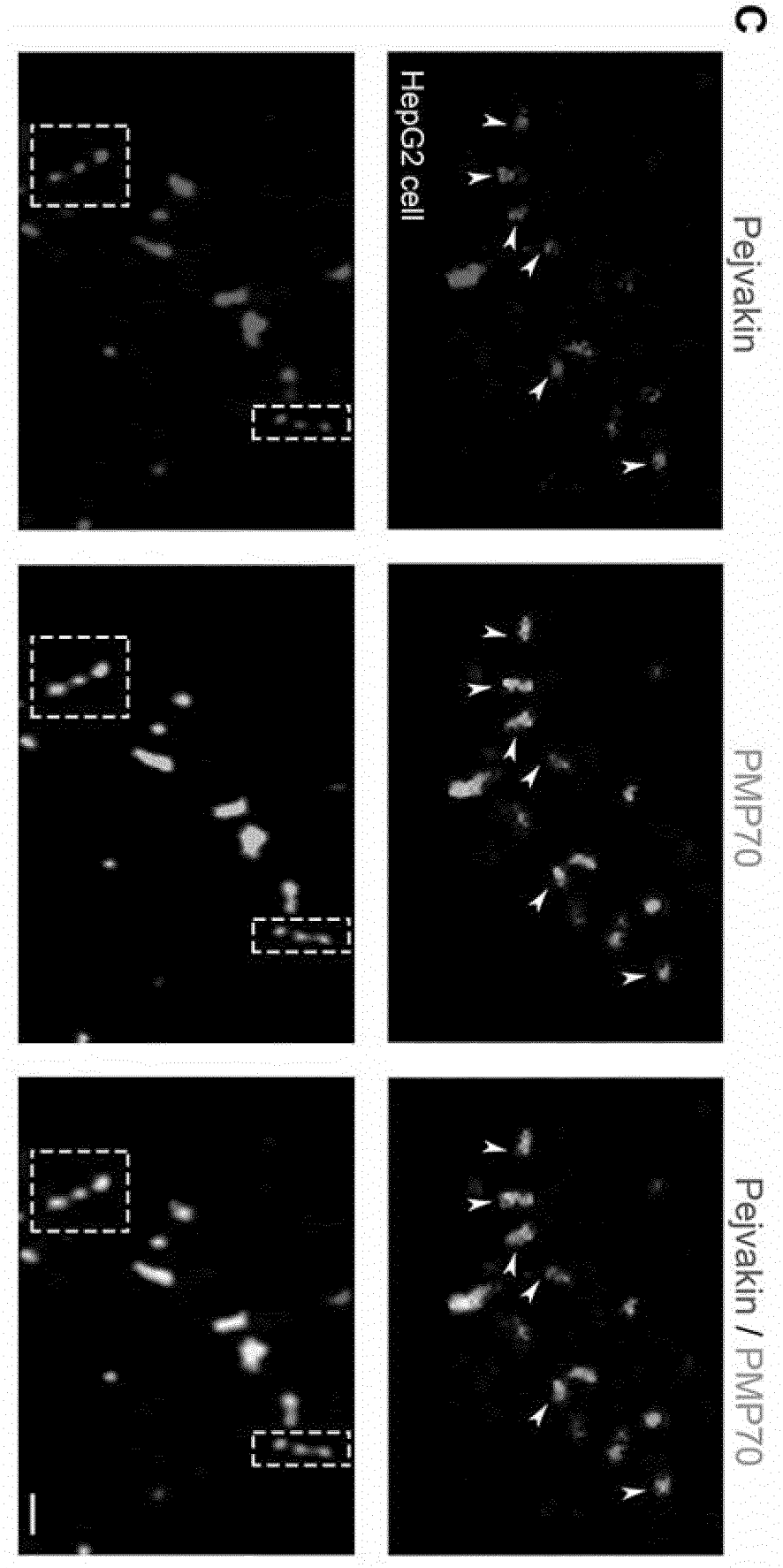

Figure 7 (continued)

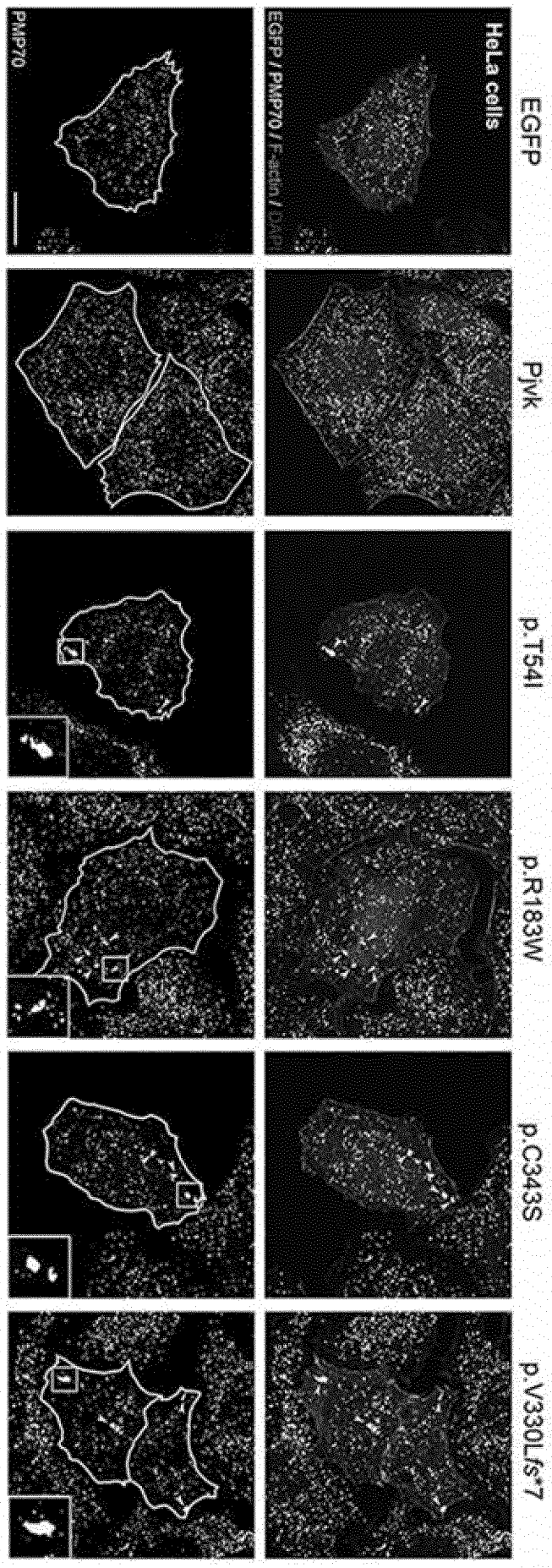
HeLa cells
EGFP / PMP70 / F-actin / DAPI
PMP70
EGFP
Pjvk
p.T54I
p.R183W
p.C343S
p.V330Lfs*7

Figure 8

Figure 9

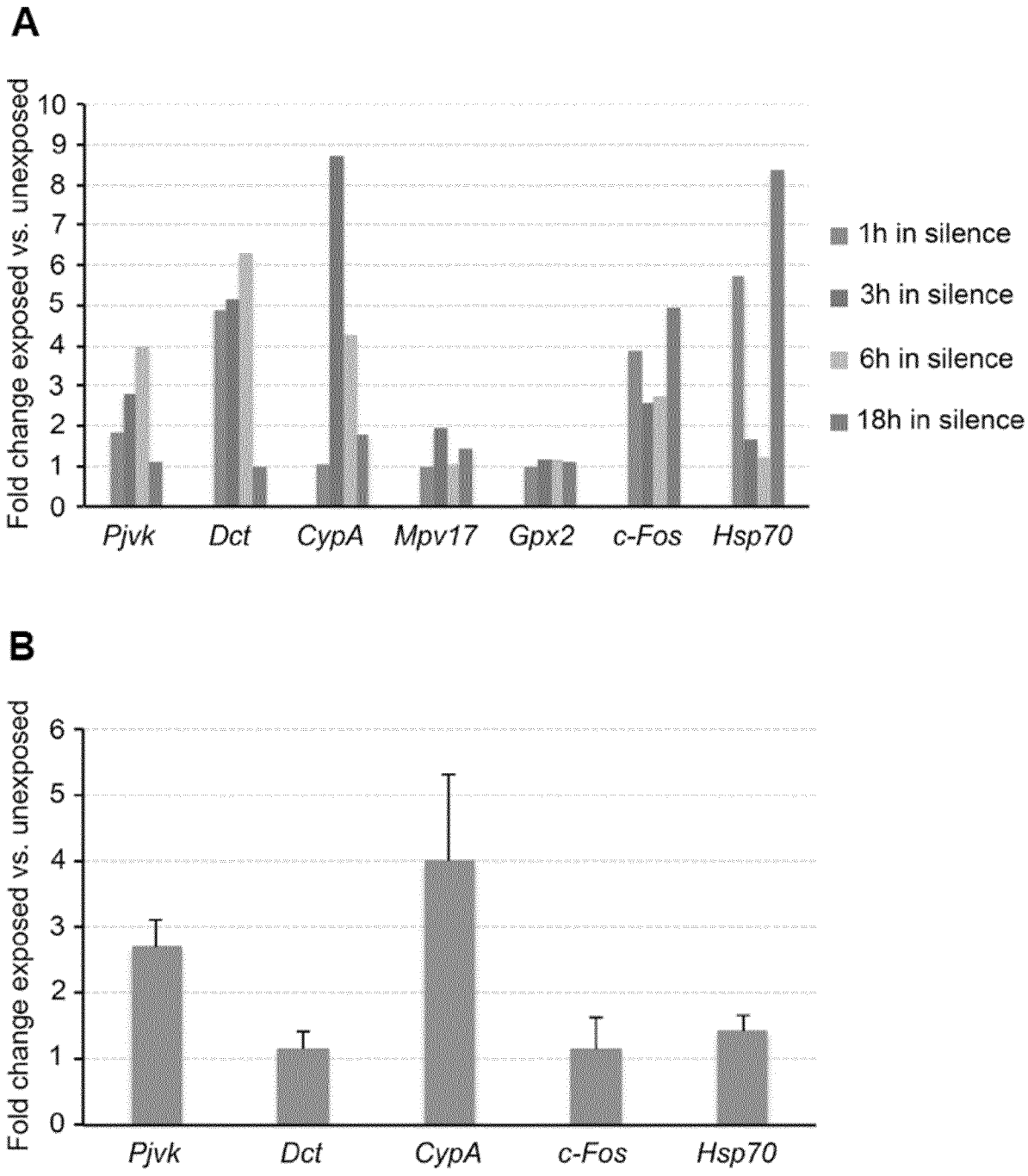
A
Fold change exposed vs. unexposed
0
1
2
3
4
5
6
7
8
9
10
Pjvk
Dct
CypA
Mpv17
Gpx2
c-Fos
Hsp70
1h in silence
3h in silence
6h in silence
18h in silence
B
Fold change exposed vs. unexposed
0
1
2
3
4
5
6
Pjvk
Dct
CypA
c-Fos
Hsp70

Figure 10

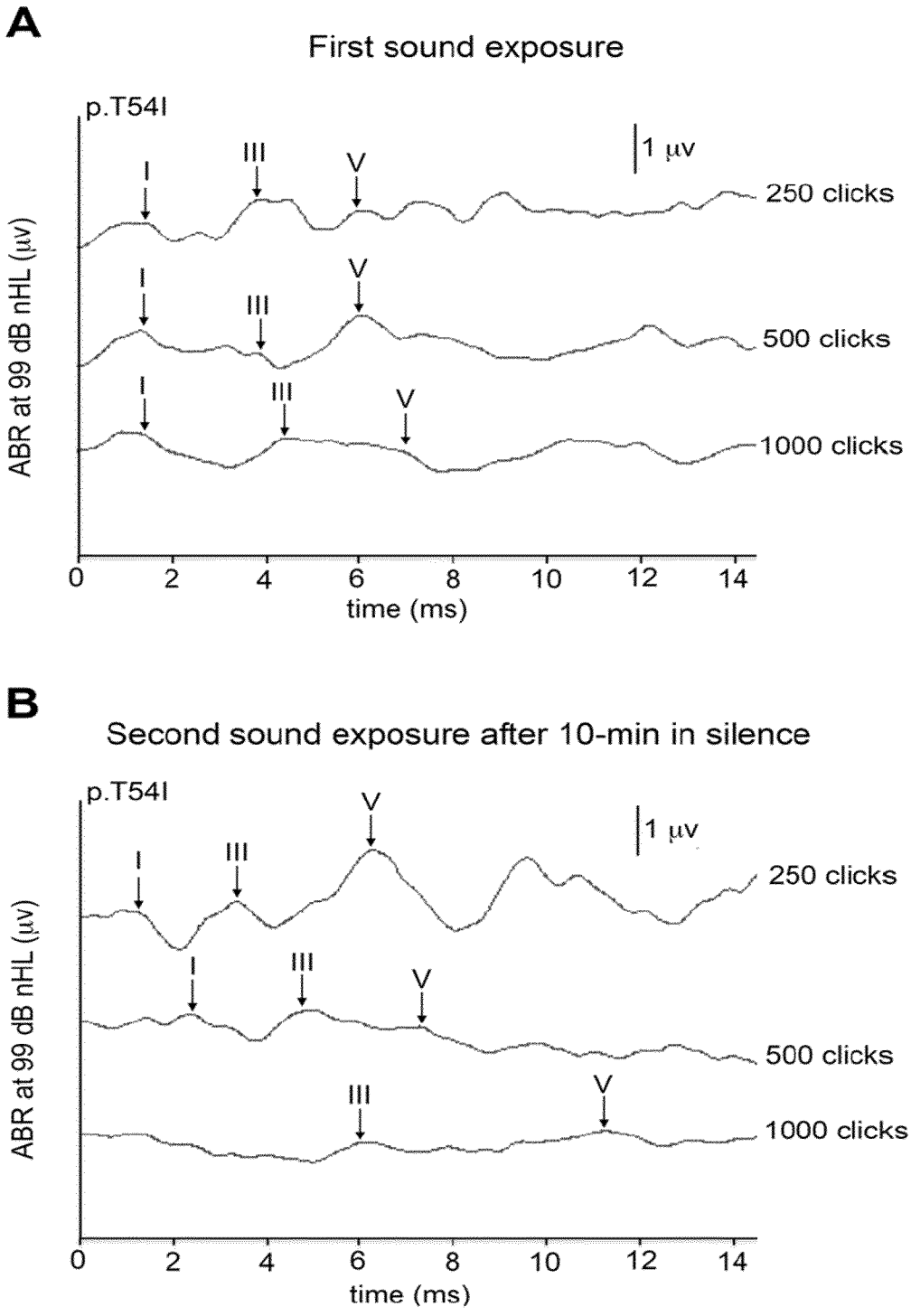
A
First sound exposure
p.T54I
1 µv
I
III
V
250 clicks
500 clicks
1000 clicks
ABR at 99 dB nHL (µv)
0 2 4 6 8 10 12 14
time (ms)
B
Second sound exposure after 10-min in silence
p.T54I
1 µv
I
III
V
250 clicks
500 clicks
1000 clicks
ABR at 99 dB nHL (µv)
0 2 4 6 8 10 12 14
time (ms)

Figure 10 (continued)

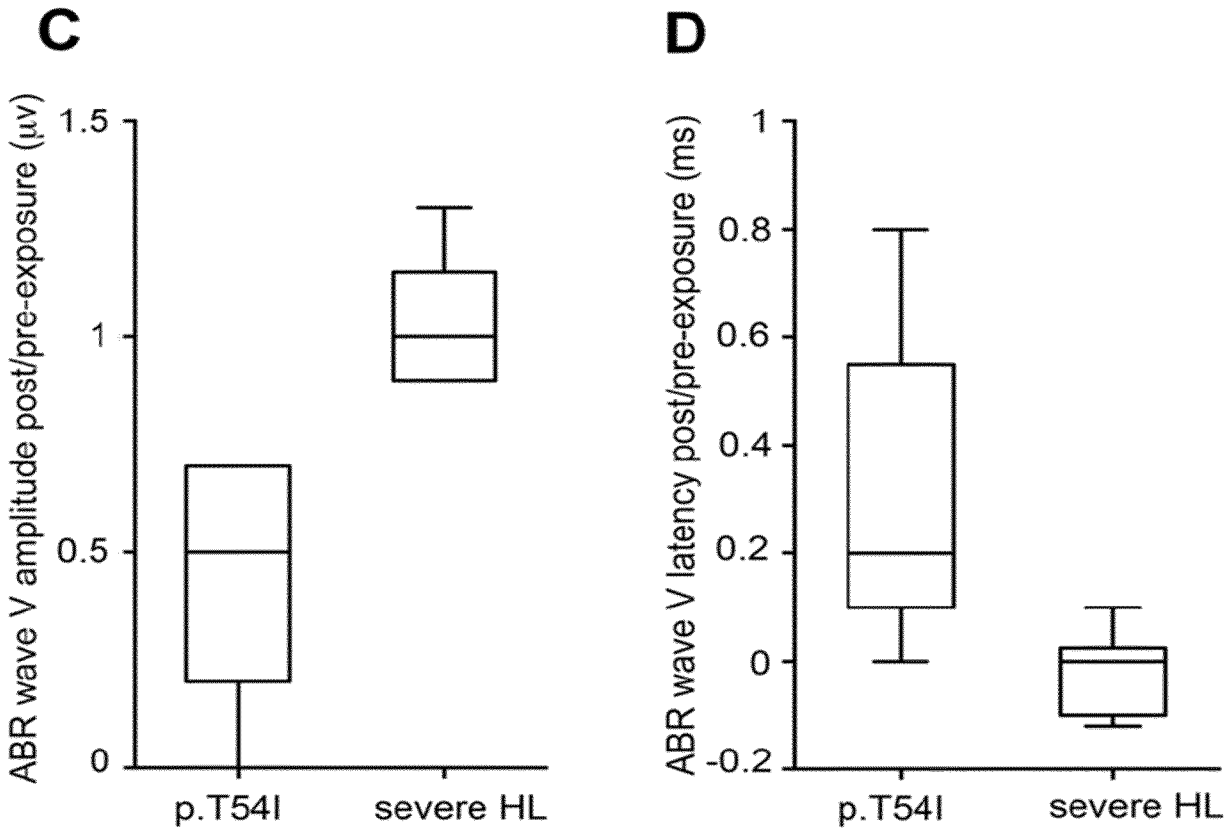

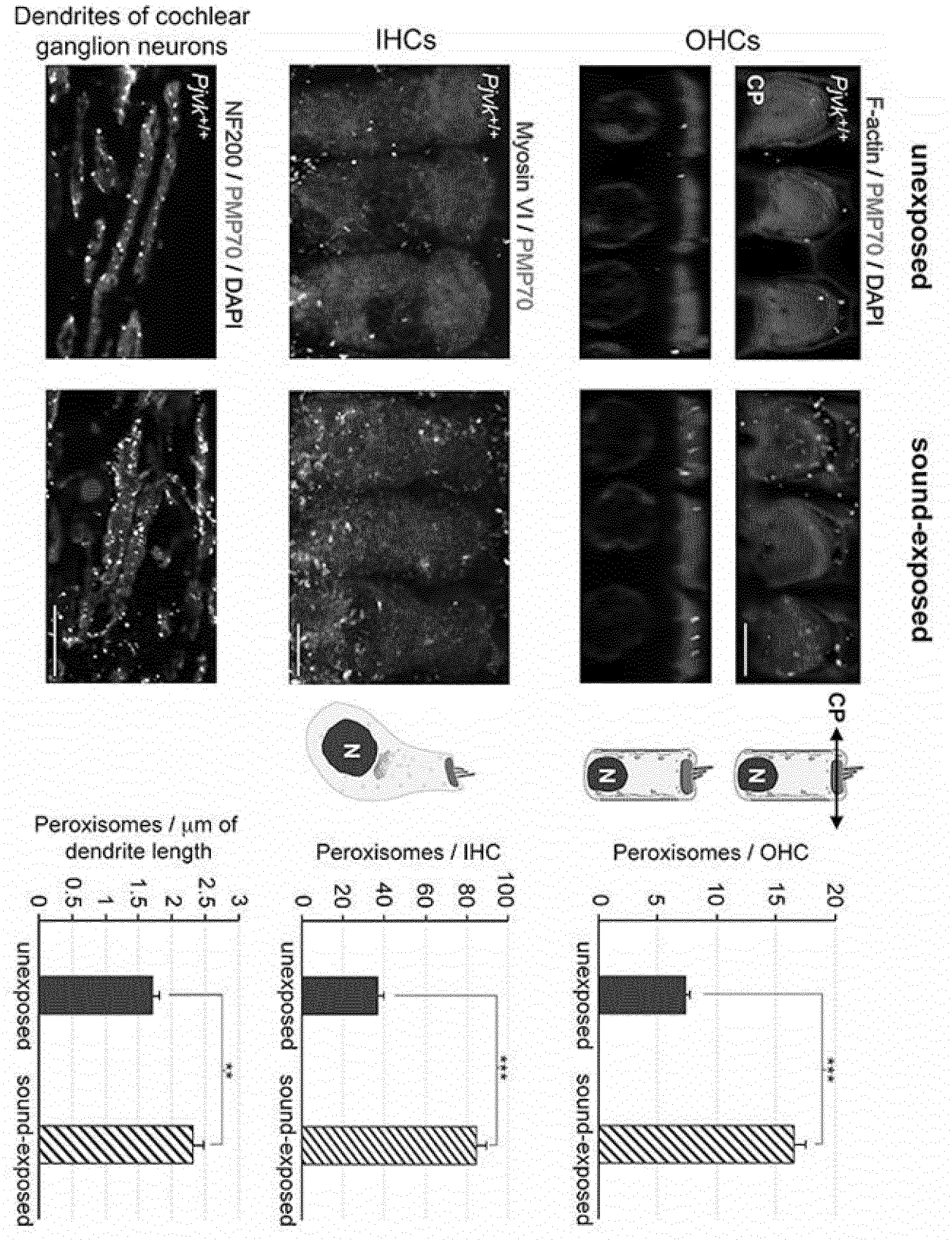
unexposed
sound-exposed
OHCs
IHCs
Dendrites of cochlear ganglion neurons
F-actin / PMP70 / DAPI
Myosin VI / PMP70
NF200 / PMP70 / DAPI
Pjvk+/+
CP
N
Peroxisomes / OHC
Peroxisomes / IHC
Peroxisomes / µm of dendrite length
unexposed
sound-exposed
***
**

Figure 11

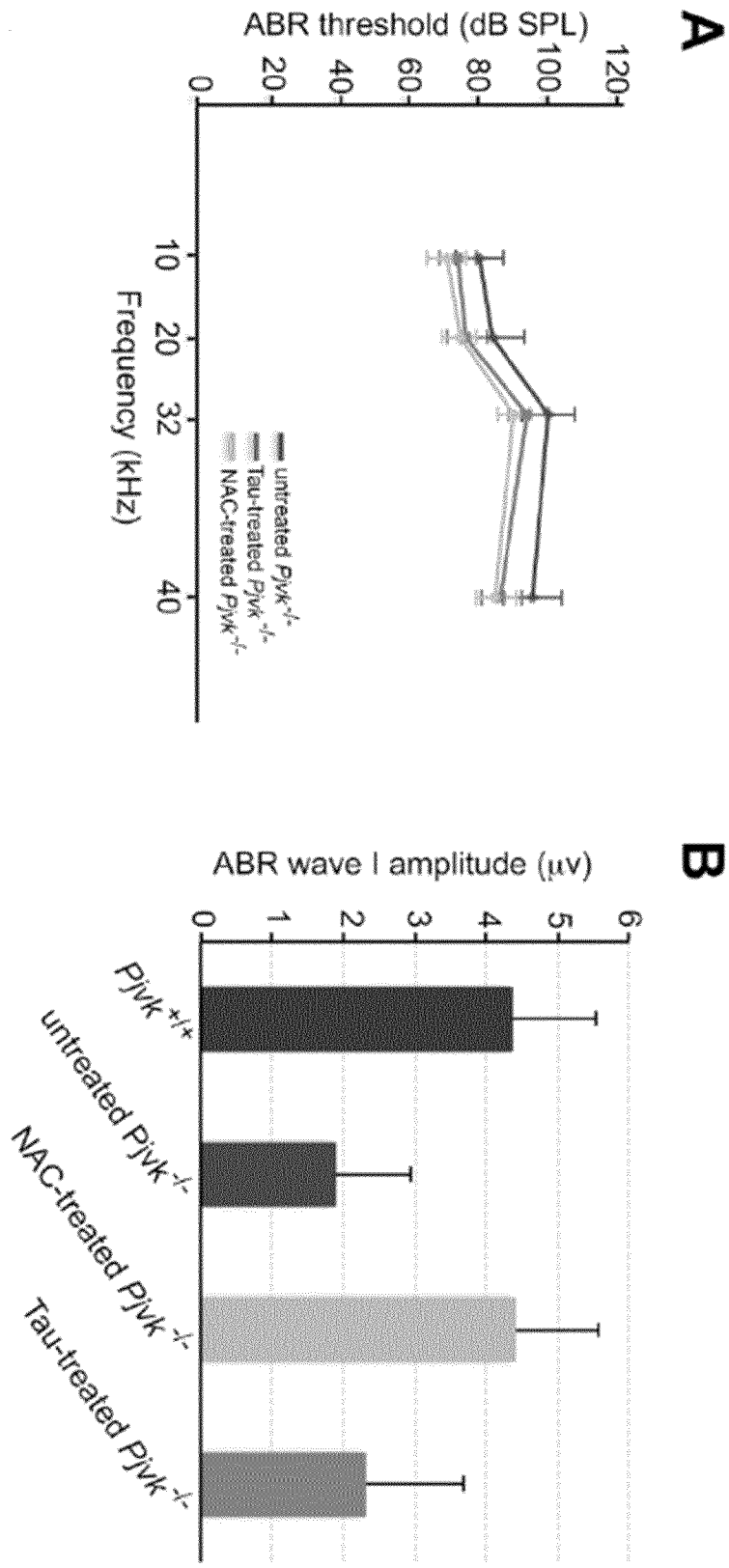
A
ABR threshold (dB SPL)
0
20
40
60
80
100
120
10
20
32
40
Frequency (kHz)
untreated Pjvk-/-
Tau-treated Pjvk-/-
NAC-treated Pjvk-/-
B
ABR wave I amplitude (μv)
0
1
2
3
4
5
6
Pjvk+/+
untreated Pjvk-/-
NAC-treated Pjvk-/-
Tau-treated Pjvk-/-

Figure 12

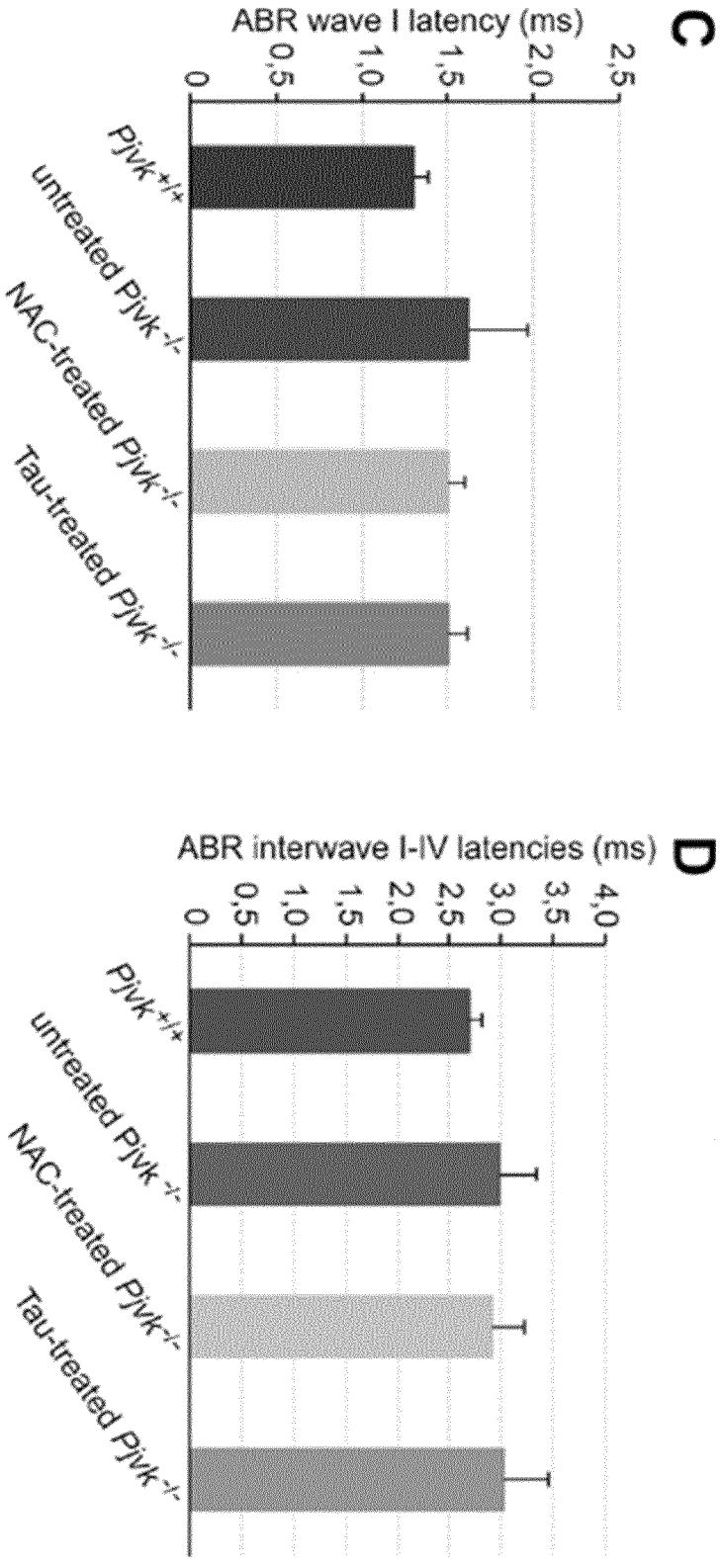

Figure 12 (continued)

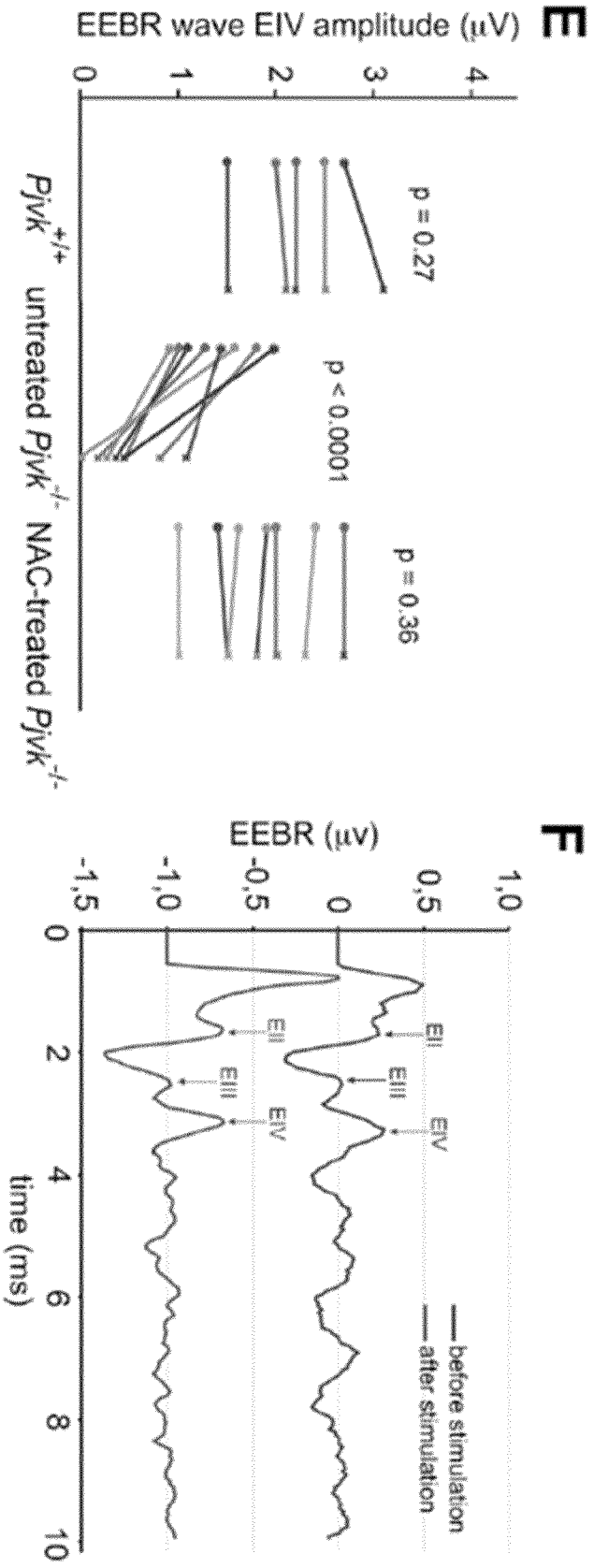

Figure 12 (continued)

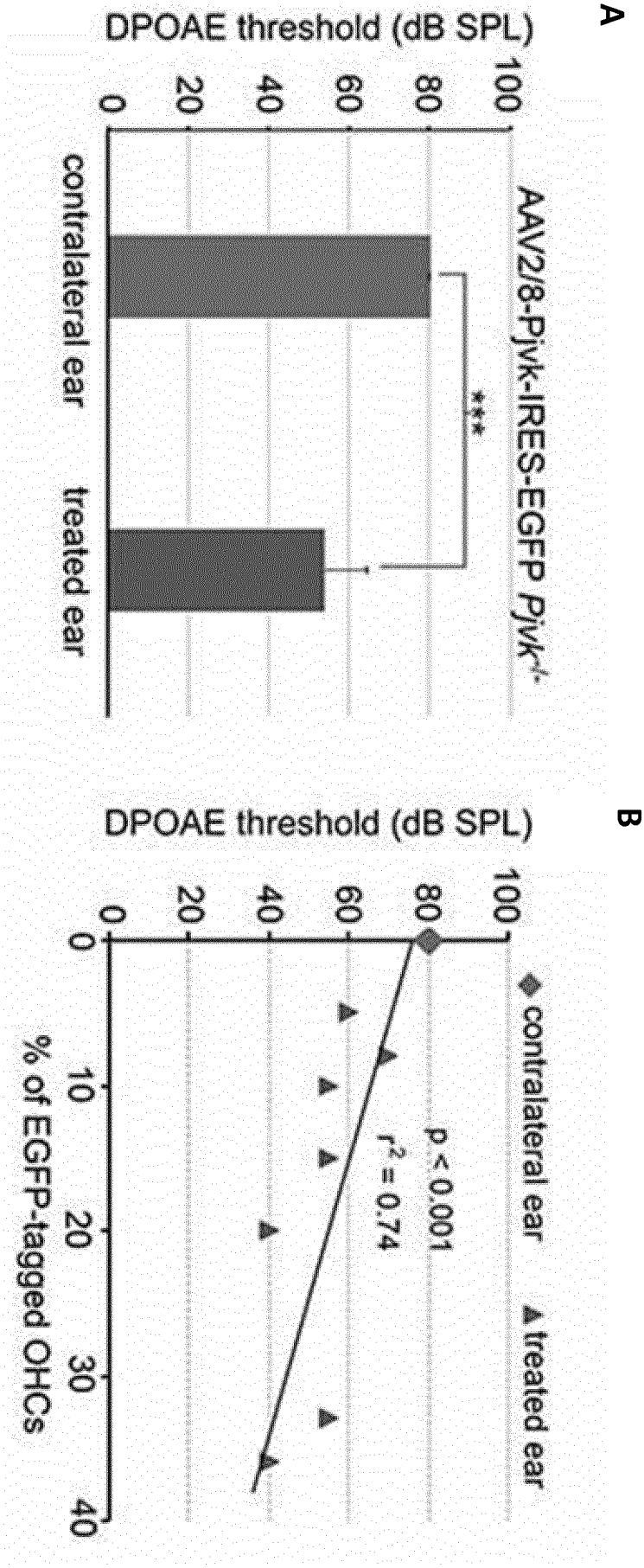
A
DPOAE threshold (dB SPL)
0
20
40
60
80
100
contralateral ear
treated ear
***
AAV2/8-Pjvk-IRES-EGFP Pjvk-/-
B
DPOAE threshold (dB SPL)
0
20
40
60
80
100
0
10
20
30
40
% of EGFP-tagged OHCs
contralateral ear
treated ear
p < 0.001
r2 = 0.74

Figure 13

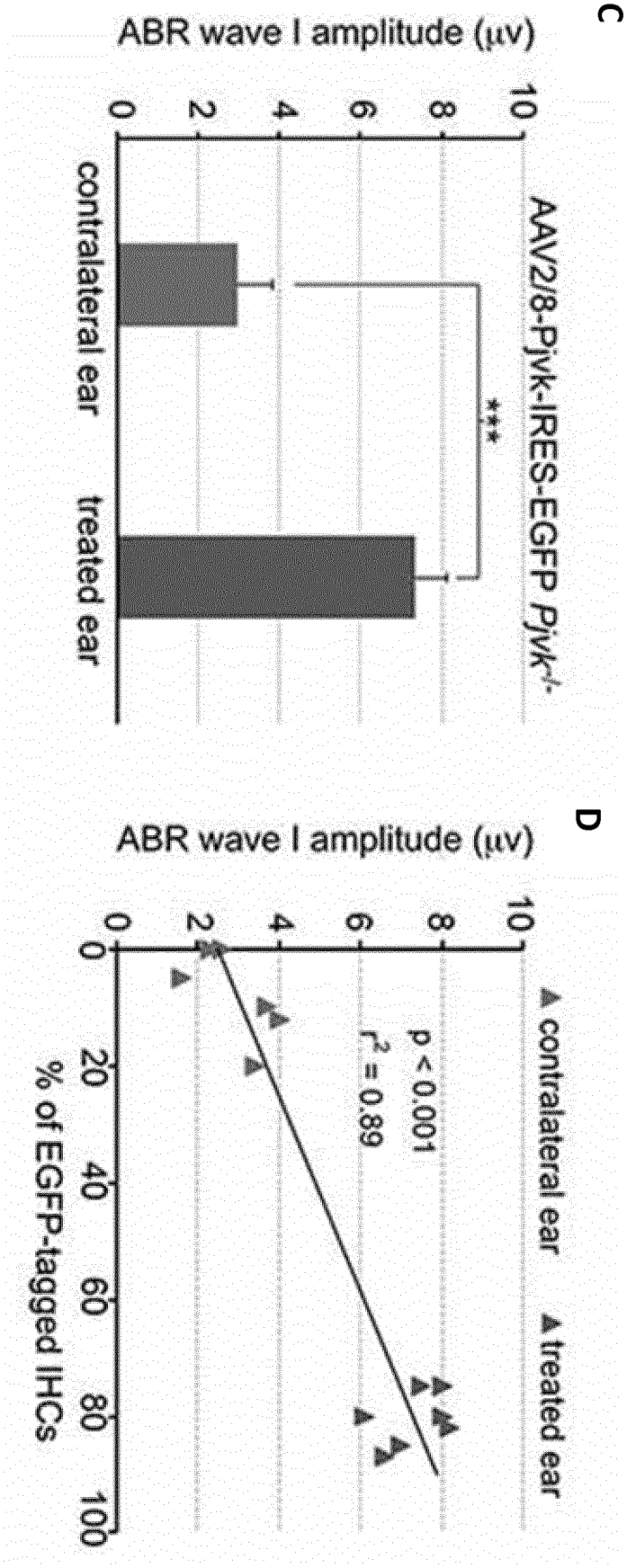

Figure 13 (continued)

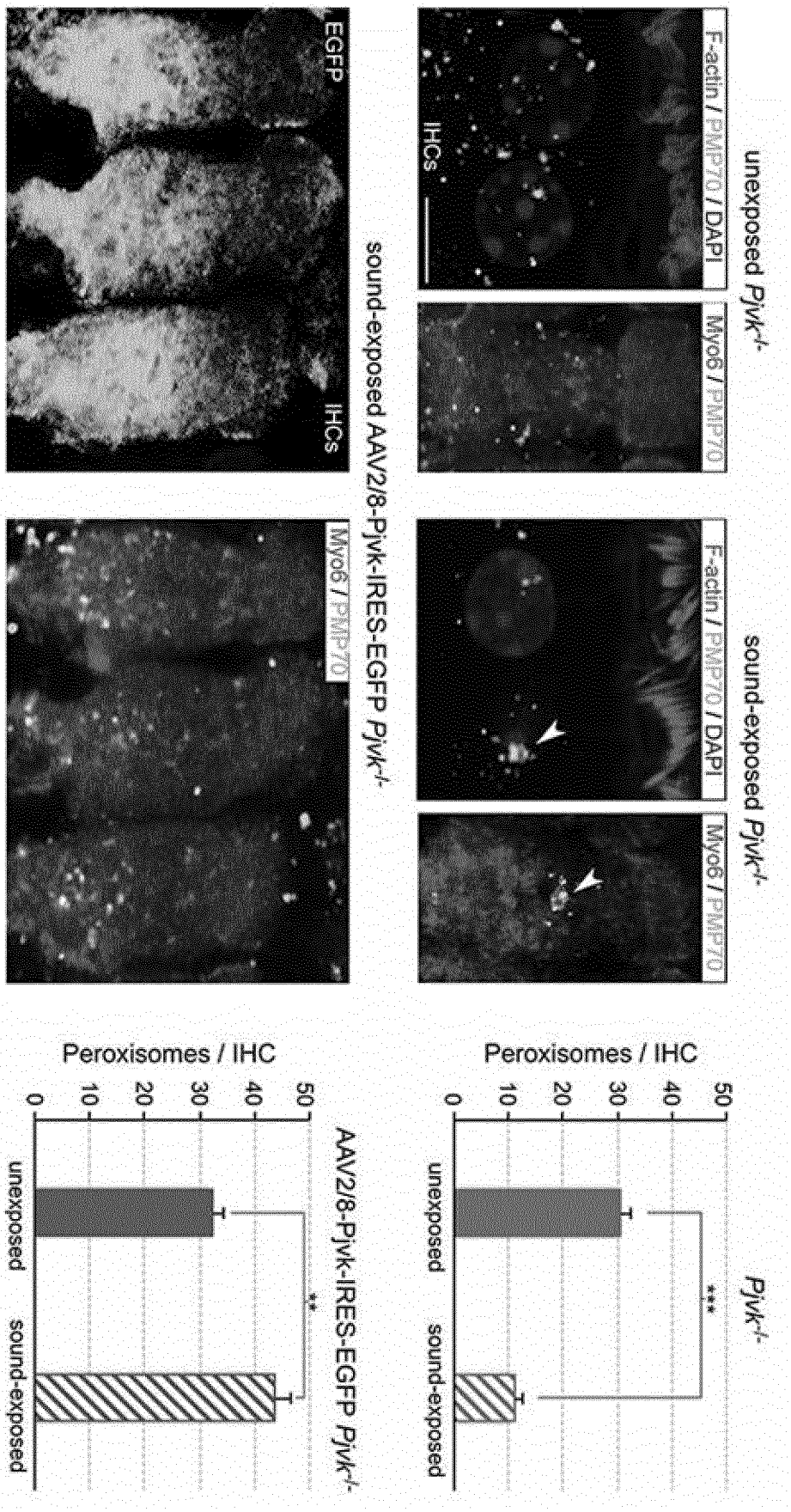
unexposed Pjvk-/-
sound-exposed Pjvk-/-
F-actin / PMP70 / DAPI
Myo6 / PMP70
IHCs
sound-exposed AAV2/8-Pjvk-IRES-EGFP Pjvk-/-
EGFP
IHCs
Peroxisomes / IHC
Pjvk-/-
AAV2/8-Pjvk-IRES-EGFP Pjvk-/-
unexposed
sound-exposed
***
**

Figure 14

Figure 15

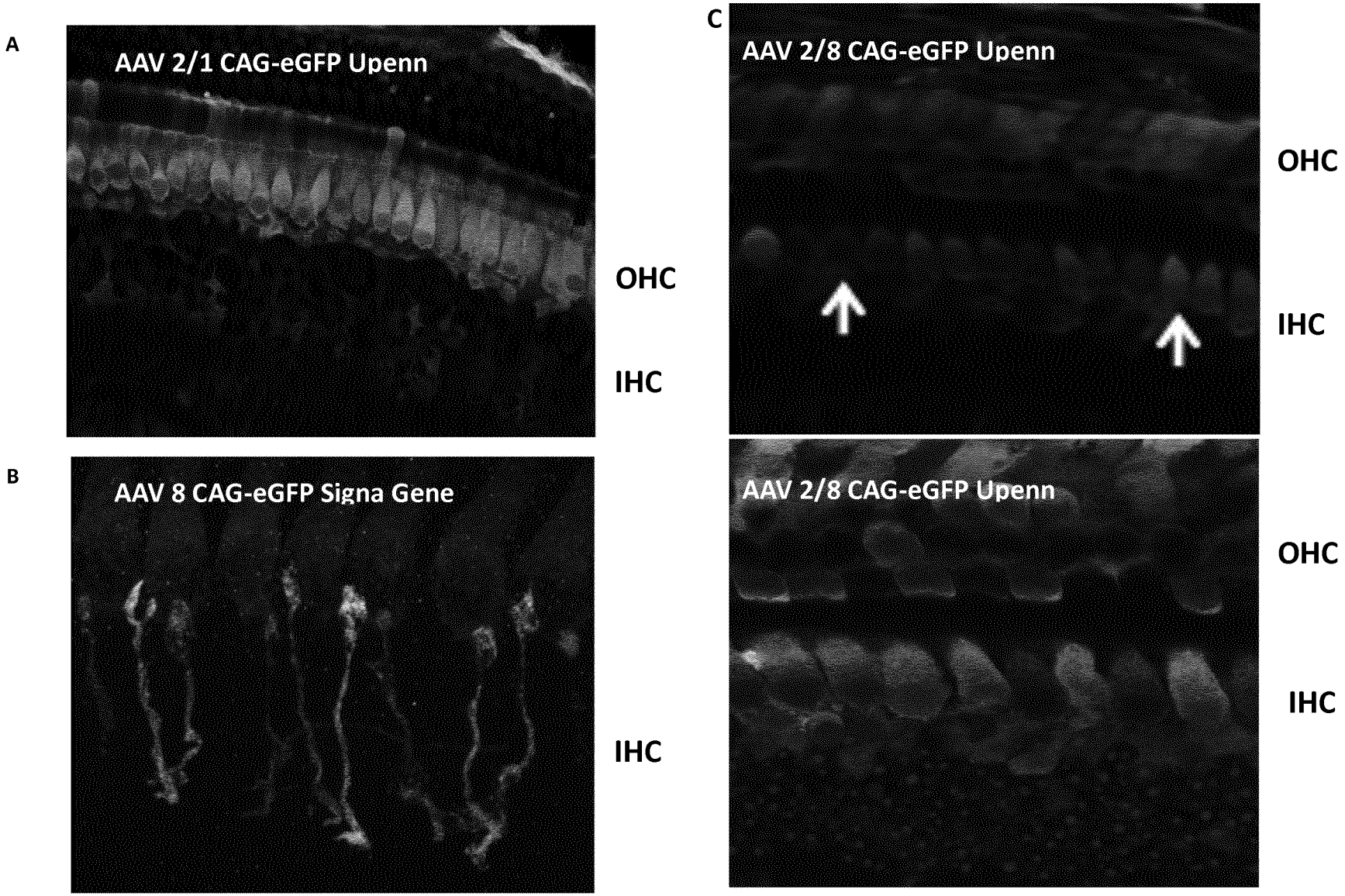
A
AAV 2/1 CAG-eGFP Upenn
OHC
IHC
B
AAV 8 CAG-eGFP Signa Gene
IHC
C
AAV 2/8 CAG-eGFP Upenn
OHC
IHC
AAV 2/8 CAG-eGFP Upenn
OHC
IHC

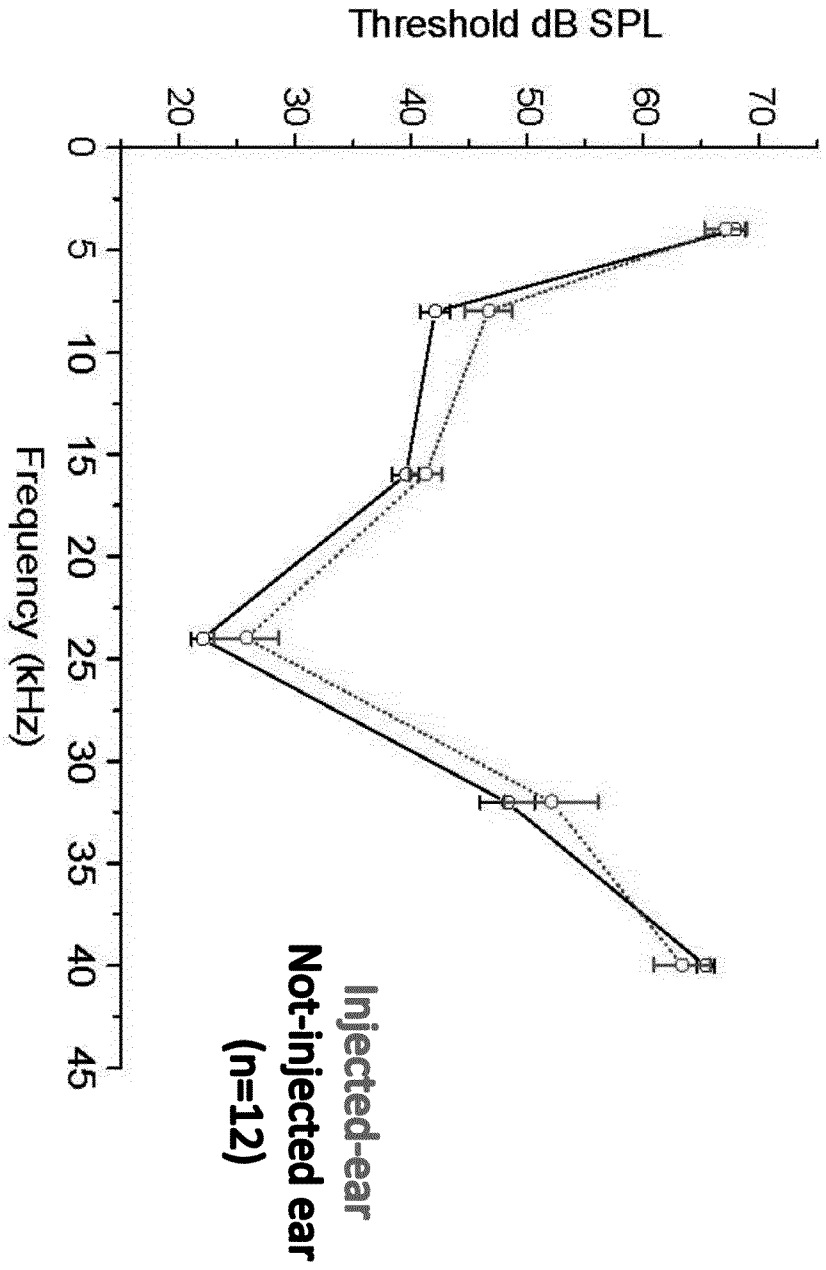

Figure 15 (continued)

Figure 16

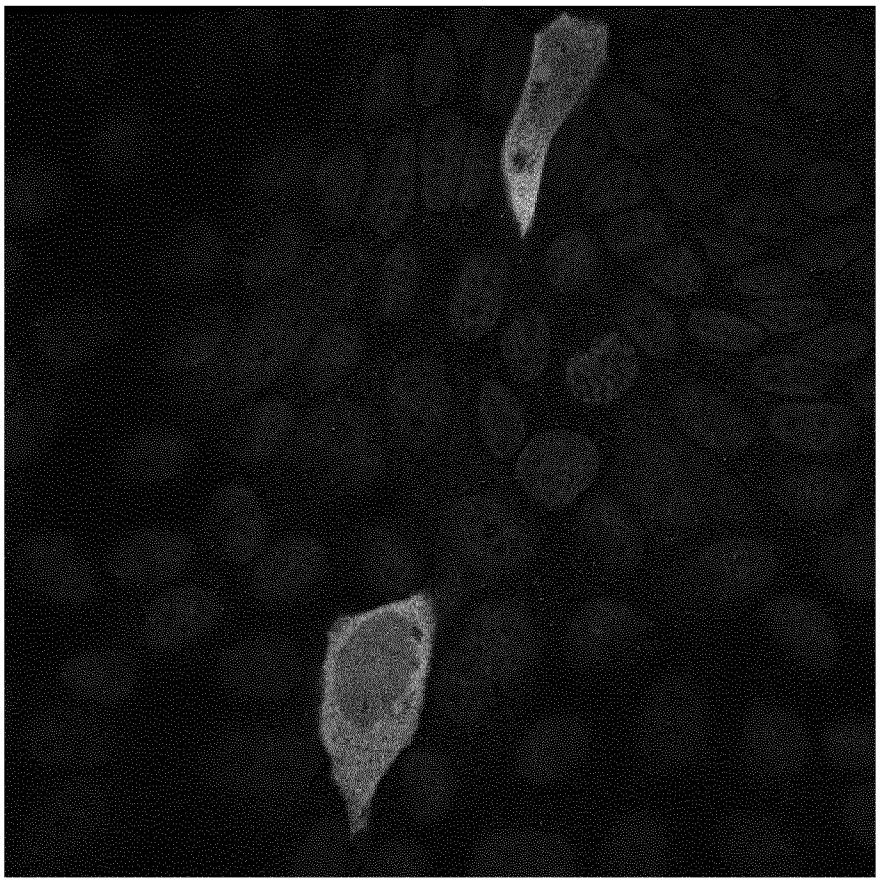

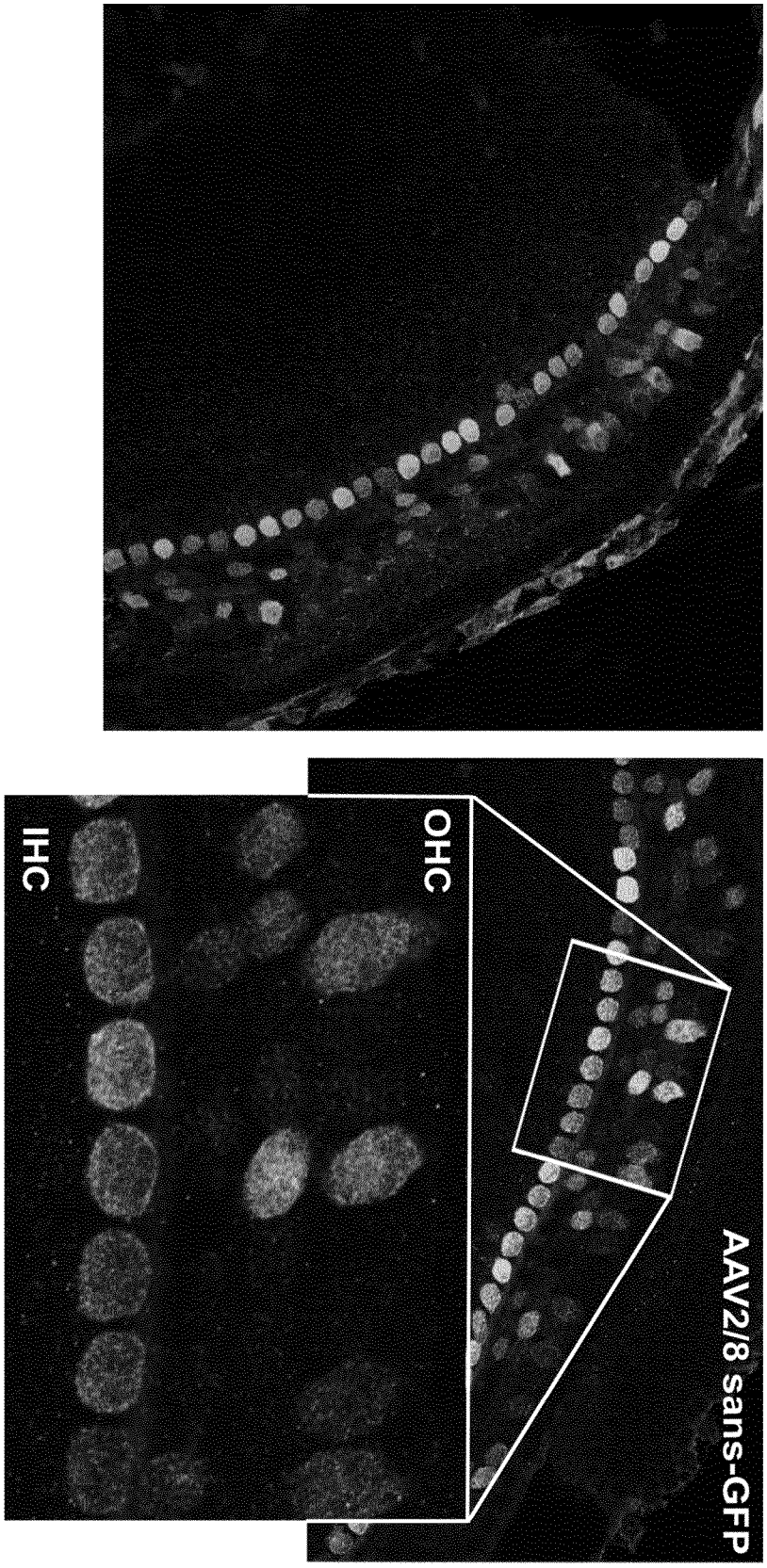

Figure 17

Figure 18

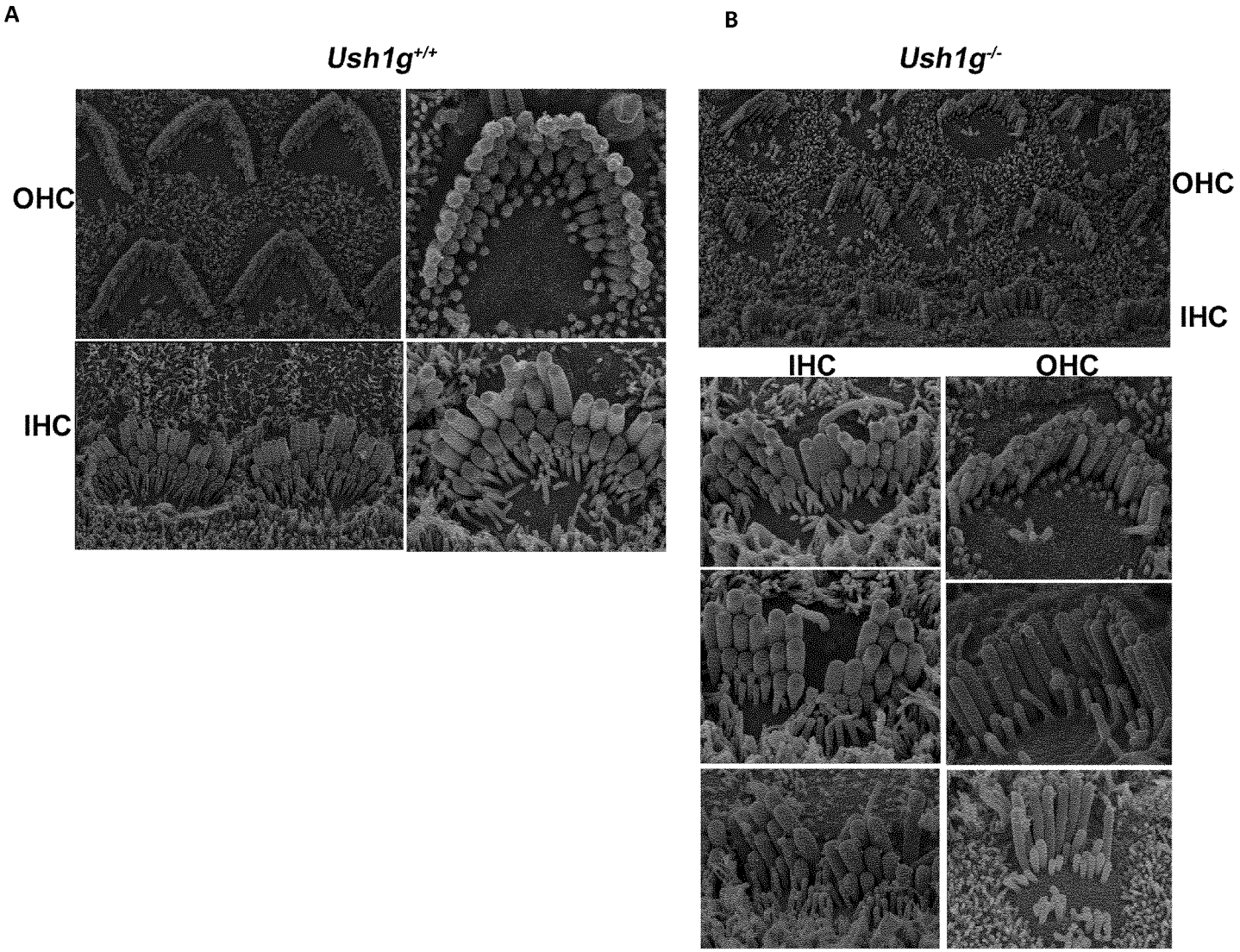

C

Treated *Ush1g* $^{-/-}$ mice

Figure 18 (continued)

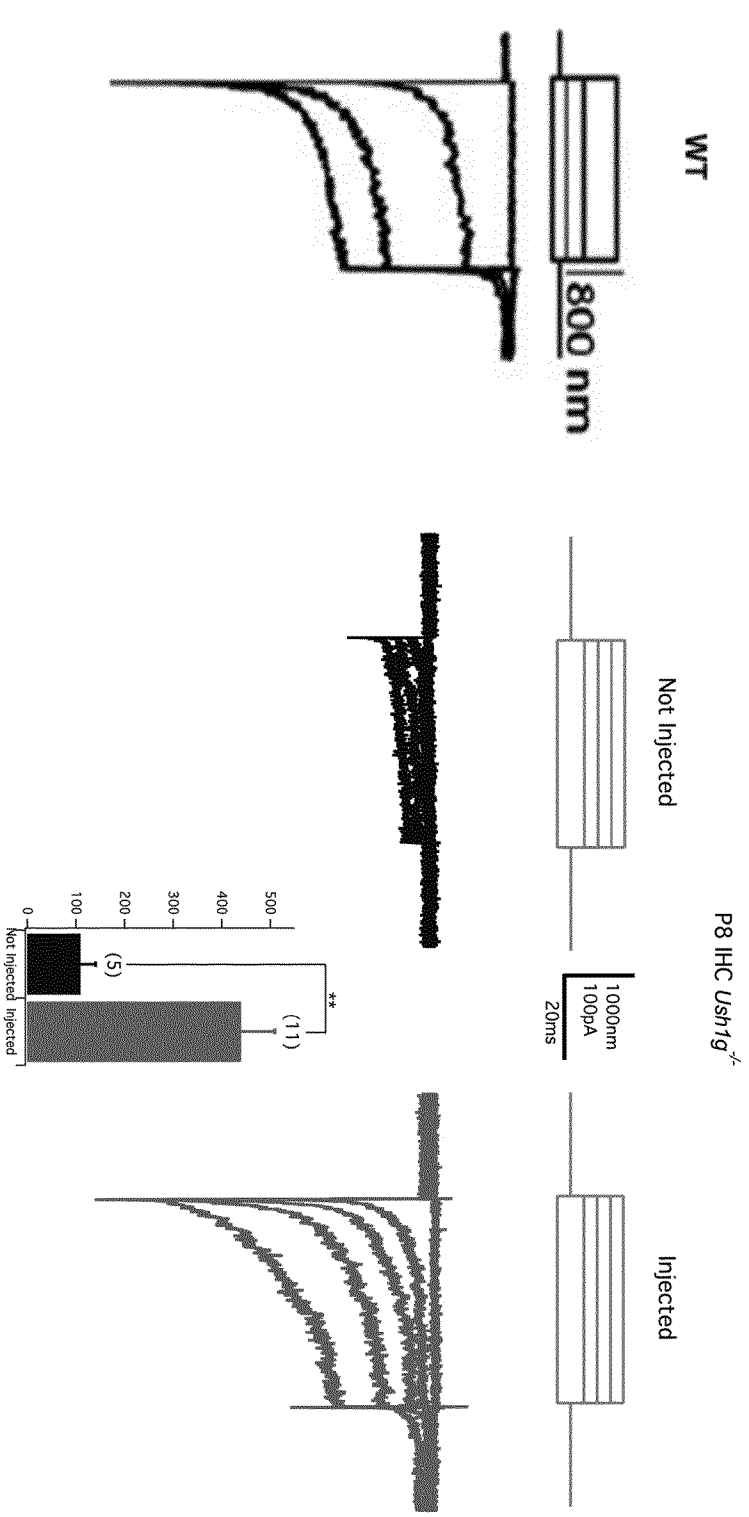
A
WT
800 nm
P8 IHC Ush1g-/-
Not Injected
Injected
1000nm
100pA
20ms
500
400
300
200
100
0
(5)
(11)
**
Not injected
Injected

Figure 19

Figure 19 (continued)

B

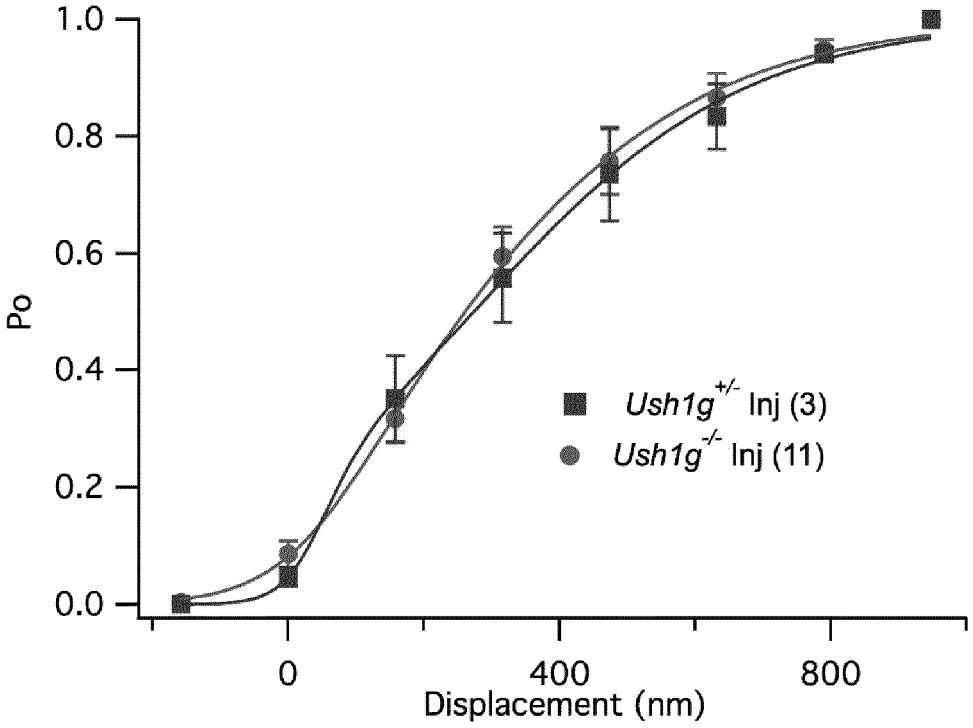

Figure 19 (continued)

C

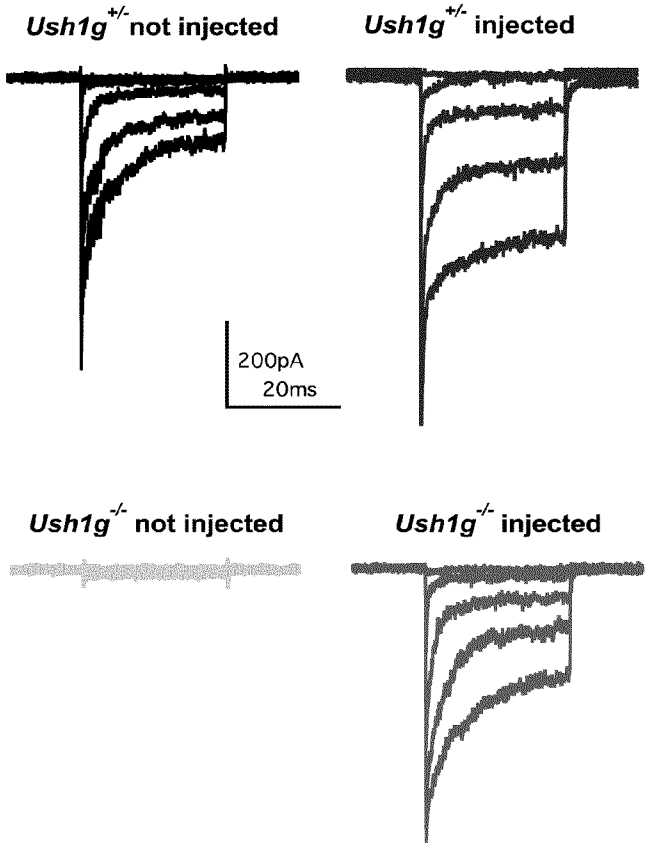

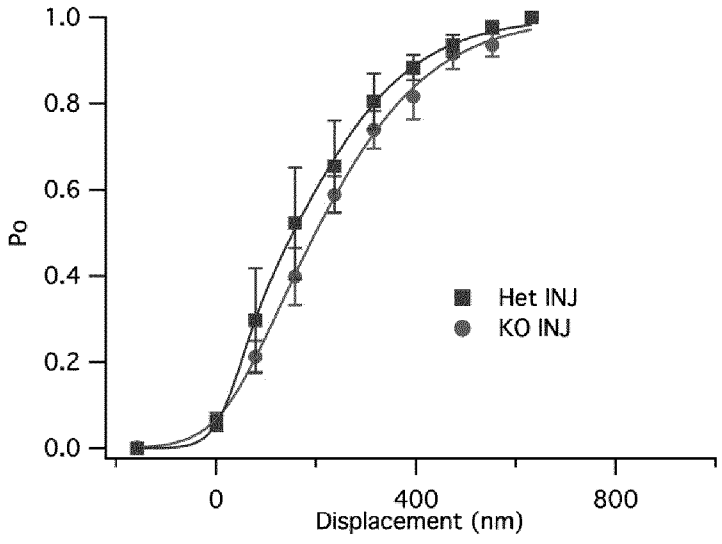

Figure 19 (continued)

D

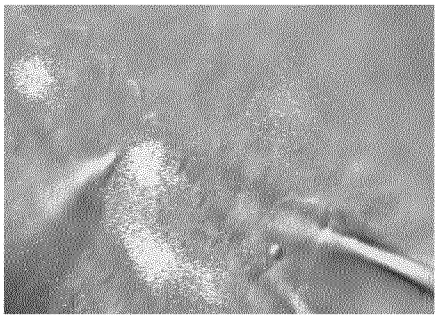

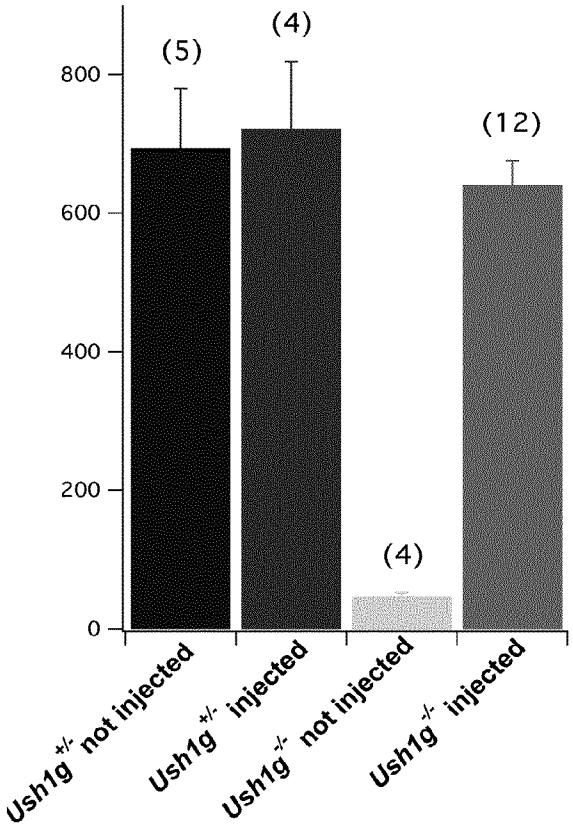

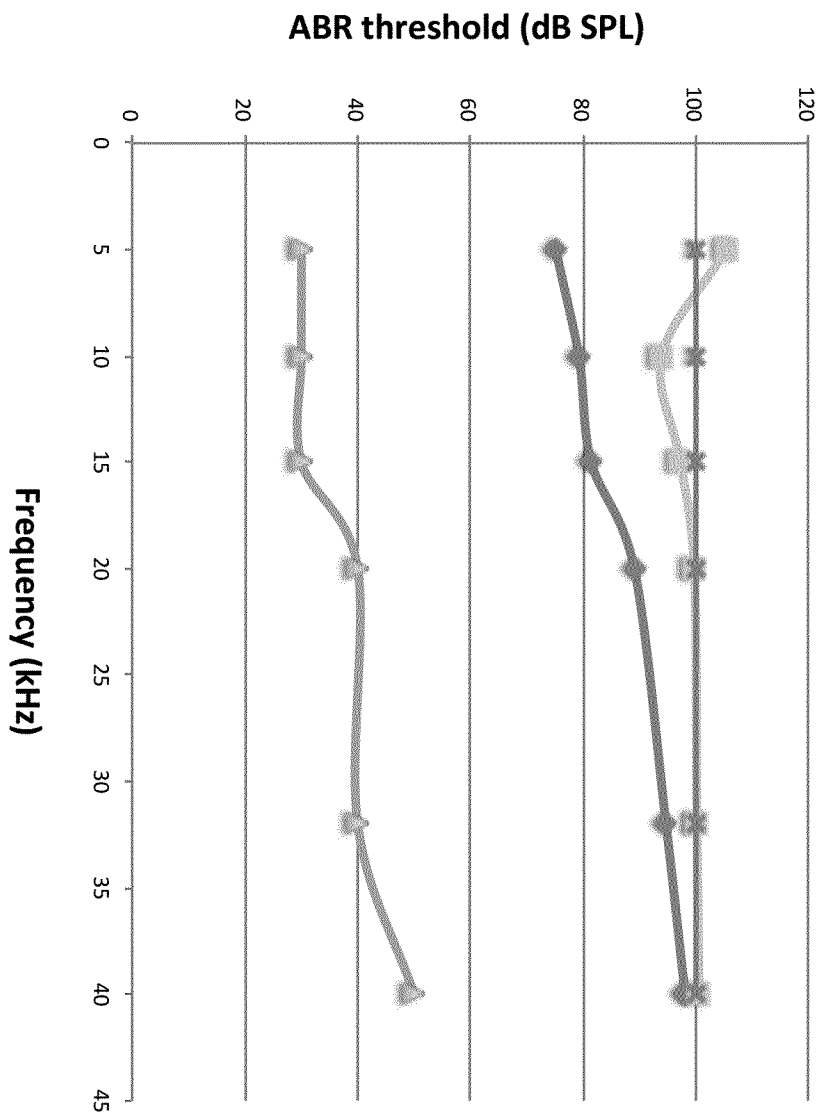
ABR threshold (dB SPL)
120
100
80
60
40
20
0
0
5
10
15
20
25
30
35
40
45
Frequency (kHz)
Ush1g -/- mice
Contralateral ear
Treated Ush1g -/- mice (n=16)
Ush1g +/- mice

Figure 20

Figure 21

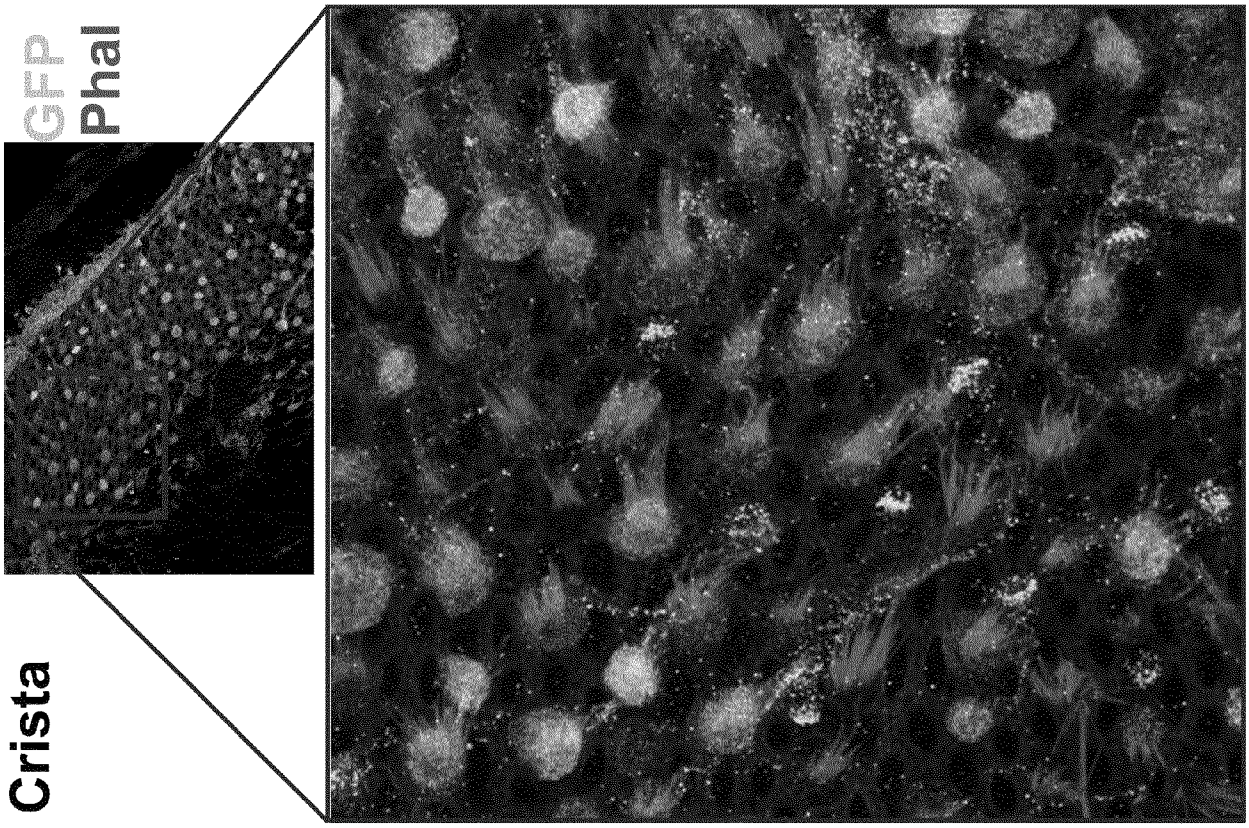

Figure 22

A

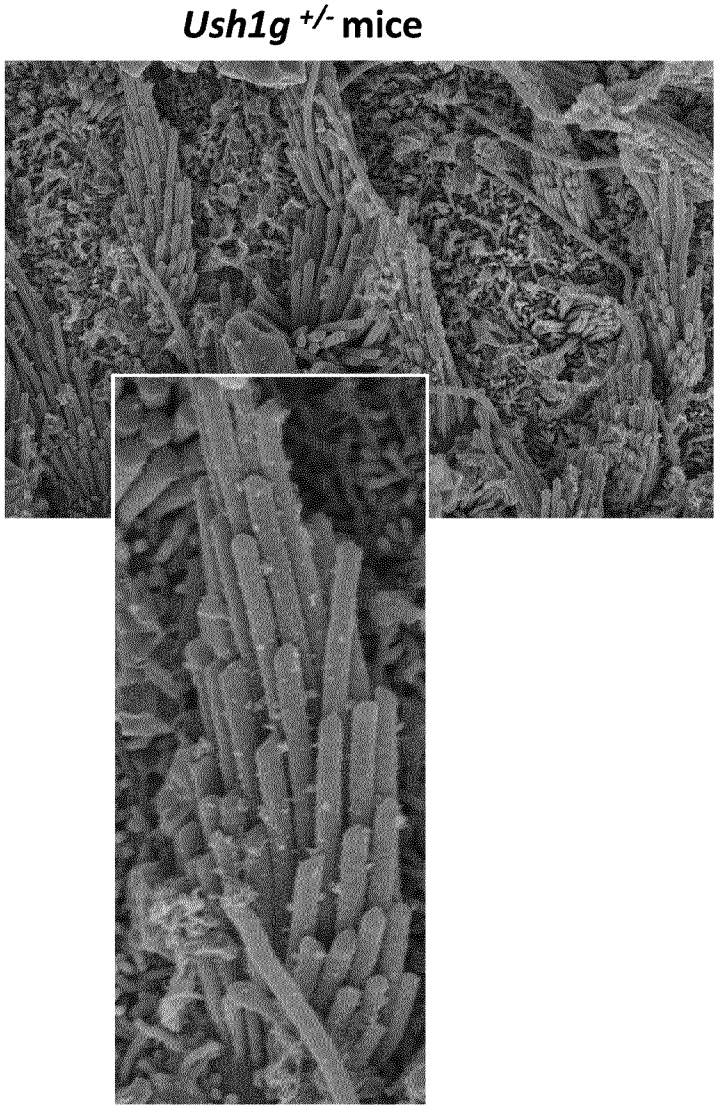

Figure 22 (continued)

B

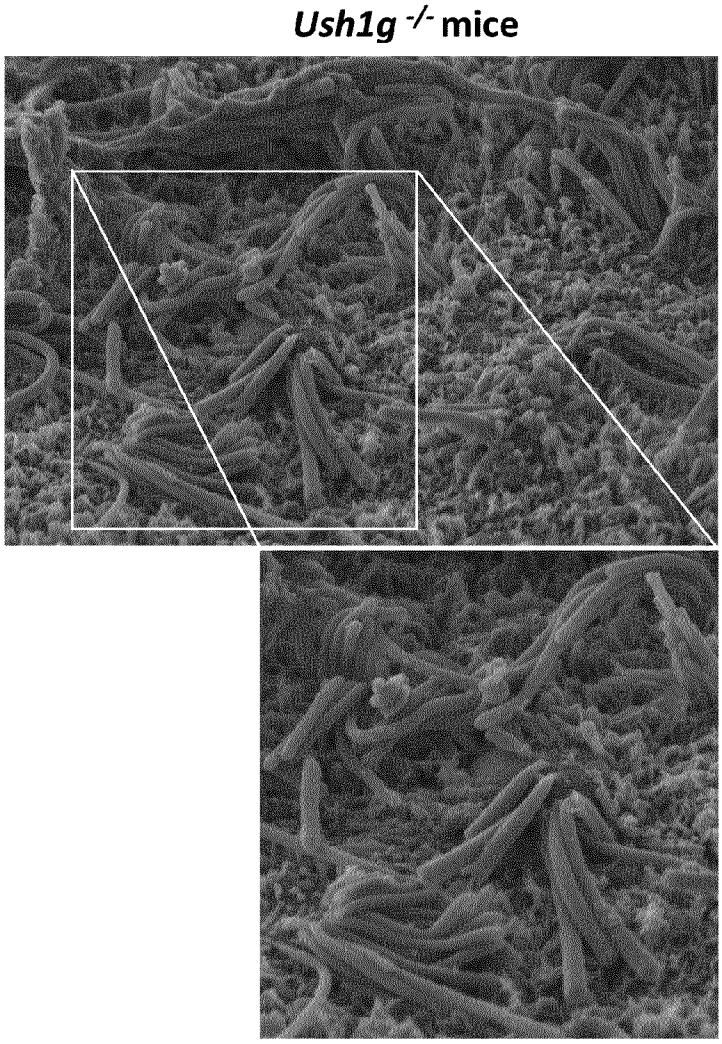

Figure 22 (continued)

C

Treated *Ush1g* $^{-/-}$ mice

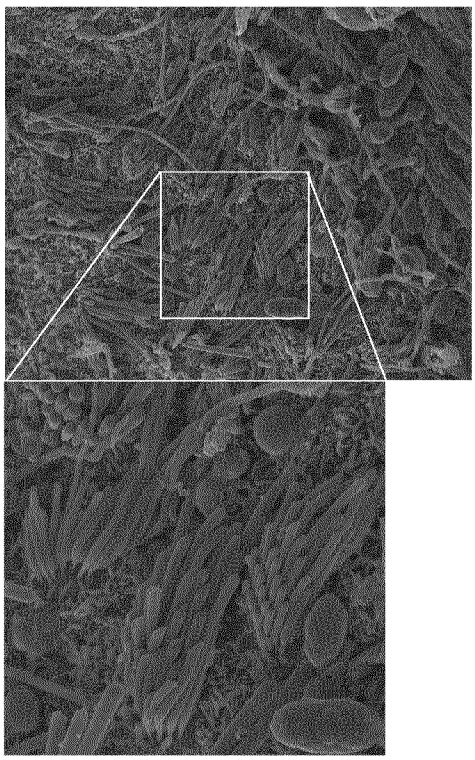

Ush1g $^{+/-}$ mice

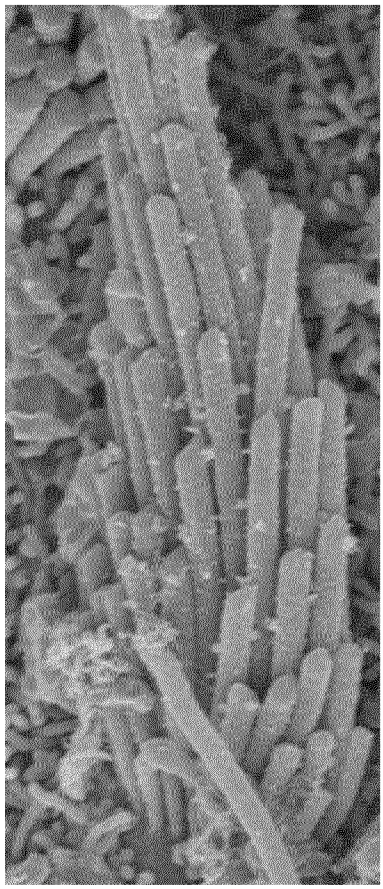

Figure 23

Ush1g $^{+/-}$ mice

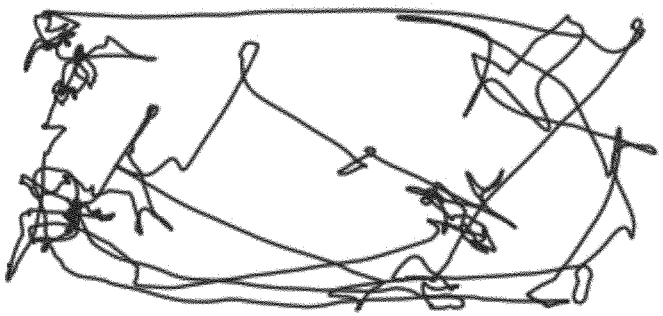

Treated *Ush1g* $^{+/-}$ mice

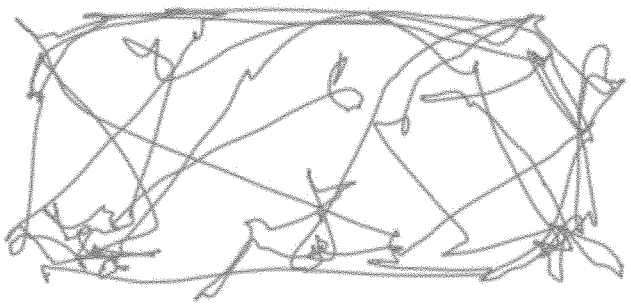

Ush1g $^{-/-}$ mice

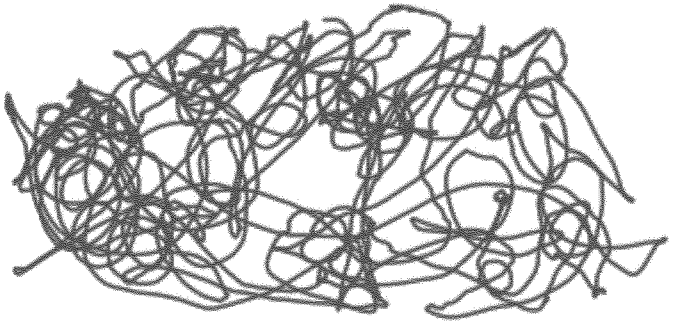

Treated *Ush1g* $^{-/-}$ mice

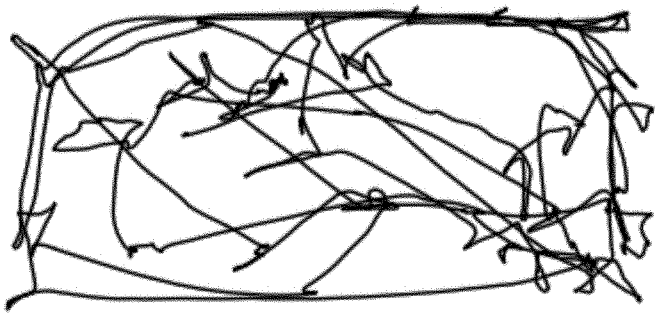

INTERNATIONAL SEARCH REPORT

International application No
PCT/EP2016/053613

A. CLASSIFICATION OF SUBJECT MATTER
INV. A61K38/17 A61K48/00 A61P27/06 A61P35/00 A61P29/00
ADD.

According to International Patent Classification (IPC) or to both national classification and IPC

B. FIELDS SEARCHED

Minimum documentation searched (classification system followed by classification symbols)
A61K A61P

Documentation searched other than minimum documentation to the extent that such documents are included in the fields searched

Electronic data base consulted during the international search (name of data base and, where practicable, search terms used)
EPO-Internal, BIOSIS, EMBASE, WPI Data

C. DOCUMENTS CONSIDERED TO BE RELEVANT

Category*	Citation of document, with indication, where appropriate, of the relevant passages	Relevant to claim No.
X	WO 2011/075838 A1 (AUDIGEN INC [CA]; BANCE MANOHAR [CA]; ROBERTSON GEORGE [CA]; WANG JIAN) 30 June 2011 (2011-06-30)	1-5,8, 10,13, 14,19-31
Y	abstract page 7	1-15, 17-19

X	WO 02/20606 A1 (BIOWINDOW GENE DEV INC [CN]; MAO YUMIN [CN]; XIE YI [CN]) 14 March 2002 (2002-03-14)	1-5,8, 10, 12-14,19
Y	abstract; sequence 2	1-15, 17-19

	-/--	

[X] Further documents are listed in the continuation of Box C.

[X] See patent family annex.

* Special categories of cited documents :

"A" document defining the general state of the art which is not considered to be of particular relevance

"E" earlier application or patent but published on or after the international filing date

"L" document which may throw doubts on priority claim(s) or which is cited to establish the publication date of another citation or other special reason (as specified)

"O" document referring to an oral disclosure, use, exhibition or other means

"P" document published prior to the international filing date but later than the priority date claimed

"T" later document published after the international filing date or priority date and not in conflict with the application but cited to understand the principle or theory underlying the invention

"X" document of particular relevance; the claimed invention cannot be considered novel or cannot be considered to involve an inventive step when the document is taken alone

"Y" document of particular relevance; the claimed invention cannot be considered to involve an inventive step when the document is combined with one or more other such documents, such combination being obvious to a person skilled in the art

"&" document member of the same patent family

Date of the actual completion of the international search	Date of mailing of the international search report
22 June 2016	01/07/2016

Name and mailing address of the ISA/	Authorized officer
European Patent Office, P.B. 5818 Patentlaan 2 NL - 2280 HV Rijswijk Tel. (+31-70) 340-2040, Fax: (+31-70) 340-3016	Weisser, Dagmar

3

Form PCT/ISA/210 (second sheet) (April 2005)

C(Continuation). DOCUMENTS CONSIDERED TO BE RELEVANT

Category*	Citation of document, with indication, where appropriate, of the relevant passages	Relevant to claim No.
X	DATABASE WPI Week 201307 Thomson Scientific, London, GB; AN 2012-R56799 XP002738790, & CN 102 732 614 A (CHINESE PLA GEN HOSPITAL) 17 October 2012 (2012-10-17)	1-5,8, 10,12,19
Y	abstract sequence 2	1-15, 17-19

X	SEDIGHEH DELMAGHANI ET AL: "Mutations in the gene encoding pejvakin, a newly identified protein of the afferent auditory pathway, cause DFNB59 auditory neuropathy", NATURE GENETICS, vol. 38, no. 7, 1 July 2006 (2006-07-01), pages 770-778, XP055184645, ISSN: 1061-4036, DOI: 10.1038/ng1829	1-5,8, 10,12, 13,19
Y	page 770, column 3 page 773, column 8; figure 4 page 776, column 8 page 777, column 2	1-15, 17-19

Y	GHULAM MUJTABA ET AL: "A p.C343S missense mutation in PJVK causes progressive hearing loss", GENE, vol. 504, no. 1, 1 August 2012 (2012-08-01), pages 98-101, XP055184677, ISSN: 0378-1119, DOI: 10.1016/j.gene.2012.05.013 the whole document	1-15, 17-19

Y	A. R. FETONI ET AL: "Noise-Induced Hearing Loss (NIHL) as a Target of Oxidative Stress-Mediated Damage: Cochlear and Cortical Responses after an Increase in Antioxidant Defense", JOURNAL OF NEUROSCIENCE, vol. 33, no. 9, 27 February 2013 (2013-02-27), pages 4011-4023, XP055184837, ISSN: 0270-6474, DOI: 10.1523/JNEUROSCI.2282-12.2013 the whole document	1-15, 17-19

	-/--	

C(Continuation). DOCUMENTS CONSIDERED TO BE RELEVANT

Category*	Citation of document, with indication, where appropriate, of the relevant passages	Relevant to claim No.
Y	SU-HUA SHA ET AL: "Antioxidants attenuate gentamicin-induced free radical formation in vitro and ototoxicity in vivo: D-methionine is a potential protectant", HEARING RESEARCH, ELSEVIER SCIENCE PUBLISHERS, AMSTERDAM, NL, vol. 142, no. 1-2, 1 April 2000 (2000-04-01), pages 34-40, XP007906532, ISSN: 0378-5955 the whole document -----	1-15, 17-19
Y	WO 2011/028503 A1 (HOUGH EAR INST [US]; OKLAHOMA MED RES FOUND [US]; KOPKE RICHARD DANA [] 10 March 2011 (2011-03-10) abstract paragraphs [0019], [0022] -----	1-15, 17-19
A	KIMBERLING W J ET AL: "Localization of Usher syndrome type II to chromosome 1q", GENOMICS, ACADEMIC PRESS, SAN DIEGO, US, vol. 7, no. 2, 1 June 1990 (1990-06-01), pages 245-249, XP024797566, ISSN: 0888-7543, DOI: 10.1016/0888-7543(90)90546-7 [retrieved on 1990-06-01] the whole document -----	20-31

INTERNATIONAL SEARCH REPORT

International application No.
PCT/EP2016/053613

Box No. II Observations where certain claims were found unsearchable (Continuation of item 2 of first sheet)

This international search report has not been established in respect of certain claims under Article 17(2)(a) for the following reasons:

1. ☐ Claims Nos.:
because they relate to subject matter not required to be searched by this Authority, namely:

2. ☐ Claims Nos.:
because they relate to parts of the international application that do not comply with the prescribed requirements to such an extent that no meaningful international search can be carried out, specifically:

3. ☐ Claims Nos.:
because they are dependent claims and are not drafted in accordance with the second and third sentences of Rule 6.4(a).

Box No. III Observations where unity of invention is lacking (Continuation of item 3 of first sheet)

This International Searching Authority found multiple inventions in this international application, as follows:

see additional sheet

1. ☐ As all required additional search fees were timely paid by the applicant, this international search report covers all searchable claims.

2. ☐ As all searchable claims could be searched without effort justifying an additional fees, this Authority did not invite payment of additional fees.

3. ☒ As only some of the required additional search fees were timely paid by the applicant, this international search report covers only those claims for which fees were paid, specifically claims Nos.:

1-15, 17-31

4. ☐ No required additional search fees were timely paid by the applicant. Consequently, this international search report is restricted to the invention first mentioned in the claims; it is covered by claims Nos.:

Remark on Protest

☐ The additional search fees were accompanied by the applicant's protest and, where applicable, the payment of a protest fee.

☐ The additional search fees were accompanied by the applicant's protest but the applicable protest fee was not paid within the time limit specified in the invitation.

☒ No protest accompanied the payment of additional search fees.

FURTHER INFORMATION CONTINUED FROM PCT/ISA/ 210

This International Searching Authority found multiple (groups of) inventions in this international application, as follows:

1. claims: 1-15, 17(completely); 18, 19(partially)

   Gasdermin (i.e. pejvakin; i.e. being regarded to have antioxidative properties) a vector encoding such a polypeptide and its use for treating a cancer, inflammatory disease, ischemic-reperfusion injury or preventing damage of cochlear cells

   ---

2. claims: 16(completely); 18, 19(partially)

   A composition comprising a RS inhibiting compound and/or an antioxidant compound exception of gasdermin (i.e. pejvakin) for use in treating congenital hearing impairment.

   ---

3. claims: 20-31

   An AVV2/8 vector expressing one USH1 gene and its use for treating Usher syndrome.

INTERNATIONAL SEARCH REPORT

Information on patent family members

International application No
PCT/EP2016/053613

Patent document cited in search report	Publication date	Patent family member(s)	Publication date
WO 2011075838 A1	30-06-2011	US 2013095071 A1	18-04-2013
		WO 2011075838 A1	30-06-2011
WO 0220606 A1	14-03-2002	AU 2045302 A	22-03-2002
		CN 1341652 A	27-03-2002
		WO 0220606 A1	14-03-2002
CN 102732614 A	17-10-2012	NONE	
WO 2011028503 A1	10-03-2011	AU 2010289838 A1	19-04-2012
		CA 2772097 A1	10-03-2011
		EP 2470015 A1	04-07-2012
		ES 2563777 T3	16-03-2016
		JP 5762414 B2	12-08-2015
		JP 2013502461 A	24-01-2013
		JP 2015172071 A	01-10-2015
		US 2012172435 A1	05-07-2012
		WO 2011028503 A1	10-03-2011